INTENSE BEDLOAD TRANSPORT IN NON-UNIFORM FLOW

By

YONAS KINFU PAULOS

B.E., Anna University, 1985

M.A.Sc., University of British Columbia, 1991

A THESIS SUBMITTED IN PARTIAL FULFILLMENT OF

THE REQUIREMENTS FOR THE DEGREE OF

DOCTOR OF PHILOSOPHY

in

THE FACULTY OF GRADUATE STUDIES

DEPARTMENT OF CIVIL ENGINEERING

We accept this thesis as conforming

to the required standard

THE UNIVERSITY OF BRITISH COLUMBIA

November, 1998

© YONAS KINFU PAULOS, 1998

In presenting this thesis in partial fulfilment of the requirements for an advanced degree at the University of British Columbia, I agree that the Library shall make it freely available for reference and study. I further agree that permission for extensive copying of this thesis for scholarly purposes may be granted by the head of my department or by his or her representatives. It is understood that copying or publication of this thesis for financial gain shall not be allowed without my written permission.

Department of CIVIL ENGINEERING

The University of British Columbia
Vancouver, Canada

Date December 02, 1998 W

ABSTRACT

A theoretical and experimental investigation of intense bedload transport in non-uniform flow has been carried out. The study includes the process of shear stress transfer from fluid to carpet; the effect of convective acceleration induced pressure field on the carpet flow; efficiency factor of intense bedload transport; the profiles of sediment and fluid velocities; and frictional behavior of carpet flow.

The theoretical study considers two aspects of carpet flow: The first deals with the dynamics of flat-bed carpet flow and the second deals with the effect of the convective acceleration of the fluid produced by flow over a bedwave. Employing Bagnold's (1954) semi-theoretical relationships, based on his rotating-drum experiments, the theoretical analysis gave two results: 1) velocity profiles for the grains and fluid; and 2) the trend of shear stress transfer from the fluid to the grains. These flat-bed relationships were then extended to the bedwave situation which deals with the effect of the pressure gradient produced by convective acceleration on a carpet flow. Control volume analysis shows that an additional shear stress, other than fluid induced turbulent shear stress, acts to mobilize the sediments. This is confirmed in two ways from the experimental measurements: 1) from the sediment transport kinematics; and 2) from the weight of sediment supported within the carpet layer.

Experiments were carried out to verify the theory and to establish the relative importance of the various stress mechanism. The experiments were conducted using a re-circulating closed conduit, which avoided the effect of surface waves and also produced the necessary high shear stress and other flow parameters.

The sediment concentration and velocity profiles were measured by using a high-speed digital camera that was able to record 1000 frames per second. The velocity profile of the overlaying fluid was measured by using an acoustic doppler velocimeter. Pressure measurements at various points were made by using pressure transducers that logged data to a computer.

A relationship for estimating frictional behavior of intense bedload on flat bed is given. It was found that the amount of resistance depends on the Shields parameter, the critical value being close to 0.8. This theory indicates that for flows with intense bedload and Shields parameter above this critical value, the frictional resistance is higher than an equivalent clear-water and rough-surface flow, and lower for values below the critical.

Identically shaped dunes were observed for a range of discharges which indicated that the fluid induced shear stress, both from friction and convective acceleration, scale almost similarly for a given range of flow. Moreover, the geometry of the dunes are possibly influenced by the scale of the experiments.

A reasonably good matching of the grain velocity profile was obtained between the theoretical and experimental results. And it appears that carpet sediment transport under the influence of convective acceleration is more efficient than the flat bed case, because the additional force on sediments from the pressure gradient is transmitted directly with less energy loss.

TABLE OF CONTENTS

LIST OF TABLES

LIST OF FIGURES

LIST OF SYMBOLS

a = coefficient of proportionality, Eq. 2.5

a_i = coefficient in Bagnold's equation, Eq. 4.8

A = area

    = coefficient in Eq. 3.45

A_d = sidewise area of the mobile part of a dune

b = ratio between the distance between two grains centers and grain diameter

B = Bagnold number

    = coefficient in Eq. 3.45

c_d = dune celerity

c_1 = coefficient defined by Eq. 4.21

c_2 = coefficient defined by Eq. 4.27

c_f = friction coefficient

c_i = coefficient in Eq. 2.21

C = grain concentration

    = Chezy's resistance coefficient

C_b = loose-poured concentration value of grains

C_d = celerity of a dune

C_i = concentration at interlocking

C_r = relative concentration

C_0 = maximum possible concentration of grains

D = grain diameter

d = conduit flow depth

D_{50} = grain diameter where 50% are finer

D_{85} = grain diameter where 85% are finer

e = efficiency factor

f = friction factor

= function

f_c = frequency of grain collision

f_1 = a function defined by Eq. 2.17

= a function in defining grain collision frequency, Eq. 4.5

f_2 = a function given in Eq. 2.21

F = force

F_p = pressure force per unit volume

g = acceleration due to gravity

G = Reynolds number equivalent for grain flow in fluid

h_d = head loss in a down pipe

h_e = expansion head loss d/s of dune crest

h_u = head loss in a riser pipe

i = hydraulic gradient

i_b = immersed weight sediment transport rate

k = roughness height

= coefficient in bed-wave propagation

= a constant in Eq. 2.16

m = mass of a grain

= correction factor for channel meander

M = momentum

n = Manning's resistance coefficient

= coefficient in bed-wave propagation

= exponential coefficient, Eq. 2.5

= a layer of sediment within a carpet flow

n' = a power coefficient

n_g = number of grains per unit area

L = length of a reach

L_d = wave length of a dune

p = pressure

P = normal stress due to *dispersive pressure*

= perimeter

q = unit discharge

Q = discharge

R = hydraulic radius

R_h = hydraulic radius for a pipe flow

Re = Reynolds number

Ri = Richardson number

s = free distance between grains

S = bed/channel slope

s_s = specific gravity

t = time

= variable thickness of carpet

u = fluid velocity

u_* = boundary shear velocity

U = grain velocity

U_c = velocity of carpet

U_i = velocity of grains at top interface of carpet layer

V = velocity of flow

W = weight of grains

x = coordinate in the horizontal direction

y = coordinate in the vertical direction for grain flow

Y = depth of flow

z = coordinate for channel elevation

α = coefficient for velocity gradient correction

α_i = angle determined by collision conditions of grains

β = coefficient in Eq. 2.18

δ_s = thickness of a carpet layer

Δ = factor given by Eq. 6.3

ε = dissipation rate of energy

   = thickness of sediment layer

ϕ' = angle of internal dynamic friction

θ = angle of inclination

   = head loss given by Eq. 6.3

κ = von Kármán constant

λ = linear concentration (ratio of grain diameter to spacing between grains)

η = local bed-wave height

   = relative depth within carpet layer

μ = viscosity of fluid

ν = kinematic viscosity

ρ = density of fluid

σ = density of grains

τ = shear stress

τ_* = non-dimensional shear stress (Shield's parameter)

ω = unit stream power

ω_0 = settling velocity

Ω = stream power

Subscripts

$1,2,3$ = sections

b = bed

BC = stationary boundary of carpet layer

c = collision

C = top boundary of carpet layer

cr = critical

d = dune

f = fluid

= friction

g = between fluid and grains within a carpet layer

m = water-sand mixture

s = sediment

= smooth

t = turbulent

T = total

$*$ = closely packed sand

ACKNOWLEDGMENT

CHAPTER 1

INTRODUCTION

1.1   General Introduction

The study of sediment-transport is an important component of hydraulic and hydrologic engineering designs, geomorphologic investigations, and other water-sediment related processes.

Sediment-transport and its complexity has been studied by many researchers over a long period of time. Mobile beds with significant sediment transport exhibit differing behavior depending upon the flow and sediment parameters. Uniform, flat bed sediment transport can occur, but the more usual behaviour is the formation of various types of sediment bedwaves, even under high transport conditions. Generally accepted categorizations of mobile beds are: ripples (for sediments of size less than 0.6 mm); dunes; plane-bed; and antidunes. The identification, development, and prediction of bedforms has been a subject of study by many investigators, and much of this work on sediment bedwave transport has followed the approach of Einstein and Barbarossa (1952) who subdivided the total resistance into grain and form resistance. The assumption is that only the grain resistance contributes to the sediment transport. This question of the sub-division of resistance is important for estimating sediment transport rates and the effect that sediment transport has on resistance to flow in a channel. This channel resistance is also important when estimating water flow from measurements of channel depth, especially

when trying to estimate extreme flood values using the slope-area method, a commonly used approach.

This thesis is concerned with intense bedload transport which occurs under conditions of high shear stress and which produces a multi-layered thickness of moving sediments, usually called a carpet flow. The classic analysis by Bagnold (1966) considered a uniform flat bed condition and this upper regime plane bed condition has been examined by a number of researchers. This flat-bed carpet flow will be re-examined and compared with earlier work. Carpet flow also occurs in the non-uniform flow conditions induced by dune sediment movement. It is this non-uniform sediment transport behavior which will be examined in this thesis, and the uniform flat-bed analysis will be extended to this non-uniform flow situation.

1.2   Research Objectives

The purpose of this research is to examine sediment carpet flow under the non-uniform flow conditions produced by intense sediment bedwaves. The objective is to develop a theoretical basis for the sediment transport process in the bedwave situation and verify the theory with experiments.

After an initial investigation of plane bed sediment dynamics, the research has concentrated on intense bedload in the presence of bedwaves. This carpet flow of sediment is not constant, but varies along each bedwave, or dune. The flow field is correspondingly variable, because the flow accelerates convectively over each dune, producing a variable shear stress field. This convectively accelerating flow field and the corresponding sediment motion will be analyzed using the theoretical basis developed by Bagnold (1966) in his well know paper on the general

physics of sediment transport. However, Bagnold's analysis of intense bedload, which he called *carpet flow*, had to be simplified to model the transfer of stress to the carpet and within the carpet. Also, in his famous rotating drum experiment (Bagnold, 1954), his theoretical and experimental work on stress within a sheared layer of particles lays the foundation for a more detailed analysis of the carpet, but does not consider the difficult problem of how the fluid induced shear stress is transferred from the open channel flow to the sediment carpet.

The present work therefore set out to investigate several of these key factors both theoretically and experimentally. These factors are:

1. the transfer of shear stress from the driving flow of water to the sediment carpet;

2. the distribution of sediment within the carpet;

3. the influence of convective acceleration on the sediment dynamics;

4. estimation of the efficiency of the sediment transport process;

5. calculation of the power requirement for transport of water and sediment;

6. evaluation of the influence of intense bedload transport on channel resistance;

7. design of experiments to evaluate the theoretical estimates, or to help in making reasonable theoretical assumptions.

All the above factors are closely inter-related and the analysis will be developed to examine these relationships. This theoretical work will then be verified against the experimental findings.

1.3 Thesis Outline

This thesis has seven chapters. The focus of Chapter 2 is literature review of previous work related to flood flow and carpet flow investigations. Chapter 3 deals with the theoretical aspects of carpet flow.analysis. The effect of convective acceleration on intense bedload is discussed in Chapter 4. Chapter 5 describes the apparatus used and experimental procedures adopted in investigating carpet flow phenomenon in non-uniform flow. In Chapter 6 the theoretical and experimental results are presented with a discussion, and conclusion is given in Chapter 7.

CHAPTER 2

LITERATURE REVIEW

2.1   Introduction

The earlier sediment transport equations are based on functions of shear stress and are therefore directly related to channel resistance. The inadequacy of this approach when bedwaves are present was recognized by Einstein and Barbarossa (1952) who proposed that total resistance be subdivided into grain and form resistance, with the assumption that only the grain resistance contributes to the sediment transport.

In general terms, the resistance to flow includes many effects such as: grain roughness; form roughness; meandering; sediment transport; channel geometry; unsteadiness; non-uniformity of flow; surface-wave resistance; etc. The additional resistance resulting from the sediment bedload transport has not been quantified and is usually ignored. However, according to Bagnold (1966), considerable energy is dissipated in moving sediment in an intense carpet flow situation, and this should result in an increase in resistance to flow in the channel. Although the aim of this thesis is to achieve a better understanding of carpet flow, both in flat bed and bedwaves, one of the important outcomes would be a better estimate of the additional channel resistance under extreme flood conditions. Therefore, this review will include a brief survey of work on channel resistance, in addition to the work on the carpet flow mode of sediment transport.

5

2.2   Channel Resistance

Many large floods are estimated using the slope-area method, which depends on accurate channel surveys and a good evaluation of the resistance factor. The accuracy of the method depends on field measurements of channel geometry and slope. The channel geometry can be variable and may change during a flood and the water surface slope is usually estimated from flood marks. Sound judgment in selecting a particular reach and estimating the Manning's n value, is of critical importance. Quite often, for ungauged rivers the n values are estimated based on two approaches; 1) given by Chow (1959) and Barnes (1967), and 2) by Limerinos (1970). Chow and Barnes provided photographs for typical reaches together with their n values. Practitioners are expected to select a particular picture which resembles the reach in question. Limerinos's method estimates the n value based on relative roughness, the ratio between the sediment size and the hydraulic radius of a channel using an equation developed from field measurements.

Another procedure given for the estimation of the n values is by Cowan (1956). According to his procedure, the basic n value, given as n_0 for a straight, uniform, smooth channel in natural materials is modified according to irregularities observed for a particular reach in order to obtain the actual gross aggregate n value. Chow (1959) summarized it as follows:

$$n = (n_0 + n_1 + n_2 + n_3 + n_4)m_5 \qquad (2.1)$$

where n_1 = correction for surface irregularity; n_2 = correction for variation in shape and size of a channel cross section; n_3 = correction for obstructions; n_4 = correction for vegetation and flow conditions; and m_5 = correction factor for channel meander. However, as Cowan himself

noted, the procedure is not applicable for unstable sand beds with high sediment transport associated with high discharges.

Quick (1991) has indicated that under high flow conditions, the resistance to flow may be underestimated for various reasons, such as erosion of the cross-section and additional resistance from sediment transport. Also among other general factors involved, one of the reasons is the n value estimates based on low flow and low sediment transport conditions. Thus, the approaches suggested by Chow and Barnes, and Limerinos in estimating the resistance value are not suited for flood conditions when the estimates provided are based on conditions totally different from floods. Furthermore, with recourse to Bagnold's (1966) stream-power approach to channels, Quick has indicated that under high flow conditions, when flat bed conditions are likely to occur, up to one-third of the total stream power may be utilized in transporting the bedload. Thus, the modification of resistance to flow due to sediment-transport has to be included in estimating the total resistance and hence the amount of flood discharge.

2.3   Stream-Power Approach

2.3.1   Introduction

The power concept in defining resistance to flow was first given by Rubey (1933) and Cook (1935) listed the different energy demands involved:

1) Resistance due to purely viscous shearing forces as in laminar flow.
2) Creating and maintaining turbulence in the fluid.

3) Transporting solids.

4) Doing work in the alteration of the channel-section.

5) Creating and maintaining waves on the surface of a stream.

6) Creating and maintaining bed forms.

Many researchers have approached the problem of sediment transport from the concept of power balance of flowing water: Graf (1971); Ackers and White (1973); McDowell (1989); and Pacheco-Ceballos (1990); and for sand transport on a beach, Bailard (1981) and Bailard and Inman (1981). It is argued that the potential energy of a flowing water is used to overcome the frictional resistance in driving the flow, i.e. in sustaining the average kinetic energy and also transporting the sediment load. The potential energy is ultimately lost and dissipated as heat. Thus, the rate of energy dissipation of flowing water is in part related to the rate of sediment transport, i.e. the rate of doing work. In a broader sense, three approaches that utilize the power concept may be identified: stream-power, Bagnold (1966); unit stream-power, Yang (1973); and gravitational theory, Velikanov (1954). Since the focus of this study is on the bedload transport mode of carpet flow, Bagnold's approach will be dealt with in detail.

2.3.2   Bagnold's approach

Bagnold (1956, 1966) made an analysis of sediment transport from a general physics point-of-view, and avoided empirical formulations as much as possible. He compared a sediment laden river to a machine working at a certain efficiency factor. By adopting such an analogy, he calculated the rate of energy dissipation to transport a given sediment flux. The basic assumptions made are: 1) steady uniform open-channel flow; 2) unlimited supply of sediment at the bed; 3) the channel slope is small so that the energy supply from the sediment is not

significant; and 4) the variables are statistically steady, and a single cross section can be used to represent the reach-averaged channel geometry.

The amount of power, ω, is equal to the drop in potential energy per unit time and unit area of channel bed:

$$\omega = \rho g Y S\, \bar{u} = \tau \bar{u} \tag{2.2}$$

where ρ = the density of water, g = acceleration due to gravity, Y = the depth of flow, S = the slope of the channel, $\bar{u}$ = average flow velocity, and τ = shear stress on the bed.

His bedload analysis, which has a direct relevance to this study, will be discussed here. Bagnold considered two levels of power transfer between the overlaying body of fluid and the grains within the carpet. The first level of transfer is between the overlaying body of fluid and the lumped carpet as a whole. The second level of transfer is between the fluid and grains in the carpet.

Fig. 2.1 is a schematic diagram for the definition of carpet flow as given by Bagnold. A fully developed carpet flow, with a thickness significantly greater than the sediment diameter but negligible compared to the total depth of flow is considered. For a carpet layer moving at an average velocity of U_c and acted upon with a shear stress of τ, the amount of work done per unit time and unit area is:

$$\omega_s = \tau U_c = e_c \omega \tag{2.3}$$

where e_c = efficiency of sediment carpet transport. Thus:

$$e_c = \frac{\tau U_c}{\tau \bar{u}} = \frac{U_c}{\bar{u}} \qquad (2.4)$$

The shear stress that acts at the top of the carpet, applied from the main body of fluid, is given as follows:

$$\tau = a\left(\bar{u} - U_c\right)^n \qquad (2.5)$$

where a = a coefficient of proportionality which is dependent on the bed roughness, and $n = 2$ for fully turbulent flow and 1 for laminar flow. Therefore, the work rate of the carpet is:

$$\tau U_c = a U_c \left(\bar{u} - U_c\right)^n \qquad (2.6)$$

The above equation, which describes the amount of energy absorbed by the carpet, has a maximum value when $U_c = \bar{u}/(1+n)$. Substitution of this value into Eq. 2.4, with $n = 2$, for turbulent flows, indicates that up to 1/3 of the total stream power is taken by carpet flow under turbulent condition, which is the case for all channel flows of practical concern. Furthermore, Bagnold made an analysis of the energy transfer efficiency within the carpet flow itself.

The fluid force, F, exerted on the sediments is assumed to be proportional to $(u - U)^{n'}$, similar to Eq. 2.5; where n' = a coefficient that varies between 1 (Stokes-law region) and 2 (for large sediments) depending on the local Reynolds number, $\text{Re} = (u - U)D/\upsilon$, where D = sediment size, and υ = kinematic viscosity of the fluid. Furthermore, Bagnold asserted that depending on the value of n, the overall efficiency of the bedload sediment transport varies between 0.11 for

10

large sediments and large flow velocities to 0.15 for very fine sediments and low flow velocities.

In his analysis, Bagnold made no attempt to determine the thickness of the carpet but assumed a constant concentration distribution of sediments within the carpet.

2.4 Review of Work by Other Researchers

2.4.1 DuBoys analysis

One of the earliest investigations and analysis of sediment transport was made by DuBoys (1879). Although his analysis was not found to be applicable for cases where saltation mode of sediment transport was dominant, the approach he used is relevant to intense bedload transport even though some of his assumptions are flawed. DuBoys assumed that sediment moves in discreet layers (n in number), each with a thickness of ε. Furthermore, the velocity profile of the layers is assumed to be linear, with zero at the bottom immobile boundary and $(n-1)U_i$ at the top boundary, where U_i = sediment velocity at the interface. Moreover, the sediment concentration is assumed to be uniform with depth. Fig. 2.2 shows the details.

At the immobile boundary, the tractive force due to the applied shear stress, τ_c, is balanced with the resisting force. The balance of forces gives:

$$\tau_c = c_f \, n\varepsilon\rho g(s_s - 1) \tag{2.7}$$

where c_f = a frictional coefficient; ρ = density of water; g = acceleration due to gravity; and s_s = specific gravity of grains. At a threshold of motion, the applied shear stress is resisted by one layer of sediment. Therefore the critical shear stress is given as:

$$(\tau_C)_{cr} = c_f \, \varepsilon \rho g (s_s - 1)$$

(2.8)

Combining the above with Eq. 2.7,

$$n = \frac{\tau_C}{(\tau_C)_{cr}}$$

(2.9)

The above expression was used in defining the rate of sediment transport from know τ_C and $(\tau_C)_{cr}$. From an historical point-of-view, du Boys's analysis was the earliest study of intense bedload transport.

2.4.2 Wilson et al.'s approach

Wilson et al. (1984-1995), at Queen's University, have investigated this intense sediment transport processes. The experiments were conducted using closed conduits and Wilson (1966) showed the advantages of using a closed-conduit flow for the investigation of high rate sediment transport. The results obtained are summarized below.

2.4.2.1   Wilson's analysis

Wilson (1984, 1987, 1989) analyzed intense bedload based on the following concepts and assumptions:

- shear stress transfer within carpet layer is by intergranular collision;

- total shear stress is divided into intergranular and fluid components;

- no slip velocity between fluid and grains exists within the carpet layer;

- Prandtl's mixing length concept is applicable within the carpet layer (velocity gradient is inversely proportional to the mixing length);

- the ratio of fluid stress to the total shear stress is a function of only relative height y/δ_s, and similarly for the ratio of mixing length to the height;

- a linear sediment concentration profile;

- velocity correction due to concentration gradient is made based on Richardson number, Ri;

The combination of the above indicates that the "virtual origin" for the velocity distribution (logarithmic function of height) of the main body of fluid is at the midpoint of the carpet layer. Moreover, by utilizing the technique of finding the average velocity in a pipe flow, Wilson showed that:

$$U_i = 8.2 u_* \tag{2.10}$$

where U_i = the sediment velocity at interface and u_* = the shear velocity (τ/ρ).

The depth of the carpet layer was obtained by balancing the intergranular normal stress with the submerged weight of the grains. For a linear concentration profile, the following was obtained:

$$\frac{\delta_s}{D} = \frac{\tau_*}{0.5 C_b \tan \phi'} \tag{2.11}$$

where τ_* = Shields non-dimensional parameter, C_b = loose-poured concentration value of grains, ϕ' = angle of internal dynamic friction, and δ_s = thickness of carpet layer. By considering the *inertial* region of grain flows, Wilson (1987) used Bagnold's (1954) experimental result which showed that $\tan\phi' = 0.32$. Moreover, with a typical value of C_b = 0.625, Wilson evaluated Eq. 2.11 as:

$$\frac{\delta_s}{D} \approx 10\tau_* \tag{2.12}$$

The grain and fluid velocity (after substituting for von Karman's constant) reduces to:

$$\frac{u}{u_*} = \frac{U}{u_*} = 7\left(\frac{y}{\delta_s}\right)^{\frac{1}{2}} \tag{2.13}$$

Wilson (1989) showed that the resistance to flow for intense bedload obeys its own frictional behavior and the friction factor was found to match neither the rough-wall nor the hydraulically-smooth behavior. Similar argument was also made by Gust and Southard (1983). Nevertheless, it is shown that the velocity distribution of flow for intense bedload and for clear water is similar, but with a different resistance length-scale. For flow with intense bedload, the length scale that is of importance is found to be $0.5\delta_s$. Therefore, combining with Eq. 2.12, the effective roughness ratio is given as:

$$\frac{k}{D} \approx 5\tau_* \tag{2.14}$$

where k = Nikuradse's roughness height.

14

2.4.2.2   Nnadi and Wilson's analysis

The analysis given by Nnadi and Wilson (1992, 1995) is an extension of the work by Wilson (1984, 1987, 1989). Based on previous experimental results they ascertained that the concentration profile is nonlinear. Moreover, the analysis was carried out for cases where the thickness of the carpet is no longer small compared to the hydraulic radius of flow. They found that the ratio between the carpet thickness and hydraulic radius, δ_s/R, is a function of the hydraulic gradient, i, and specific gravity of particles, s_s, so that:

$$\frac{\delta_s}{R} = 7.5\frac{i}{(s_s - 1)} \tag{2.15}$$

Combining the above with a rough-wall law, they found that the frictional resistance of flow with carpet layer is higher than the equivalent clear water rough-wall flow. Moreover, it was found that the friction factor is independent of particle size.

2.4.3   Wang and Qian's approach

Wang and Qian (1987) conducted closed-conduit experimental studies and theoretical work of, what they called, "laminated load motion in the developing stage," and "laminated load in its fully developed stage." The theoretical work is based on collisional theory of grain motions similar to that given by Bagnold (1954). In the developing laminated load motion, they identified three different zones; 1) laminated load region where interparticle collision dominates to the extent that the flow behaves as laminar due to the damping of the interstitial water; 2) contact load region where the mechanism of sediment movement is due to sliding, rolling and saltation; and 3) suspended load region where the main mechanism for suspension of particle is

fluid turbulence. Of interest to this study is the discussion of the developing stage of the laminated load which resembles a carpet flow mode of bedload.

Similar to Bagnold's formulation but differing in form, Wand and Qian derived the following formula for granular shear stress:

$$\tau_s = k f_1(\lambda) \rho \delta_s (\omega_0/u_*)^2 U\left(\frac{dU}{dy}\right) \tag{2.16}$$

where k = a constant, f_1 = a function that depends on λ, λ = linear concentration (ratio between sediment size and spacing between grains), δ_s = the thickness of the laminated load, and ω_0 = settling velocity of sediment. Eq. 2.16 differs from Bagnold's formulation in that the shear stress is made proportional to the product of sediment velocity and gradient, whereas Bagnold and others such as Savage and Sayed (1985), Hanes and Inman (1985), Takahashi (1991) etc. have shown that the shear stress is directly proportional to the square of the strain rate, i.e. the velocity gradient. This is even more so for higher concentrations.

The value of the function that depends on the linear concentration is given as follows in its simplified form:

$$f_1(\lambda) = \beta \frac{1 - y/\delta_s}{\sqrt{y/\delta_s}} \tag{2.17}$$

in which case

$$\beta = \frac{\sqrt{2\pi}}{12}\left[1 - \frac{(1 + 1/\lambda)^2}{12}\right] \approx \text{constant (assumed)}$$

The sediment shear stress is taken to vary linearly within the laminated load; with maximum value (τ_c) at the interface with the stationary boundary, and zero at the upper interface. Thus:

$$\tau_s = \tau_c(1 - 1/\delta_s) \tag{2.18}$$

Combining Eqs. 2.16 with 2.17 and equating it with Eq. 2.18 they obtained the following expression for the velocity distribution of sediments:

$$\frac{U}{U_i} = \left(\frac{y}{\delta_s}\right)^{3/4} \tag{2.19}$$

where U_i = sediment velocity at $y = \delta_s$ (at interface to the overlaying body of water).

Wang and Qian compared their results with findings for debris flow given by Takahashi (1978) and Tsubaki et al. (1983). Such a comparison is not reasonable for the simple reason that the propelling force for carpet flow comes from the main body of fluid unlike debris flow where the weight component of particles is the main driving force. Moreover, the sediment concentration profile estimated from debris flow measurements is not directly related to the carpet flow mode of sediment transport. No expression was given by them for flow resistance under intense bedload condition.

2.4.4 Hanes and Bowen's approach

Hanes and Bowen (1985) presented an analytical solution of intense bedload transport based on Bagnold's constitutive model for granular flow in the inertia region and in conjunction with certain boundary conditions. Three flow regions were identified: 1) overlying clear water; 2)

saltation (water-sediment mixture); and 3) granular-fluid region. The shear stress within the granular layer was taken to be constant, which means that the fluid shear stress is negligible. Moreover, a linear sediment concentration profile was assumed in order to obtain a closed solution

Based on the condition of fluid continuity between the different regions, the velocity profile of the main body of fluid was given as:

$$u = U_i + \frac{u_*}{\kappa} 2.303 \log \frac{y + \delta_s}{\delta_s} \qquad (2.20)$$

The above expression is basically a logarithmic velocity profile with moving boundary, U_i, and with the position of the origin at the lower boundary (stationary) of a carpet layer.

The thickness of the carpet layer was calculated by assuming a linear concentration profile between the stationary boundary and the interface of the granular-fluid and saltation region, and also by considering additional normal stress due to saltation. The shear stress within the carpet layer was taken constant, with no fluid shear stress acting. This assumption is not reasonable since shear stress is gradually transferred to the grains within the depth of a carpet layer.

An expression for the velocity of grains was obtained by utilizing Bagnold's (1954) formulation for grain inertial region as follows:

$$U = \frac{(\tau_c)^{\frac{1}{2}} 3 C_0 \delta_s f_2(\lambda)}{(c_i \sigma)^{\frac{1}{2}} 2 D (C_b - C_i)} \qquad (2.21)$$

where

$$f_2(\lambda) = \frac{\lambda + 1/3}{(1+\lambda)^3}$$

and c_i = a coefficient in Bagnold's equation.

Efficiency factors, as defined by Bagnold, both in the transfer of energy from the flowing water to the carpet (ε_c) and that from the carpet (interstitial water) to the sediments (ε_g) were also given. For the efficiency factor between the main body of fluid and carpet layer, the grain velocity at the interface was used. Moreover, the shear stress was taken to be constant. As mentioned before, the latter assumption is not reasonable.

In the computation of the efficiency factor in the transfer of energy from the carpet to the grains, power dissipation associated with the saltating grains was also included. But such a formulation does not correspond with the definition that was given originally by Bagnold.

2.4.4.1   Hanes analysis of the frictional resistance

Hanes (1984, 1986) argued that frictional bed resistance due to moving sediments is lower than for equivalent clear-water flow. The argument is based on the comparison of equations of motion for a granular-fluid and clear-water cases. Bagnold's (1954) equation of motion for grains in the inertial region may be re-written as follows:

$$u_*^2 = c_i \left(\sigma/\rho\right)(\lambda D)^2 (dU/dy)^2 \tag{2.22}$$

But for a wall bounded shear flow of clear-water, a similar and equivalent expression may be given as follows:

$$u_*^2 = (\kappa y)^2 (du/dy)^2 \qquad (2.23)$$

In Eqs. 2.22 and 2.23 the coefficients of the velocity gradient are equivalent to the frictional resistance. Therefore, resistance coefficients may be defined for each equation as follows:

$$\varepsilon_s = c_i (\sigma/\rho) D^2 \lambda^2 \qquad (2.24a)$$

and

$$\varepsilon_t = \kappa^2 y^2 \qquad (2.24b)$$

where κ = von Kármán constant.

Thus, the ratio of the two terms becomes:

$$\frac{\varepsilon_s}{\varepsilon_t} = \frac{c_i \sigma D^2 \lambda^2}{\rho \kappa^2 y^2} \qquad (2.25)$$

The above equation compares the magnitude of shear resistance for a given shear rate between a clear-water flow and a granular flow. Hanes argued that for a typical value of variables, the granular flow offers less shear resistance suggesting that transporting grains is more efficient than an equivalent fluid. Hence, the carpet layer may be viewed as a layer of lower viscosity and the whole system may be treated as two-layer flow of different viscosity. Based on data

obtained by Williams (1970) for upper plane bed regime, Hanes further argues that a plotting of the non-dimensional sediment transport versus friction factor indicates a lower frictional resistance for higher sediment transport rates.

2.4.4.2   Comments on Hanes' analysis

The shear stress was assumed to be constant throughout the granular-fluid layer, but this is not the case, since the shear stress is gradually transferred to the grains within the carpet layer and ultimately to the stationary boundary. Because of the assumption of constant shear stress within the carpet layer, Hanes and Bowen did not consider an interstitial fluid.

Instead of two flow regions, the main body of water and the granular-layer, an additional saltating layer was assumed. One of the main reasons given was that an additional vertical stress is necessary to contain the granular-fluid from dilating indefinitely. But Bagnold (1956) has shown that the submerged weight of grains is able to balance the dilation pressure that is generated due to shearing. Therefore, the consideration of a saltating layer is not reasonable.

It was estimated that sediment transport by saltation could amount to about 90% of the total bedload. The estimate is unrealistic given that a mainly intense bedload transport has been widely reported by other researchers such as Wilson (1966), Wang and Qian (1987), Nnadi and Wilson (1992), and Eshagira and Ashida (1992).

In computing the efficiency values, the sediment bedload transport due to saltation was included, whereas the accompanying energy dissipation rate was excluded. There is no justification for such an exercise.

2.4.5   Sumer et al.'s approach

Sumer et al. (1996) conducted extensive closed-conduit laboratory experiments on intense bedload as an extension of Wilson's (1987, 1989) and Nnadi and Wilson's (1992, 1995) investigation. They divided the carpet flow mode of sediment transport, *sheet-flow* as they called it, into three regimes based on arbitrary values of the dimensionless fall velocity of particles, ω_0/u_*. The three regimes identified were: no-suspension regime, transition regime and suspension regime. The no-suspension regime, which is of interest to this study, will be considered here.

Sumer et al. used Nikuradse's resistance relation for flow on rough surfaces in order to obtain relative roughness values, k/D, from their experimental data. Based on their experimental results, they obtained the following empirical expression:

$$\frac{k}{D} = 2 + 0.6\tau_*^{2.5}$$

(2.26)

A power-law form of velocity profile was obtained based on velocity measurements, but no slip velocity between grains and fluid was mentioned. By using Wilson's expression $\delta_s/D = 10\tau_*$, the formulation given is as follows:

$$\frac{u}{u_*} = \frac{U}{u_*} = 14\left(\frac{y}{\delta_s}\right)^{3/4}$$

(2.27)

2.5   Bedwave Sediment Transport

The previous sections dealt with the intense sediment transport under uniform flow condition. No work had been done on the effect of pressure gradient, produced by convective acceleration, on sediment flux. The traditional approach in estimating the sediment transport rate for bedforms is to find the effective grain resistance and thus the shear stress that is effective in moving the sediments. To do this, the total flow resistance, which is equivalent to the total shear stress, is partitioned into grain and form components. Different methods and technique were suggested by Meyer-Peter and Müller(1948); Einstein and Barbarossa (1952); Engelund and Hansen (1967); and Ackers and White (1973); among others.

Nelson et al. (1993) concluded that the estimation of sediment transport rate by using local bottom skin shear stress to be erroneous. There are two ways that the local shear could be estimated. One is based on Reynolds stresses, and the other is based on local velocity profile. The main reason the local shear stresses are not valid in obtaining the sediment transport rate, is because they do not include the effect of convective acceleration, that is created by the bedwave topography, on the flow and effective boundary shear. McLean et al. (1994) showed that the estimated local sediment transport rates based on skin shear stress differ significantly from actual measured rates.

2.6   Summary

Bagnold's (1956, 1966) analysis of carpet flow did not consider the variation of sediment concentration within a carpet layer. Although he recognized the existence of slip between the average velocities of fluid and grains, the estimates were highly approximate. He calculated the

efficiency values for energy transfer from the main body of fluid to the grains in two steps: between the main body of fluid and the carpet in general, and between the carpet layer and the moving sediments. Therefore Bagnold's lumped approach to the analysis does not the gradual shear stress transfer to the grains within the carpet, nor the grain velocity and concentration variation. These aspects will be considered in the next chapter.

Wilson (1984), found that the variation of sediment concentration within a carpet layer can be approximated to be linear, however Nnadi and Wilson (1992) showed the sediment concentration variation to be non-linear, although they indicated that the linear variation is a good approximation. Moreover, they found that the ratio between carpet thickness and hydraulic radius is a function of the hydraulic gradient and specific gravity of particles.

Wilson (1987) showed that the frictional behavior of flow with a carpet layer is different from hydraulically-smooth and -rough surfaces. And he also found that the relative roughness height to be a function of Shields parameter. The shortcomings of Nnadi and Wilson's analysis are that they did not consider a slip velocity, between fluid and grains, within the carpet layer.

Wang and Qian (1987) used sediment concentration data obtained from debris-flow experimental results in their analysis of carpet flow. But the driving forces for debris-flow and sediment carpet layer arise from different sources. Therefore, direct comparison between the two cases is not possible. They assumed the shear stress profile within the carpet layer to be linear, for which there is no supporting evidence. No expression for flow resistance due to sediment transport was given.

Bowen and Hanes (1985) presented an analytical solution of a carpet flow and derived the velocity profile of sediments and the efficiency of sediment transport by assuming that the grain shear stress within the carpet layer to be uniform. Since the transfer of shear from the fluid to solids is gradual, the assumption is not valid. Hanes (1984, 1986), based on his analysis and also data obtained by Williams (1970), suggested that flow resistance due to sediment transport to be lower than an equivalent rough-surfaced clear-water flow.

Sumer et al. (1996) conducted extensive experiments on intense bedload and obtained a relationship for flow resistance and velocity profile of fluid and grains, but did not consider slip velocity between grains and fluid.

Taking into account the previous studies discussed above, this study will first focus on the dynamics of carpet flow under flat bed condition. Theoretical analyses will be developed which account for the gradual transfer of shear stress to the grains and detailed analysis of grain velocity and concentration will also be made.

The findings from the flat bed case will be extended to include the effect of convective acceleration under the non-uniform flow conditions produced by bedwaves. This convective acceleration creates a pressure gradient, and detailed analysis of the effect of this pressure gradient on the carpet flow motion will be made in the subsequent chapters. Moreover, the overall efficiency of sediment transport for bedwaves, where expansion loss is also associated, will be discussed.
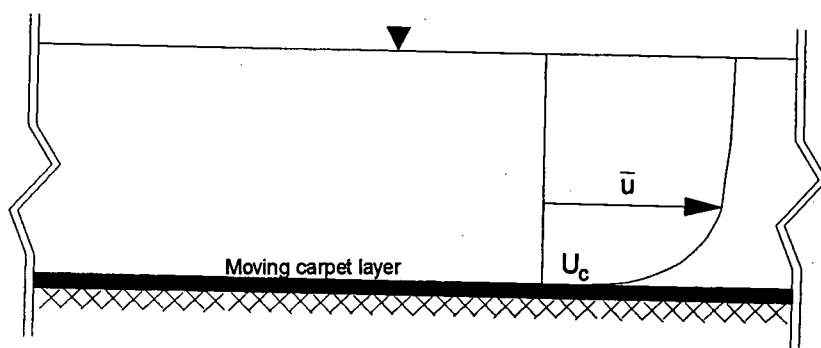
Figure 2.1. Definition diagram for Bagnold's carpet flow analysis
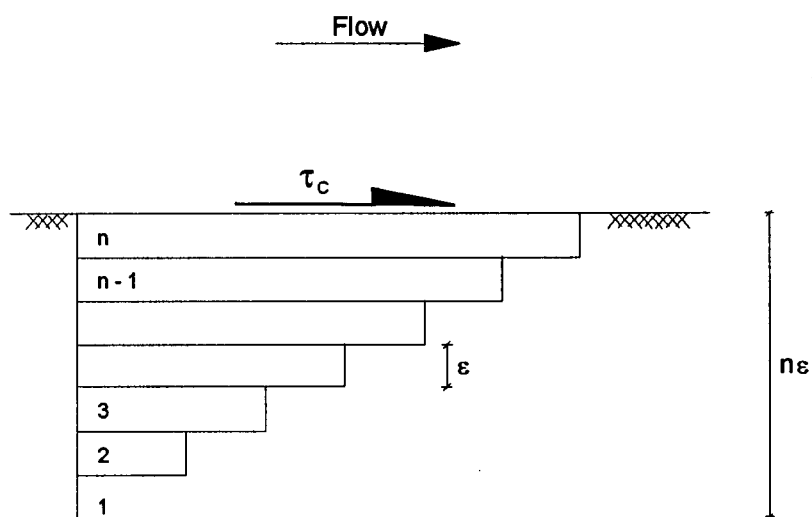
Figure 2.2. Definition sketch for du Boys' bedload model

CHAPTER 3

CARPET FLOW ANALYSIS

3.1   Introduction

This Chapter deals with the theoretical basis for the analysis of intense bedload for the flat bed condition. This flat bed case will be used in Chapter 4 as a basis for the work on non-uniform flow introduced by bedforms where fluid induced shear is additionally increased by the convective acceleration.

Open channel and closed-conduit flows with a loose mobile boundary (sand and fine gravel) exhibit various types of bed forms depending on the flow parameters. For flows with no sediment transport, and a plane bed, the frictional resistance is dependent on the relative roughness height for hydraulically rough flow, and on the viscous effects at the stationary boundary for hydraulically smooth flow. As the stream power increases in open channels, the bed forms change sequentially to ripples (for grains with diameter less than 0.6 mm), to dune and then to plane bed condition with appreciable sediment transport (Richardson and Simons, 1967). Similar changes of bed forms are also observed for closed-conduits transporting sediments. Discussions of different classification schemes are given in Chapter 2, the literature review.

In open channels under high shear stress conditions, it is reported that the bed forms are washed away to form a plane mobile bed. Under such circumstances, sediments move in a layer

27

with a thickness of several grain diameters, usually termed a *carpet flow*. This layer of sheared grains is sometimes referred to as a *shear layer* (Wilson, 1984). The shear stress from the fluid body is transmitted into the carpet flow and to the stationary boundary of the mobile bed.

The fluid turbulent shear stress must first be transferred to the sediment grains by the fluid. For effective shear stress transfer to take place, there has to be a relative velocity between the particles and the fluid; i.e. a slip velocity has to exist. Once the shear stress has been transferred to the grains, the transfer of shear stress between successive layers of grains is accomplished through inter-granular collision. This random collision of grains creates a stress vector in space which may be resolved into vertical and horizontal components. The horizontal component is the resistance to shear stress which is equivalent to the shear stress transferred to the grains. The vertical component is the normal stress, which is found in the shearing of solid particles. The normal stress at a particular layer is balanced by the weight of solid grains above that layer as first shown by Bagnold (1956) and this basic concept is to be used later on in the analysis. Also Bagnold argued that this normal stress of the sediment grains is proportional to the grain shear stress. For a sloping channel bed, the weight of the carpet has a significant downslope component and hence this downslope component contributes to the total shear stress that acts on the carpet itself. The extreme case of such contribution is a debris flow where the channel slope is large and the weight of the solids is the major driving force. However, for a small thickness of carpet relative to the total depth of flow and for a low bed slope, the shear stress was assumed by Bagnold to be constant within the carpet layer, Fig. 3.1, so that the change between γYS and $\gamma(Y - \delta_s)S$ was considered to be small.

For dunes or an adverse slope, the weight component of grains acts in the opposite direction to that of the flow. Therefore, the submerged weight of grains within a carpet flow will partly resist the shear stress exerted by the main body of flow, Fig. 3.2.

For open channel flow, the shear stress at the free surface is zero, so that the total shear stress at the base of the carpet layer, from Fig. 3.1, is:

$$\tau_{BC} = \gamma Y S \left(1 + \frac{(s_s - 1)\delta_s}{Y} \right) \qquad (3.1)$$

where γ = specific weight of fluid, Y = depth of flow (including carpet), S = slope of channel, s_s = specific gravity of grains, and δ_s = thickness of carpet layer.

In a closed conduit, with no free surface, the shear stress can still be assumed to be zero near the centerline of the flow. Fig. 3.3 shows a horizontal and wide conduit, where the vertical coordinate y is measured from the center of the conduit. For this case, the total shear stress at the base of the carpet layer is:

$$\tau_{BC} = \gamma Y S_f \qquad (3.2)$$

where for the above equation S_f = energy gradient. In the above equation the specific weight of sediments is not important since the bed slope is zero. Also δ_s is included in Y and, for zero slope, δ_s does not appear.

3.1.1   Stress within the carpet

The shear stress in the fluid above the carpet layer must be transferred into the carpet. Assuming a thin carpet and a low slope or horizontal channel, the total shear stress in the carpet layer can be considered to be constant, as assumed by Bagnold (1966). However, the shear stress must be transferred gradually from the fluid to the sediment carpet layer, as can be seen from the following argument.

At the top of the carpet, the shear stress carried by the grains must be zero, because the overlaying weight of grains is also zero and there must be a balance between grain shear and dispersive grain stress, as established by Bagnold, therefore at the top of the carpet the total shear stress is carried by the fluid.

Therefore, throughout the depth of carpet there must be a gradual transfer of fluid shear stress to the carpet. Consequently, at the top of the carpet, the total shear is carried by the fluid. Then as the depth into the carpet increases, the shear is gradually transferred to the grains, but the balance is carried by the fluid until at the base of the carpet all the shear is carried by the carpet.

Therefore, at the base of the carpet, the shear stress carried by the grains is equal to the total weight of the grains per unit area carpet multiplied by $\tan \phi'$, where ϕ' is the friction angle for the grains. This is consistent with Bagnold's original work.

The transfer of shear from the fluid to the grains will now be examined.

3.2   Constitutive Equations

Sediment transport is a two-phase flow phenomenon whereby the water phase and the sediment phase interact. There have been various attempts to obtain constitutive relationships that define the mechanical interaction between fluid and solid phases and also the flow of grains (Savage and Jeffrey, 1981; Ackermann and Shen, 1982; Shen and Ackerman, 1982; Savage and McKeown, 1983; Savage and Sayed, 1984; etc.). A comprehensive analysis that defines such an interaction and flow is far from complete. A great deal of theoretical and experimental work has been done to develop a reasonable approximation of fluid-solid and grain flows. The simplest granular flow is a special case of two phase flow in which the effect of the fluid is assumed negligible and in which grains under shearing stress behave like fluids.

For this study, the approach used by Bagnold (1954, 1956) will be used to obtain an analytical solution to carpet flow. Some of the other approaches proposed by other researchers are discussed and are seen to be similar to that given by Bagnold.

3.2.1   Theoretical approach

The theoretical work proposed by various researchers have different approaches. In the later part of the last century, Reynolds (1885) had shown that stationary grains subjected to shear stress have a tendency to dilate and disperse. Bagnold (1954) considered the dynamic relationship between shear and dilation and found that the ratio between the shear stress and the normal stress corresponds to the tangent of the angle of repose.

3.2.1.1   Assumptions made in Bagnold's equations

Bagnold (1954) developed semi-empirical equations for grain flows in interstitial fluid based on theoretical considerations and experiments. He found that, depending on the ratio between the grain inertia stress and interstitial viscous stress, two distinct flow regions exist. The first region, known as *micro-viscous* region, is when viscous stresses dominates and the effect of the grains is mainly to change the viscosity of the interstitial fluid. The second region, know as *grain-inertia* region, is when the inertia stress of grains dominate. By default, a third region exists between the two, which is termed a "transition region." This whole process of categorization is analogous to that found in fluid flows: namely, laminar flow when viscous effects dominate; turbulent flow when inertia forces dominate; and the transition between the two.

Bagnold's drum experiments had the following characteristics:

• uniform grain concentrations and velocity gradients;

• the grains had the same density as the water so that the density difference between the fluid and grains was not significant;

• the interstitial fluid was under the same strain rate as the grains;

Although the above are very different from the case of a carpet flow, Bagnold's results are still applicable as a fundamental governing equations for a grain continuum.

Therefore in Bagnold's experiments,

- the dispersion is in a state of uniform shear strain, and the mean relative velocity between the grains and the interstitial fluid is everywhere zero, i.e. no slip velocity between grains and fluids is necessary because shear is not being transmitted from fluid to grains;

- the shear strain of grains is maintained constant through time by externally applied forces in the direction of flow acting on all the grains;

- the kinetic energy per unit volume of the system is maintained constant by the applied rotational torque which balances the frictional losses so that the grain flow is in a steady state;

- the motion of the grains consists, in addition to the average velocity in the direction of flow, of oscillations in all three directions, involving approaches to and recessions from neighboring grains.

3.2.1.2   Derivation of equations

For the definition of the geometrical variables involved, Bagnold considered first the uniform dispersion of rigid spheres of uniform diameter, D, and mass density, σ, initially arrayed in tetrahedral-rectangular piling which give maximum packing. In dispersion, the free distance between the grains, s, increases. Alternatively, it is equivalent to the increase between the centers of two grains, which may be given as a fraction/multiple of the grain diameter, bD. Thus, we have,

$$b = (s/D) + 1 = (1/\lambda) + 1 \tag{3.3}$$

where λ is the ratio between the grain diameter and the free distance between grains, so that $\lambda = D/s$.

The volumetric grain concentration, the volume occupied by grains in a unit volume of space, is given by:

$$C = \frac{C_0}{b^3} = \frac{C_0}{(1/\lambda + 1)^3} \tag{3.4}$$

where C_0 is the maximum possible concentration under maximum packing of grains, where $s = 0$. For spheres, $C_0 = 0.74$.

Bagnold considered moving layers of uniform sized grains. Fig. 3.4 is the definition schematic diagram used for the analysis. For simplicity, he argued that the slower moving layer A can be considered stationary relative to the faster moving layer B, so that only the relative movement, or velocity (δU), is considered between the adjacent layers.

Then he further argues that for a unit time, the frequency of collision is directly proportional to the relative velocity, δU, and some function of the linear concentration, $f_1(\lambda)$, and inversely proportional to the free distance between the grains. Thus,

$$f_c = \frac{f_1(\lambda) \delta U}{s} \tag{3.5}$$

But, at the same time, the number of grains per unit area perpendicular to the direction of grain movement is:

$$n_g = \frac{1}{b^2 D^2}$$ (3.6)

And the total change of momentum at each collision of a grain, considering the inelastic case, is:

$$\delta M = 2m \, \delta U \cos \alpha_i$$ (3.7)

where m is mass of each grain ($\frac{3}{4}\rho\pi D^3$), and α_i angle determined by the collision conditions of grains.

Therefore, the vertical repulsive force per unit area, the normal stress, between successive layers of grains is obtained by multiplying Eqs. 3.5, 3.6, and 3.7. Thus, after multiplying and making the necessary simplification, we have an expression for the normal stress as:

$$P(y) = a_i \, \sigma \lambda f_1(\lambda) D^2 \left(\frac{dU}{dy}\right)^2 \cos \alpha_i$$ (3.8)

where a_i = a coefficient.

Furthermore, Bagnold argued that the shear stress, the horizontal component of the stress due to grain collisions, is related to the normal stress as follows:

$$\tau = P \tan \alpha_i$$ (3.9)

Therefore, according to Bagnold, random collisions between adjacent layers of moving grains produce a stress vector whose horizontal and vertical components correspond to shear stress and normal stress, respectively.

Combining Eqs. 3.8 and 3.9, and adopting simplification given by Bagnold (1954) a stress relationship for the *grain-inertia* regime, where the grain inertia is significant and the stresses produced are due to random collisions, is as follows:

$$\tau = a_i \sigma D^2 \lambda^2 \left(\frac{dU}{dy}\right)^2 \sin \phi'$$

(3.11)

The above equation is reminiscent of turbulent fluid flow where the shear stress is proportional to the square of the velocity gradient. Such formulation and resemblance is one of the main reason that a rapid-granular-flow is taken as analogous to fluid flow. However, unlike Prandtl's boundary layer assumption, the mixing length in the granular flow of Bagnold's experiment appears to be a constant fraction of λ and D. In its simplest form, the mixing length is simply λD, and not a function of distance from the boundary.

In the *macro-viscous* regime, viscosity of the interstitial fluid is dominant and the stresses are a linear function of the velocity gradient. Similar to fluid flow, the grain-inertia and macro-viscous regimes are defined by the Bagnold number, $B = \lambda^{1/2} \sigma D^2 (dU/dy)/\mu$ and where μ = fluid viscosity, which is a special form of the Reynolds number.

The total shear stress for the *macro-viscous* regime (where the presence of the grains modifies the overall effective viscosity of the mixture) was given as follows:

$$\tau = (1+\lambda)(1+\lambda/2)\mu\left(\frac{dU}{dy}\right)$$

(3.10)

In Bagnold's later analysis of carpet flow, he considered a simplified process for shear transfer. He assumed the carpet to be like a solid conveyor belt and the total fluid shear was transferred directly to the top of this moving layer. This transfer required a slip velocity between the fluid and the rigid carpet. Bagnold argued that the carpet moved a 1/3 of the speed of the fluid for turbulent flow and 1/2 for laminar flow.

In reality, the shear stress cannot all be transferred to the carpet at the top, as assumed by Bagnold, because the shear stress is directly related to the vertical dispersive stress, which must be equal to the weight of the sediment above any given level. Therefore, the shear stress must be gradually transferred so that the shear stress and the dispersive stress build up to balance the weight of the carpet.

However, Bagnold's formulations are utilized in this study as basic governing equations, to analyze the dynamics of a carpet flow.

An analysis will now be developed which considers this transfer of stress to the carpet flow.

3.3   Analysis

3.3.1   Definition of the problem

Intense transport of sediments, at higher Shields parameter, τ_*, can happen in both open channel and closed conduit flows. In uniform open channel flows, no pressure variation along

the direction of flow exists. Therefore, only shear force from the flowing fluid is transferred to a carpet layer. In closed-conduit flows, a pressure change along the direction of flow exists whether the mobile bed is flat or not. Therefore, in addition to the shear force that is exerted by the flow, a pressure change is also felt by a carpet layer. Thus, in closed-conduits there is an extra pressure force that is exerted on the sediments of a carpet layer.

For a pipe flow with flat bed, the pressure drop can be written in terms of the boundary shear stress as follows:

$$\frac{dp}{dx} = \frac{\tau_c}{R_h} \tag{3.12}$$

where p = pressure, x = axis of the direction of flow, τ_c = boundary shear stress and R_h = hydraulic radius of a pipe flow cross-section. But with a non-flat mobile bed, where convective acceleration is significant, the total shear stress acting on the lower boundary of a carpet layer is the sum total of the fluid shear stress acting on the interface between a carpet and main body of fluid, and the pressure gradient due to convective acceleration. Therefore:

$$\frac{\tau_{BC}}{R_h} = \left(\frac{dp}{dx}\right)_{uniform\,flow} + \left(\frac{dp}{dx}\right)_{convec.\,accel.} \tag{3.13}$$

where τ_{BC} = shear stress at the lower boundary of a carpet layer. In the above equation an assumption is made that the carpet thickness compared to the dimension of flow is small enough that the hydraulic radius is the same with and without the inclusion of the carpet layer.

The same is also true for non-uniform open channel flow where convective acceleration due to the change of mobile-bed elevation exists. The pressure forces due to the drop in pressure caused by the convective acceleration also act on sediments of a carpet layer.

The effect of the pressure drop on the moving sediments is similar to that of a buoyancy effect. Buoyancy force is equivalent to the product of specific weight times volume of object under consideration. Therefore, pressure force on sediments can be written as:

$$F_p = \left(\frac{dp}{dx}\right)C \qquad\qquad (3.14)$$

where F_p = pressure force per unit volume and C = volume concentration of sediments.

3.3.2   Basic assumptions and approaches utilized

The following are the basic assumptions and approaches utilized in the present analysis:

- uniform grain size;

- the thickness of a carpet is several grain diameters so that collision of grains is significant;

- the statistical average of variables such as velocity, grain concentration, etc. to be constant over sufficient period of time at a given location;

- continuum mechanics is applicable to the constituents of a carpet flow, fluid and grains;

39

- Prandtl's mixing length concept is applicable to the fluid within the carpet flow;

- a slip velocity exists between fluid and grains within the carpet so that shear stress is transferred from the fluid to grains;

- the tractive shear stress applied by the main body of flow is gradually transferred to the grains within the carpet;

- at the lower boundary of the carpet flow all the shear stress is carried by the grains and the grain concentration reaches a maximum possible value above which motion ceases;

- the normal stress due to shear dilation of grains at any level within the carpet is in equilibrium with the submerged weight of grains above the particular level;

- the slope of the flow conveyance system is very small, so that the component in the flow direction of the submerged weight of sediment is negligible (unlike debris flow where the driving force is the weight of the sediments themselves);

- Bagnold's (1954) results from his drum experiments and his semi-empirical formulations are applicable to carpet flow analysis;

- where a pressure change exists along the direction of flow, the pressure force that acts on the fluids also acts on the sediments throughout the depth of carpet flow.

3.3.3 Carpet flow with no pressure gradient

To analyze the dynamics of carpet flow, let a shear stress, τ_c, be assumed to act on a carpet layer with a thickness of several grain diameters. Figs. 3.5 and 3.6 give the definition sketch. As shown in Fig. 3.7, at level y some of the fluid shear stress is transferred to the particles as τ_s and the remaining is the residual shear stress of fluid, τ_f. As suggested by Bagnold (1956), the grain shear stress is obtained from the equilibrium condition of vertical forces acting within the carpet, so that the weight of grains above a particular level is balanced by the normal stress of grains at the point. Therefore, the balance of the normal stress and the submerged weight of sediments at any given level may be written as:

$$P_y = \rho g(s_s - 1)\int_0^y C\,dy \qquad (3.15)$$

where the right hand side is the submerged weight of sediments contained between the top of carpet, where the concentration of grains is negligible, and the particular level considered. But, also, the normal stress and the corresponding shear stress are related through the coefficient of dynamic friction, as given by Eq. 3.9. Therefore,

$$\tau = \rho g(s_s - 1)\tan\phi'\int_0^y C\,dy \qquad (3.16)$$

where τ = the shear stress related to the normal stress as given by Eq. 3.9; ρ = the fluid density, g = gravity acceleration; s_s = is grain specific gravity; ϕ' = dynamic friction angle; C = volumetric concentration; and y = the distance of a particular level within a carpet from the top boundary.

Bagnold (1954) in his shear experiments has related the grain shear to different grain and fluid parameters as follows.

When grain inertia dominates:

$$\tau = a_i \sigma D^2 \lambda^2 \left(\frac{dU}{dy}\right)^2 \sin \phi' \qquad (3.11)$$

where a_i = a coefficient (obtained from experimental results), D = grain diameter, λ = is linear concentration (grain diameter/clear distance between grains) and U is velocity of grains.

When fluid viscosity dominates:

$$\tau = (1+\lambda)(1+\lambda/2)\mu\frac{dU}{dy} \qquad (3.10)$$

where μ is fluid viscosity.

Bagnold introduced an equivalent Reynolds' number, $G^2 = \sigma D^2 \tau_s / \lambda \mu^2$, which when greater than 3000, the grain inertia dominates, and when it is below 100, fluid viscosity is dominant. Transition is observed in the range between 3000 and 100. For this transition region, no formulation was given by Bagnold. Therefore, for this study a scheme was developed to obtain a formulation for the transition region depending on the G value. A solution was obtained by interpolating for the transitional region between the laminar and the grain-inertia regions.

For $100 < G^2 < 3000$, the strain rate was obtained as follows:

$$\frac{dU}{dy}\bigg|_{transitional} = \left(\frac{3000 - G^2}{2900}\right) * \frac{dU}{dy}\bigg|_{laminar} + \left(\frac{G^2 - 100}{2900}\right) * \frac{dU}{dy}\bigg|_{inertial} \tag{3.17}$$

The above is basically a weighted average approach of estimating the strain rate in the transitional region from laminar and grain-inertia values.

Moreover, Bagnold's results were given for λ values up to 17, but interlocking of particles doesn't take place unless the λ value exceeds 22. Therefore a scheme was developed that extrapolated for the value of a_i as given in Eq. 3.11, depending on the λ value of concentration. A trend for the change of a_i with λ was obtained as follows based on Bagnold's (1954) experimental results:

$$a_i = 0.04 + \frac{(\lambda - 14) * (0.427 - .04)}{(22 - 14)} \tag{3.18}$$

Bagnold's (1954) experiment was not designed to include the transfer of shear from fluid to solids. For his case, a slip velocity between the grains and fluids did not exist. But, his results are used as governing equations to build a model that simulates the shear stress transfer from fluid to grains. This analysis must be carried out subject to the necessary boundary conditions as previously set out.

3.3.4   Simplified approach

To prepare for the detailed analysis, two simplified cases are considered first, one assuming uniform sediment concentration and another one assuming a linear increase in sediment concentration with carpet depth.

3.3.4.1   Carpet flow with uniform sediment concentration

Bagnold (1966), in his carpet flow analysis, implicitly assumed the sediment concentration to be uniform throughout the depth. An analytical solution is obtained as follows.

For a uniform concentration profile, grain shear stress varies linearly; being zero at the carpet interface with the main body of fluid and a maximum, τ_{BC}, at the stationary boundary of the carpet. Therefore,

$$\tau_s = \tau_{BC} \left(\frac{y}{\delta_s} \right) \tag{3.19}$$

Combining the above with Eq. 3.11 (assuming inertial regime of flow within the carpet) gives:

$$\tau_{BC} \frac{y}{\delta_s} = a_j \overline{\lambda}^2 D^2 \left(\frac{dU}{dy} \right)^2 \tag{3.20}$$

where $\overline{\lambda}$ = the linear concentration of sediments and $a_j = a_i \sin \phi$. After integrating the above equation with the limit that grain velocity is zero at the stationary boundary, the expression for grain velocity is as follows:

44

$$U = c_1 \left(\delta_s^{3/2} - y^{3/2} \right)$$ (3.21)

where,

$$c_1 = \frac{2}{3\sqrt{a_j \lambda D}} \left(\sqrt{\frac{\tau_{BC}}{\delta_s}} \right)$$ (3.22)

3.3.4.2   Carpet flow with a linear concentration profile

The denominator of Eq. 3.4 may be expanded as follows:

$$\left(1 + \frac{1}{\lambda} \right)^3 = 1 + 3\left(\frac{1}{\lambda} \right) + 3\left(\frac{1}{\lambda} \right)^2 + \left(\frac{1}{\lambda} \right)^3$$ (3.23)

Since the value of λ is higher than unity, the first two terms of the right hand side of the above equation will dominate.

Also, for a linear concentration profile, the value of concentration at any point below the top of carpet is as follows:

$$C = C_0 \frac{y}{\delta_s}$$ (3.24)

Combining Eq. 3.4 with Eqs 3.23 and 3.24, an expression for λ can be obtained as follows:

$$\lambda = \frac{3y}{(\delta_s - y)}$$ (3.25)

And for a linear sediment concentration profile, the grain shear stress distribution is given as follows (Wilson, 1984):

$$\tau_s = \tau_{BC} \left(\frac{y}{\delta_s} \right)^2$$

(3.26)

Therefore, combining the above equation with Eq. 3.11, and rearranging, we have:

$$U = c_2 \left[\frac{\delta_s}{2} - \left(y - \frac{y^2}{2\delta_s} \right) \right]$$

(3.27)

where

$$c_2 = \frac{1}{\sqrt{a_j} 3D} \sqrt{\tau_{BC}}$$

(3.28)

3.3.5 Numerical analysis

In the above sections, simplified approaches were used to obtain the velocity of grains within a carpet layer, and various assumptions and approximations were made. This section deals with a numerical analysis of carpet flow dynamics.

Between Eqs. 3.16 and 3.10 or 3.11 there are three unknowns, i.e. τ_s, C, and U. The grain concentration, C, is approximated in order to obtain a closed solution to the equations, and solutions are obtained based on the following assumptions:

1) Uniform concentration profile: the concentration is taken to be constant within the carpet depth, with $C = 0.27$, an average value between $C = 0.0$ at top of carpet and $C = 0.54$ at the bottom of carpet. When $C = 0.54$ the grains are stationary due to interlocking.

2) Linear concentration profile: the concentration is assumed to vary linearly (with $C = 0$ at top to $C = 0.54$ at the bottom of carpet), which is the same as given by Wilson (1984).

3) Non-linear concentration profile. This concentration profile was derived by Nnadi and Wilson (1992) as an improvement on the linear profile.

The non-linear concentration profile was defined by the following expression,

$$\left(\frac{C}{C_i}\right) = 1 - 4\eta^{1.5} + 3\eta^2 \qquad (3.29)$$

where C_i = the maximum concentration, which for this study will be taken as the concentration where interlocking of grains occurs, and η is the relative depth given as,

$$\eta = \frac{y}{\delta_s} \qquad (3.30)$$

where δ_s is thickness of carpet given by ,

$$\delta_s = \frac{\tau_t}{\rho g(S-1)\overline{C}_r \tan\phi'} \qquad (3.31)$$

where $\overline{C}_r$ is average relative concentration equal to 0.4 and $\tan\phi'$ is taken as 0.53.

A non-uniform sediment concentration causes a density gradient which can have a significant effect on the velocity gradient. A correction procedure is based on Wilson (1984) in which an approximate correction of the velocity gradient is made based on the Richardson number, Ri, given as:

$$Ri = \frac{-\dfrac{g}{\rho_m}\dfrac{d\rho}{dy}}{\left(\dfrac{dU}{dy}\right)^2} \tag{3.32}$$

Correction of the velocity gradient is introduced by multiplying the velocity gradient by the factor $(1+\alpha Ri)$. The value of the coefficient α is approximately equal to 5 as given by Turner (1973).

3.3.6 Fluid velocity

Once the grain shear stress was obtained, the fluid shear stress was calculated by subtracting the know grain shear stress from the total applied shear stress:

$$\tau_f = \tau_c - \tau_s \tag{3.33}$$

where τ_f is the fluid shear stress and τ_c is the shear stress applied to the carpet.

Then Prandtl's mixing length concept was used to obtain the velocity of the fluid. This idea was also used by Wilson (1987, 1989). The basic formulation that was adopted is as follows:

48

$$\tau_f = \rho(\kappa y)^2 \left(\frac{du}{dy}\right)^2 \tag{3.34}$$

where κ = von Kármán constant (0.41) and u = local average fluid velocity in the direction of flow. The above equation was solved from known fluid shear stresses and the boundary condition that the velocity of fluid is zero at the stationary boundary, the level where all the shear stress is taken by the interlocking of the grains.

3.3.7   Solution method

A finite difference numerical computer solution was obtained for the governing equations, Eqs. 10, 11 and 16, using specified boundary conditions.

This analysis has the advantage that the flow region does not have to be specified in advance. For the simplified cases, it was already assumed that the grain flow was in the inertial region.

The computer program that was used is given in Appendix A.

3.4   Power and Efficiency within the Carpet

According to Bagnold (1966), there are two levels of power transfer between the main body of flow and actual movement of sediments. The first level is the lumped transfer of power to the carpet as a whole which includes the interstitial fluid and also sediments. The second level is the transfer of power within the carpet which is effective in transporting the sediment. In order to compute the different efficiency factors involved, the amount of power available in each phase has to be obtained.

3.4.1 Power and efficiency concepts

The rate of energy dissipation per unit area of channel bed and in unit time is the stream power within the main fluid body and is given as follows:

$$\omega = \bar{u}\tau_C \qquad (3.35)$$

where $\bar{u}$ = average velocity of flow, and τ_C = shear stress exerted by flow at the bed.

The total amount of power supplied to a flow per unit volume, which is also lost to heat ultimately, is the product of the shear stress and the velocity gradient (Daily and Harleman, 1966). In order to obtain the efficiency value of energy transfer within the carpet, from the fluid to the sediments, the rate of energy dissipation of the fluid will be considered first. The rate of energy dissipation per unit width and time for a unit volume of fluid is as follows (Daily and Harleman, 1966):

$$\varepsilon_f = \int_0^{\delta_s} \tau_f \frac{du}{dy} dy \qquad (3.36)$$

where τ_f = residual shear stress within the fluid. The velocity profile of the fluid within the carpet is obtained by utilizing Prandtl's (1926) mixing-length hypothesis. The same mixing length approach was also used by Wilson (1987, 1988), but the slip velocity between sediment and fluid was ignored.

In the same way, the amount of power involved in moving sediments is given as follows:

$$\varepsilon_s = \int_0^{\delta_s} \tau_s \frac{dU}{dy} dy \qquad (3.37)$$

where τ_s = shear stress of the moving sediments and U is the local mean grain velocity. The velocity profile for the sediments was obtained from the numerical analysis.

Finally the efficiency of power transfer between the main body of flow and the carpet as a whole is given as follows:

$$e_c = \frac{\varepsilon_s + \varepsilon_f}{\omega} \qquad (3.38)$$

where e_c = efficiency of power transfer between the main body of fluid and the carpet layer, ε_s = power dissipation per unit width and time for a unit volume of fluid; and ε_f = power dissipation in moving sediments.

Secondly the efficiency for the transfer of power between the fluid within the carpet and the moving sediments is:

$$e_g = \frac{\varepsilon_s}{(\varepsilon_s + \varepsilon_f)} \qquad (3.39)$$

where e_g = efficiency of power transfer between the fluid and grains within the carpet layer. Therefore, combining Eqs 3.38 and 3.39, to account for the two levels of energy transfers, the overall bedload transport efficiency may be given as follows:

$$e_b = e_g \times e_c = \frac{\varepsilon_s}{\omega} \qquad (3.40).$$

Eq. 3.40 directly links the amount of power that is transferred from the main body of fluid to the sediments in motion, or in other words, to the sediment bedload under intense flow condition. Eq. 3.40 could have been written directly, but for comparison with Bagnold's analysis the two stage process has been followed. In the present work, the efficiency can be calculated in a single step.

3.4.2   Flow resistance

From Keulegan's (1938) resistance equation for wide rectangular channel flow with a free surface, we have:

$$\frac{\bar{u}}{u_*} = 5.75\log\frac{Y}{k} + 6.25 \tag{3.41}$$

where $\bar{u}$ = depth averaged flow velocity, Y = depth of flow, u_* = shear velocity, and k = Nikuradse's equivalent sand roughness. The above equation may be arranged to provide an expression for unit discharge, q,

$$q = Yu_*\left(5.75\log\frac{Y}{k} + 6.25\right) \tag{3.42}$$

Wilson (1989) gave a relationship between the effective roughness height and Shields parameter based on sediment size. The relationship (for $\tau_* \geq 1$) is as follows:

$$\frac{k}{D} = 5\tau_* \tag{3.43}$$

The constant in this equation depends on the assumed friction coefficient. As indicated previously, in section 2.4.2.1, the above estimate is based on the value obtained by Bagnold (1954) for the dynamic coefficient of friction (0.32) for his experiments. But, Bagnold (1973), based on experimental data, later indicated that the value he obtained for the dynamic coefficient of friction from his experiments was based on the value for his spherical particles and was about half the value for natural sediments. Therefore, for the present study a value of 0.64 has been used. The same argument was also verified by Hanes and Inman (1985a) in their experimental evaluation of dynamic coefficient of friction. Therefore, the following formulation is used after modifying Eq. 3.43:

$$\frac{k}{D} = 2.5\tau_*$$
(3.44)

3.4.3   Analysis of power transfer to the carpet

To test the analytical formulations presented in this chapter, numerical solutions will be carried out, and various assumptions tested. For illustrative purposes, a shear stress value of 10 Pa and uniform sediment size of 1 mm was considered for analysis: the same was also considered by Wilson and Pugh (1988). The value considered is in the range found in natural situations. Detailed relationships for carpet flow are given in section 3.3.3, and these relationships are utilized to obtain shear stress and velocity profiles for both the fluid within the carpet and also the moving sediments.

The results obtained from section 3.3.3 were combined with Eqs. 3.35 to 3.40 to obtain the energy and efficiency values. Starting with a known value of shear stress value and grain size, the gradual transfer of shear stress from the fluid to the grains is calculated beginning from the

top carpet boundary. Table 3.1 shows the results that where obtained for the different sediment concentration profiles. Both the linear and non-linear concentration profiles are close and also seem to be reasonable. The value obtained for efficiency of power transfer between the fluid within the carpet and sediments is close to one-fourth. Bagnold (1966), based on certain approximations and assumptions, obtained a value close to one-third, and this difference is expected because of the general nature of the assumptions used by Bagnold: details are given in Chapter 2.

For this analysis, Eqs. 3.43 and 3.45 were used to compute the efficiency values of sediment transport. For a given stream power, which is the product of the average velocity of flow and shear stress on the bed, there could be different combinations of discharges and depths of flow. Therefore, Eq. 3.43 was solved for different values of discharges, but values within the range of the Froude number for a channel were selected. For each discharge that was selected, the depth of flow was obtained from Eq. 3.43 by iteration. Table 3.2 gives the details of the results. As is indicated in the table, the efficiency factor for the transfer of power from the main body of flow to the carpet as a whole is about one-fifth. This is lower than was estimated by Bagnold (1966); who gave a value of about one-third, which is different because of the assumptions and approximation made by Bagnold.

3.4.4 Analysis of power transfer within the carpet

Results such as the variation of grain shear stress and slip velocity within the carpet layer were obtained for three different types of concentration profiles shown in Fig. 3.8. The corresponding shear stress distributions obtained by solving the governing equations for applied

shear stress of 10 Pa and grain size of 1.0 mm are indicated in Fig. 3.9. As it can be seen from the figure, the linear and non-linear concentration profiles yield similar results.

The fluid velocity profile was obtained by using the mixing length model given by Prandtl. The fluid shear stress was obtained by subtracting the grain shear from the total stress. Fig. 3.10 indicates the calculated slip velocity between the grains and the fluid. The assumption of uniform concentration gives negative slip velocity values which are not realistic.

The comparison of the velocity profile of the simplified analysis with the numerical solution is shown on Fig. 3.11. The assumption of uniform concentration has a larger variation compared to the linear concentration assumption. Although the simplified analysis with linear concentration is closer to the numerical solution, the shape of the velocity profile is quite different. Therefore, the details that were considered in the development of the numerical solution are important factors.

In order to solve the equations 3.15 to 3.17 it was necessary to formulate a model for the transfer of stress from fluid to grains. A possible model for the transfer of shear from fluid to grains was formulated and verified based on physical reasoning. To investigate the transfer mechanism of shear stress from fluid to grains it was hypothesized that the transfer of shear stress to be proportional to (or function of) the grain shear stress and linear concentration, λ. Thus, the following expression was used,

$$\frac{d\tau_s}{dy} = A \ln\left(\frac{\tau_s}{\tau_T}\lambda\right) + B \tag{3.45}$$

where $A = 650 N/m^3$, $B = 280 N/m^3$, τ_s and τ_T are in N/m^2, and y is in m.

By using Eq. 3.45, τ_s was generated starting the computation from the bottom boundary with known value, i.e $\tau_s = \tau_T$. The grain shear stress generated by the Eq. 3.45 and the one obtained by integrating, Eq. 3.16, are shown in Fig. 3.12. There is a good agreement between the two solutions for all cases, except for the uniform grain concentration.

3.6   Conclusions

Two governing equations were utilized to define the carpet flow phenomenon. But, three unknowns were involved in the equations. To obtain a closed formed solution, any one of the following have to be known before hand: grain velocity, grain or fluid shear stress, or grain concentration profile. The assumption of a linear concentration profile gave good results which agree reasonably with measurements. Further analysis established a relationship for shear stress transfer from fluids to grains.

In addition, simplified mathematical solutions were obtained for the specified boundary conditions. These solutions were approximate because simplified concentration profiles were considered and an assumption of inertial behaviour was made for the grain flows within a carpet layer. The numerical analysis has shown that such a condition does not hold for all cases.

This new analysis of carpet flow presented in this chapter takes into consideration the slip velocity between the fluid and grains, because, for the shear stress to be transferred from the fluid to the grains, there has to be a slip velocity between the two. Also within the carpet depth, the ratio between the inertia stress and viscous stress is not constant. The ratio between the two stresses determines the condition of the stress-stress relationship of the grains. Bagnold identified three regions: the macro-viscous, grain-inertia and transitional depending on the ratio

between the inertia and viscous stresses. The present analysis takes into account which part of the flow is governed by grain-inertia, transitional and viscous stresses. It was found that the viscous stress region was limited and there was significant region where the inertia and transitional stress was important.

Power transfer from the main body of fluid to the sediments occurs in two ways. The first is between the main body of fluid and the carpet as a whole; and the second is between the fluid within the carpet and the moving grains.

Close to 20 % of the power available in the main body of flow is absorbed by the carpet in contrast to Bagnold's (1966) result of close to one-third. The efficiency of power transfer from the fluid within the carpet to the moving sediments is close to 25 % which is almost the same as given by Bagnold (1966). Therefore, taking the product of these two efficiencies, close to 5% of the total power available would be utilized in moving sediments as intense bedload. This value was estimated by Bagnold to be close to 11 %. The difference between the two values is because: 1) Bagnold modeled the carpet layer as a mobile 'belt," where as in reality the carpet is a layer of dispersed grains; and 2) an approximate formulation was used by Bagnold in analyzing fluid and grain velocity profiles.

So far the analysis has been carried out for the plane bed uniform flow situation. In the next chapter the analysis will be extended to non-uniform flow.

In non-uniform flow, in addition to the boundary shear stress from fluid turbulence, pressure forces caused by the convective acceleration also act on the moving grains. Carpet flow analysis that incudes the additional pressure forces is discussed in Chapter 4. Calculations and

measurements will be presented which indicate a higher efficiency for the bedwave situation for which convective acceleration is important.

Table 3.1. Theoretical estimates of velocity, energy and efficiency values within the

carpet layer

Conc. profile	Avg. sed. vel. - $\overline{U}$ (m/s)	Avg. fluid vel. - $\overline{u}_f$ (m/s)	Energy dissp., sed. -ε_s (N/m-s)	Energy dissp., fluid - ε_f (N/m-s)	$\dfrac{\overline{u}_f}{\overline{U}}$	$e_s = \dfrac{\varepsilon_s}{(\varepsilon_s + \varepsilon_f)}$
Uniform	0.253	0.277	2.53	1.65	0.9	0.61
Linear	0.110	0.431	1.09	2.90	3.9	0.27
Non-linear	0.109	0.460	1.08	3.42	4.2	0.24

Table 3.2. Theoretical estimates of discharge, energy, bed slope, and efficiency values for a

range of Fr

Unit dis. q (m^2/s)	Y depth (m)	Ave. vel. $\overline{u}$ (m/s)	Steam-power ω (N/m-s)	Slope %	e_c %	Froude number
0.6	0.307	1.955	19.55	0.33	23	1.13
1.1	0.526	2.090	20.90	0.19	22	0.92
1.6	0.736	2.174	21.74	0.14	21	0.81
2.1	0.940	2.235	22.35	0.11	20	0.74
2.6	1.139	2.283	22.83	0.09	20	0.68
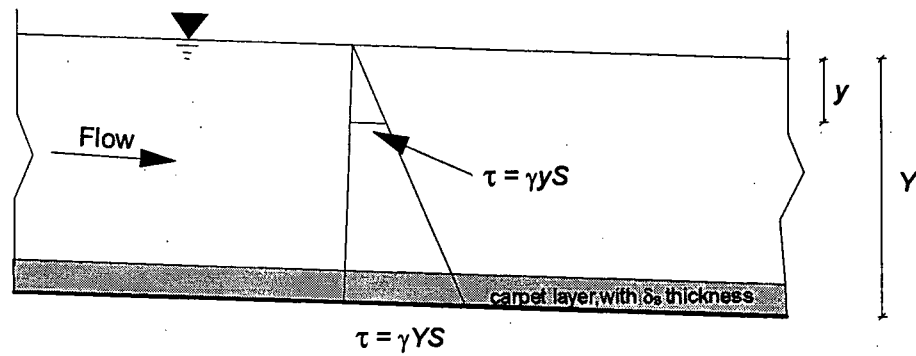
Figure 3.1. Shear stress distribution in open channel flow
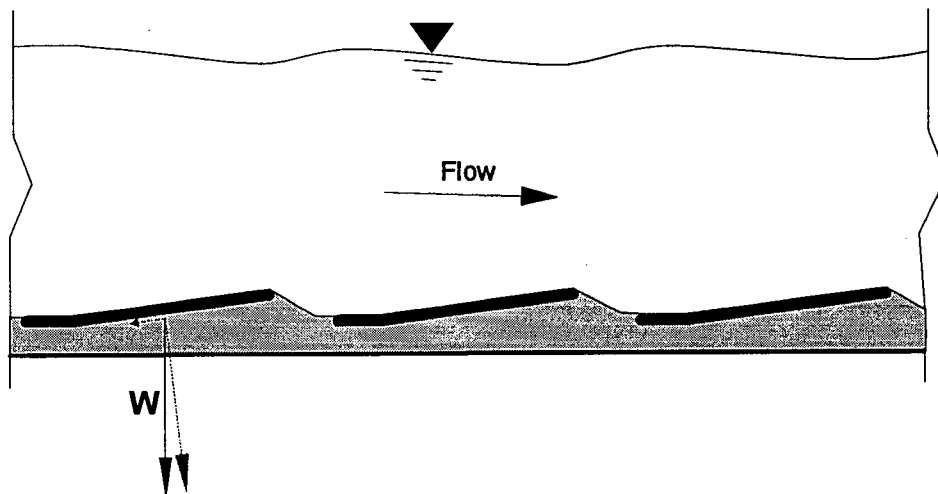
Figure 3.2. Weight component of grains in dunes
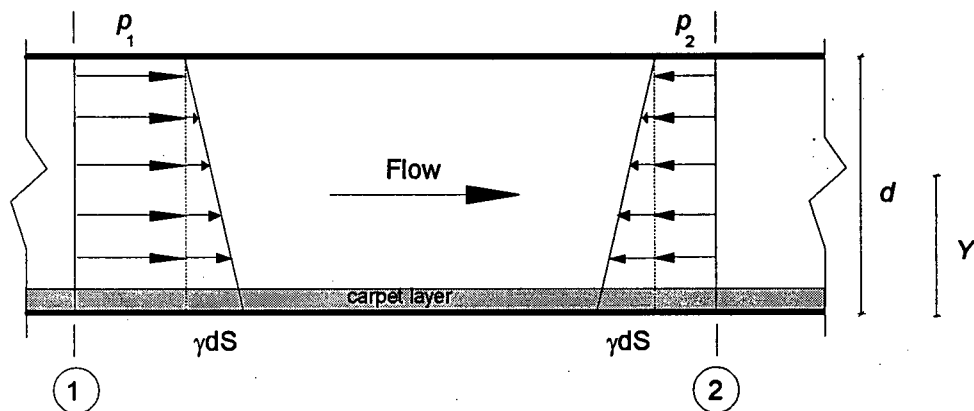
Figure 3.3. Pressure distribution for a closed-conduit flow
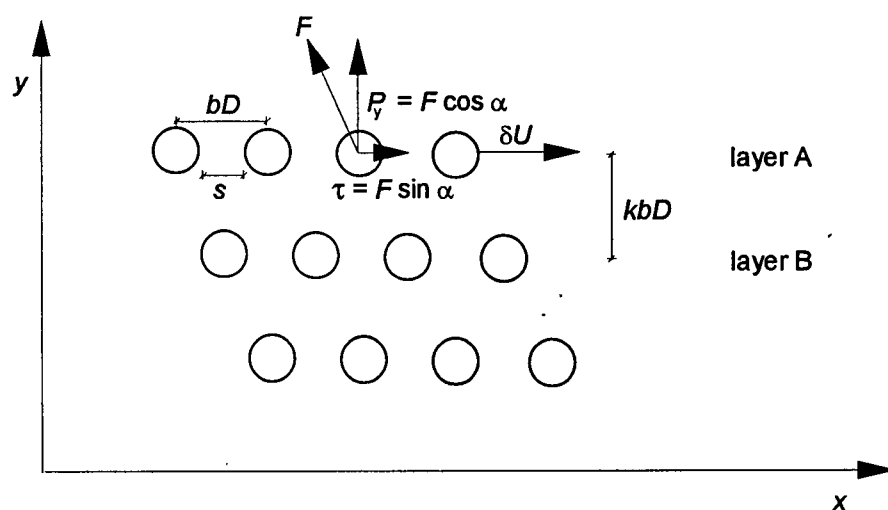
Figure 3.4. Dynamic dispersion of grains

a)

b)
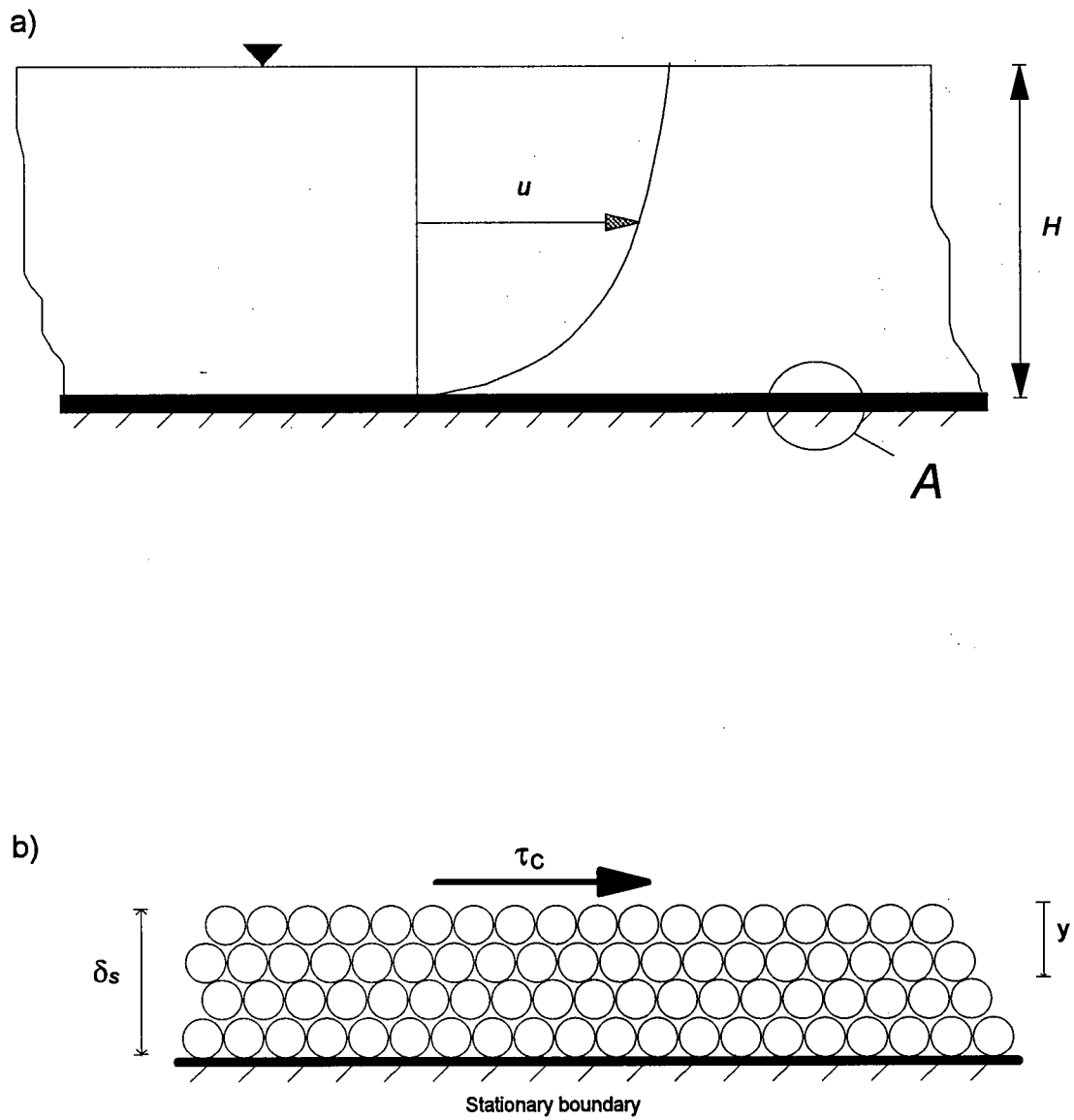
Figure 3.5. a) Open channel flow with a carpet layer; and
b) Detail A: Definition sketch for a carpet flow
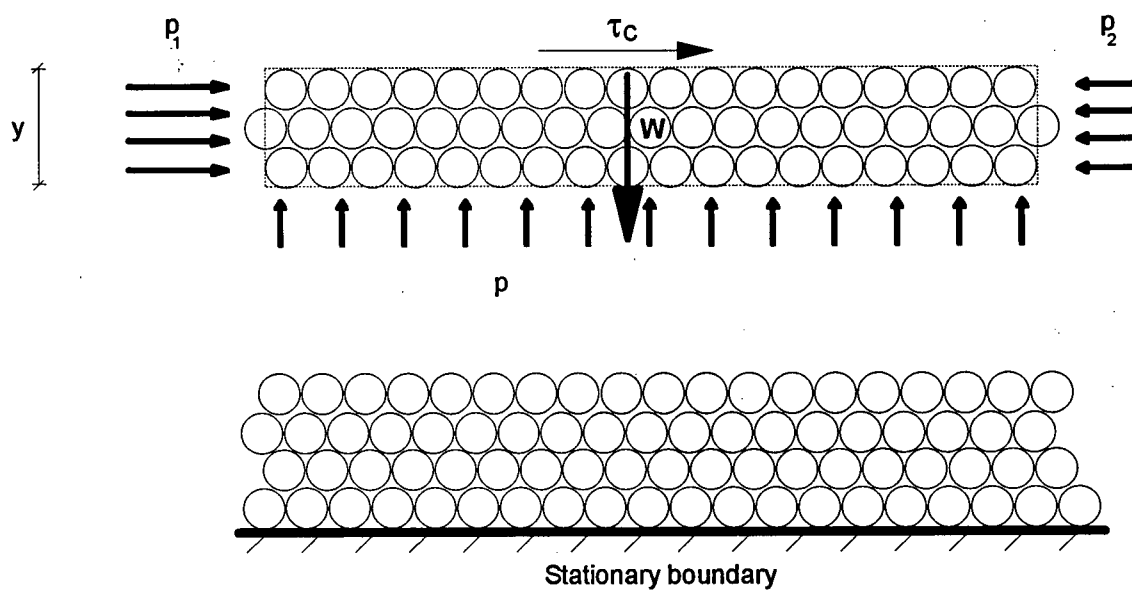
Figure 3.6. Free body diagram for the equilibrium of the vertical forces
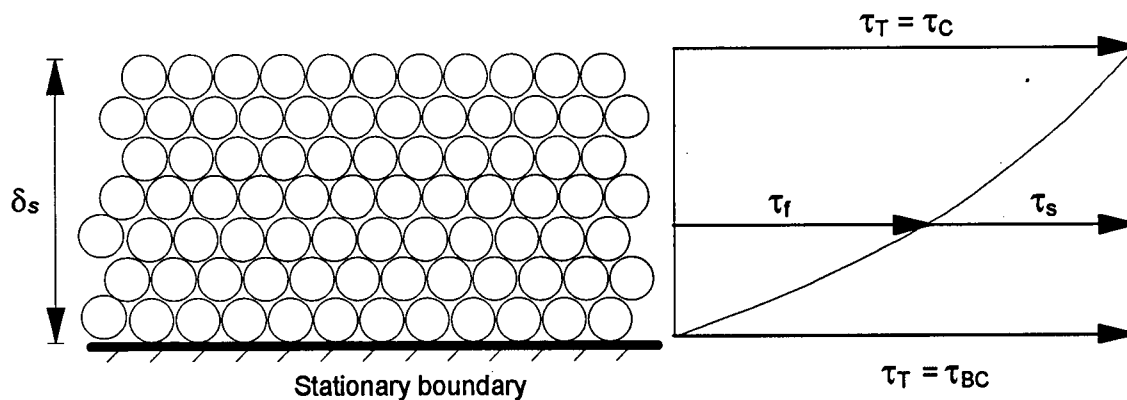
Figure 3.7. Shear transfer within a capret layer
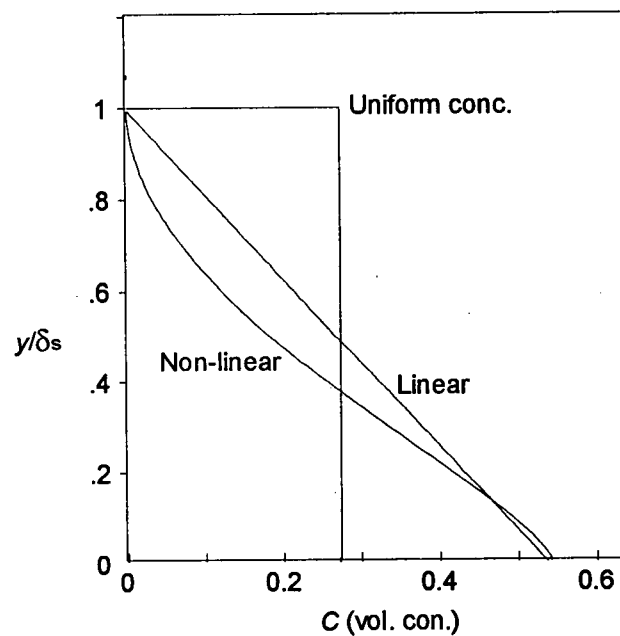
Figure 3.8. Assumed variation of grain concentration with relative depth
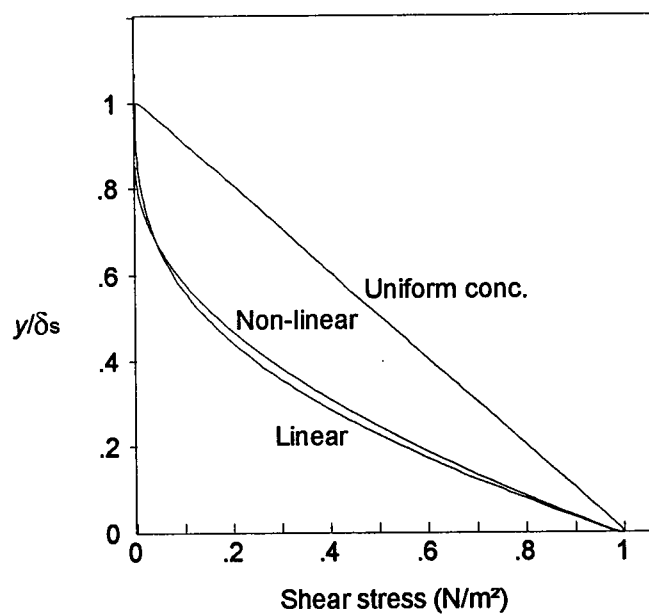
Figure 3.9. Computed variation of shear stress with relative depth
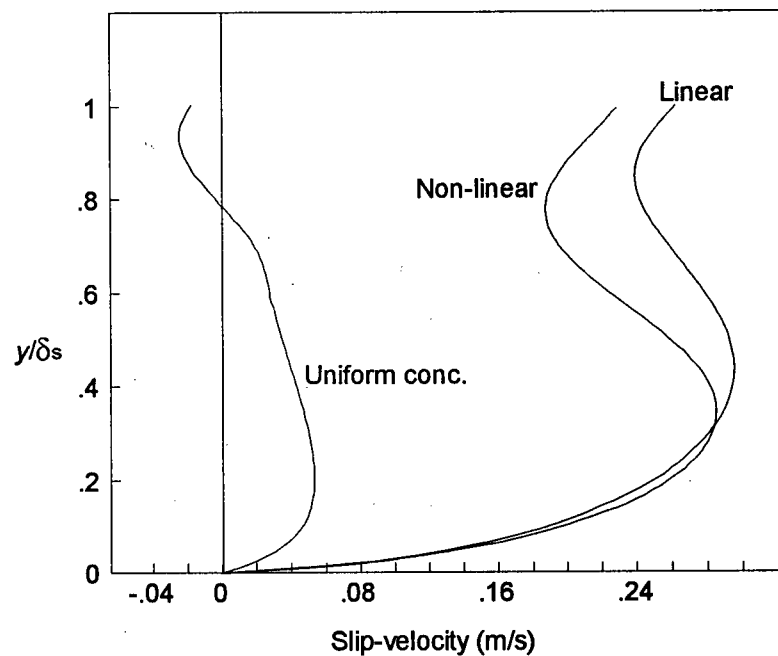
Figure 3.10. Computed variation of slip velocity (u-U) with relative depth
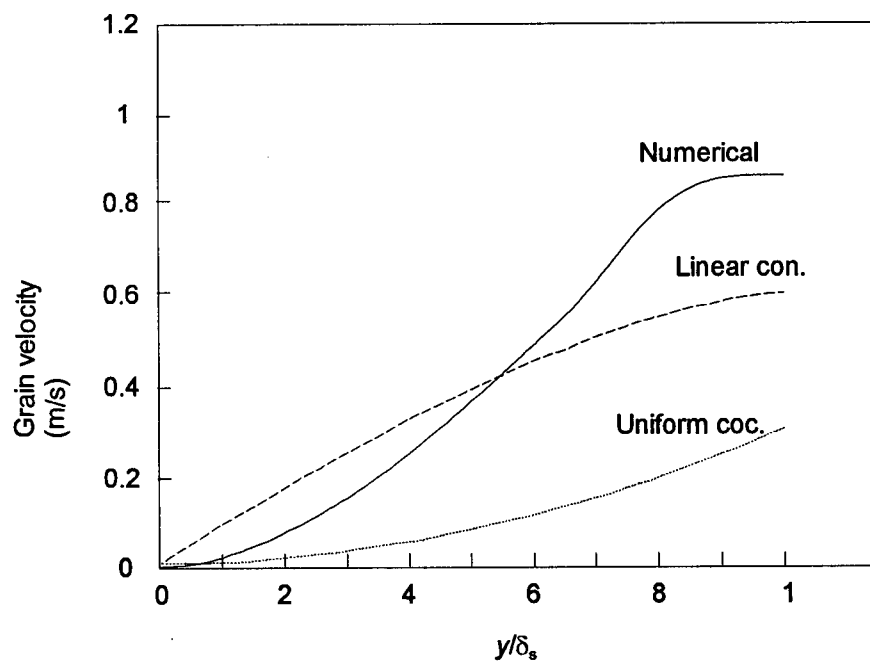
Figure 3.11. Comparision of simplified and numerical solutions

65
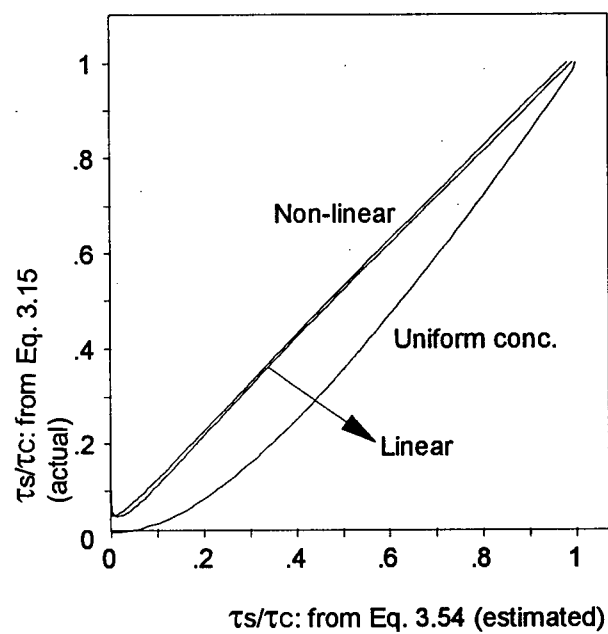
Figure 3.12. Variation of actual and estimated shear stresses with relative depth

CHAPTER 4

CONVECTIVE ACCELERATION AND CARPET FLOW ON BEDWAVES

4.1 Introduction

This chapter deals with the theoretical aspect of carpet flow under non-uniform flow condition, such as dunes and stationary waves. In the past carpet flow analysis had been carried out for a plane-bed condition where the fluid and carpet flows are uniform. Bagnold (1956, 1966) carried out carpet flow analysis by assuming that the shear stress exerted by the flowing fluid is transmitted to the carpet of moving grain and then ultimately down to the stationary bed. Similar analysis was also done by Hanes and Bowen (1985), Wang and Qian (1987), and Kinfu and Quick (1994). Wilson (1966), Nnadi and Wilson (1992) have made the same assumption that the shear stress from the fluids is transmitted through the *shear-layer* (as they called it) to the stationary interface.

The fundamental stress relationships within the carpet flow as defined in Chapter 3 must still apply to carpet flow under non-uniform flow conditions. In summary these conditions are as follows. At a particular level within the carpet, the total shear stress that is exerted by the flowing fluid on the top of a carpet is equal to the sum of shear stresses taken by the grains and the residual shear stress in the fluid. At the top interface of the carpet within the fluid, the grain shear stress is negligible, but it increases progressively towards the stationary bed, where the interlocking of the grains resists the total transferred shear stress. Reynolds (1885) indicated that a *dispersive pressure* exists when a layered group of spheres are subjected to a shearing

67

stress. Such an important concept was verified by Bagnold (1954) in his analysis of carpet flow. In addition, Bagnold showed that at a particular level within the carpet, the *dispersive pressure* exerted by the shearing of the grains has to balance the submerged overburden weight of the grains. But the analysis did not estimate the rate of transfer of the shear stress from the fluid to the grains, nor the kinematics of the moving grains. Detailed discussions are given in Chapters 2 and 3.

An inclined bed, or a bedform, introduces a non-uniformity in a flow. And under such a circumstance, a flow is bound to accelerate due to the constriction of the flow and hence convective acceleration occurs. Not only the shear stress due to frictional resistance plays an important role in defining the carpet flow, but also the associated pressure gradient due to the acceleration of flow caused by the configuration of a bedwave have an important significance.

The carpet flow analysis given in the previous chapter will now be extended to include the effect of convective acceleration under non-uniform flow.

4.2   Theoretical Development

4.2.1   Origin of carpet shear stress

The shear stress that causes the motion of intense bedload over a dune has its origins in two sources: Fluid shear stress and shear stress induced by the pressure gradient that is produced by a convective acceleration.

The fluid shear stress is generated within the fluid and is defined by the Reynolds stress. This stress at the interface of fluid and carpet is transferred into the carpet flow and is part of the tractive shear stress that disperses and moves the sediments.

In addition, the pressure gradient, which results from the convective acceleration that is produced as the flow is forced to accelerate on the stoss side of the dune, creates additional shear stress. This pressure gradient has two effects: 1) it increases the fluid shear stress due to the increased velocity gradient; and 2) it produces an additional direct stress on the carpet thickness, t. The pressure gradient is a Bernoulli effect which, in an ideal fluid, can occur without any energy loss. In reality, there will be some increased energy loss due to the increased shearing of the accelerated fluid flow. Moreover, there will be an expansion loss at the lee side of a dune where separation of flow occurs.

4.2.2 Transmission of shear stress in the carpet

Shear stress from the fluid, the Reynolds stress, is transmitted through the carpet layer to the stationary part of the dune beneath the carpet layer. The transmission of this shear stress introduces energy loss. The discussion of this inefficiency, or power dissipation, involved in the transmission of shear stress is given by Bagnold (1966) and is also outlined in Chapter 3 of this thesis.

In the presence of non uniform flow, a pressure gradient acts on the carpet thickness and has a similar effect to that of a buoyancy force that acts on immersed bodies. This pressure force requires no transmission by shearing of the flow and therefore is more efficient than the transmission of fluid shear stress. However, the transmission of pressure force results in causing

a shear stress in the carpet layer which is in balance with the required dispersive pressure which supplies the extra sediment flow induced by this extra stress. Therefore the additional pressure induced shearing causes an additional power dissipation within the carpet, exactly similar to the power dissipation calculated by Bagnold (1966) within the carpet, which he estimated to have an efficiency of 33 %. However, part of this pressure induced shear does not require a slip velocity between the fluid and the grains because it acts directly on the grains themselves.

Within the carpet layer there are both water and grains. Therefore, the pressure force accelerates both water and grains. The water accelerates more because of its lower mass, so that the pressure force induces an additional slip velocity between water and grains. The pressure force therefore accelerates the grains in two ways, by direct action which is very efficient, and by additional fluid shear induced by the faster moving water. The overall efficiency of these processes is very difficult and complex, but it can be seen to be more efficient than the effect of fluid shearing alone.

The pressure drop of a real-fluid flow in a converging flow comprises of two components: 1) due to frictional loss, and 2) the Bernoulli effect caused by the increase of flow velocity. But, the two components are not entirely independent. As the flow velocity increases in the flow direction, the boundary layer thins out and increases the shear stress on the boundary. This complex situation is automatically handled by a control volume analysis which will be presented in the next section.

The pressure drop due to frictional resistance is dependent on the development of the boundary layer, which is a function of flow velocity, geometry of flow, and the roughness of the boundary. The frictional resistance can be estimated from the turbulent Reynolds shear stresses,

from instantaneous velocity measurements or by using boundary layer relationships or, approximately, by utilizing the Moody diagram for an equivalent pipe flow.

The above discussion has implications on flow with mobile boundaries. For flows in closed conduits, the pressure at a given cross-section is essentially uniform. Therefore, the pressure gradient due to convective acceleration, along the direction of flow, is also felt at the mobile boundary and will have the tendency of moving the sediments in a fluid-like manner, producing an additional shear stress within the carpet which is finally resisted at the stationary interface. Therefore, the mobilization of the sediments at the bed is not only due to fluid induced tractive shear stress, but also to shear stress generated by the streamwise pressure gradient associated with the convective acceleration.

4.3   Dunes and Intense Bedload

4.3.1   Kinematics of dunes

Two-dimensional dunes move in progression along the direction of flow. This shifting of dunes' positions, or migration, is due to the movement and transportation of sediments. There have been different approaches to understanding and analyzing the origin and behaviors of dunes. Detailed discussion of those approaches is beyond the scope of this study, but the basic kinematics will be considered here. Fig. 4.1 gives the definition sketch.

The sediment continuity equation that relates the spatial variation of local sediment transport per unit width, q_s, to the rate of change of dune height, η, is given as follows:

71

$$\frac{\partial q_s}{\partial x} + \frac{\partial \eta}{\partial t} = 0 \tag{4.1}$$

For the sediment kinematics for dunes in such flows as a river or steady tidal flow, Quick (1978, 1982) defines four cases: 1) dunes developing from flat bed; 2) fully developed and steadily progressing waves; 3) steady standing waves and 4) regressive waves, such as antidunes. This theory is based on the kinematic wave theory given by Lighthill (1955), and sediment transport relationships which satisfy Eq. 4.1, and are dependent on the local bed-wave height, η; and initial value of sediment transport, q_{so}, as given below:

$$q_s = k\eta^n + q_{so} \tag{4.2}$$

where nk = the speed of wave propagation. Depending on the values of n and q_s, which also define the state of sand-waves, Eq. 4.2 takes different forms. For steady and progressive dunes, $n = 1$ and $q_{so} = 0$ (at point of flow reattachment). It can be shown that for such a case k is constant and is also the speed at which the dunes move.

For a progressive dune of constant dimensions, Eq. 4.2 reduces to:

$$q_s = k\eta \tag{4.3}$$

When the porosity of dune is considered, the above equation is modified as follows:

$$q_s = kC_o\eta \tag{4.4}$$

where C_0 = concentration of sediment of loose deposited sand, which accounts for the dune.

For the steady case, as shown on Fig. 4.2, where the bed-form is stationary, Eq. 4.1 reduces to:

$$\frac{\partial q_s}{\partial x} = 0 \tag{4.5}$$

which indicates that the rate of sediment transport is uniform along the direction of flow or sediment movement. The first experiment conducted corresponded to such a case and the validity of Eq. 4.5 was verified.

Alternatively, the sediment transport rate can be obtained from grain velocity and concentration measurements as follows:

$$q_s = \int_0^t U_s C \, dy \tag{4.6}$$

where U_s = velocity of sediments; t = thickness of carpet layer; C = average sediment concentration and y = coordinate in the vertical direction.

Eq. 4.6 may be rewritten in terms of the maximum grain velocity, U_{sm}, and maximum sediment concentration at the stationary bed, C_0. Based on the experimental measurements, both the velocity and concentration variation within the carpet layer has a profile close to linear. Therefore, a linear approximation of velocity and concentration will be used.

For linear velocity variation with depth we have,

$$U_s = U_{sm} \left(\frac{y}{t} \right) \tag{4.7}$$

where y = vertical coordinate measured from the stationary boundary.

And for linear concentration variation with depth we have,

$$C = \left[C_0 - C_0 \left(\frac{y}{t} \right) \right]$$ (4.8)

Thus, substituting Eqs. 4.7 and 4.8 into Eq. 4.6, we have:

$$q_s = \frac{C_0 U_{sm} t}{6}$$ (4.9)

The above result will be used for comparison with Eq. 4.4 that was derived from dune kinematics consideration.

4.4   Control Volume Analysis of Fluid and Carpet Flow

A control volume approach is used to relate the various shear stresses, pressures, and momentum flux terms involved in the dynamics of a carpet and fluid flow. This analysis is used to obtain the total shear stress that acts on the carpet layer, and also the application of the same principle to the carpet flow helps to explain the importance of the different terms and factors that are important for different flow conditions. Experimental results will be used to confirm some of the theoretical aspects of this study.

Figs. 4.3 and 4.4 show the general schematic diagrams for the control volume analysis, for a stationary bedwave and a dune, respectively. Fig. 4.5 gives the detail of the control volume *acdf* considered. The different forces involved and the velocity field are indicated.

The equilibrium of horizontal forces and momentum flux, between sections 1 and 3, for the control volume considered gives the following expression:

$$(\overline{p}_1 A_1 - \overline{p}_3 A_3) - \frac{(p_f + p_d)}{2}(A_1 - A_3) - \tau_{BC} P_b L \cos\theta - \tau_f P_s L = \rho \beta_3 u_3^2 A_3 - \beta_1 u_1^2 A_1 \quad (4.10)$$

$$\text{(I)} \qquad\qquad \text{(II)} \qquad\qquad \text{(III)} \qquad \text{(IV)} \qquad\qquad \text{(V)}$$

where $\overline{p}$ = average pressure on a cross-section; A = area of a cross-section; p = pressure at a specific point; P_b = perimeter of bed; P_s = perimeter of the smooth surface; L = length of reach; ρ = mass density of fluid; β = coefficient of momentum; $\overline{u}$ = average velocity along a cross-section and θ = slope of the stoss side of dune (practically $\cos\theta \approx 1$).

For Eq. 4.10, term (I) is related to the pressure force due to the drop in pressure; (II) is related the pressure force acting on the inclined surface of the control volume; (III) is the force acting at the stationary bed; (IV) is the net force acting on the smooth surface of the conduit; and (V) is the net momentum flux due to the acceleration of the flow. Term (V) does not include the change of sediment momentum flux, but this flux is small compared with total fluid momentum flux.

In the experiments to be described later, all terms of Eq. 4.10 will be measured directly except for τ_{BC}, which will be calculated. Alternatively, the boundary shear stress may be obtained by estimating the weight of sediment supported by the dispersive pressure. The shearing of grains produces an upward dispersive pressure that supports the weight of the moving sediments, so that the shear stress and the dispersive pressure are interrelated by the internal angle of friction. Therefore, considering the equilibrium condition at the stationary interface, where the moving sediments within the carpet layer cease to move, the following expression may be obtained:

$$\tau_{BC} = \rho g (S_s - 1) \overline{C}_r C_b \delta_s \tan \phi' \cos \theta \tag{4.11}$$

where ρ = density of fluid; g = acceleration due to gravity; S_s = specific gravity of grains; ϕ' = internal angle of dynamic friction ($\cong 32°$); $\overline{C}_r$ = a factor for averaging the grain concentration (0.4); C_b = grain concentration at the bed (0.54, where interlocking of grains occurs); and δ_s = thickness of carpet layer. Eq. 4.11 will be used to give another estimate of τ_{BC} and will be compared with the estimate from Eq. 4.10.

4.4.1 Convective pressure gradient

The measured pressure gradient due to the convective acceleration can be verified by checking against the maximum velocities of a flow. For a conduit flow, maximum velocity occurs usually at or close to the center of flow depth, where the velocity gradient is negligible. Therefore, the shear stress values are negligible at this point of zero velocity gradient so that the Bernoulli equation can be applied.

Because p_1 and p_3 are measured from the common datum of the top of the conduit, as shown on Fig. 4.3, the remaining pressure plus elevation term for each section is the same and cancels out leaving the following:

$$\frac{p_1 - p_3}{\gamma} = \frac{u_{max3}^2 - u_{max1}^2}{2g} \tag{4.12}$$

where p = pressure measured at a given cross-section; γ = specific weight of fluid; u_{max} = maximum velocity; and g = acceleration due to gravity.

Because this region of the flow is free from viscous shearing, the pressure change calculated from Eq. 4.12 can be used directly in Eq. 4.10 and will be used in the analysis of the experimental results in Chapter 6.

4.4.2 Momentum consideration within the shear layer

The momentum equation for intense sediment transport, both under uniform and non-uniform flow, quasi-steady and stationary bedwave movement is derived and discussed in this section.

A differential approach may be used to show the different components that are involved in contributing to the driving force that moves a carpet layer of sediments. Fig. 4.6 shows the general dune profile with an intense bedload movement at the interface of the main flow and dune. Fig. 4.7 shows the schematic diagram of the control volume of the carpet layer, $a'b'c'd'$. For a unit width and for a quasi-steady process, the conservation of momentum gives:

$$pt + (p + \delta p/2)\delta t - (p + \delta p)(t + \delta t) + (\tau_c - \tau_{BC})\cos\theta\,\delta x$$
$$= \rho_m (q_m + \delta q_m)(U_m + \delta U_m) - \rho_m q_m U_m \tag{4.13}$$

where p = pressure (taken at the top of a dune) and is assumed constant across the depth of the carpet because the carpet is thin.

After neglecting second order terms and applying the approximation $\cos\theta \approx 1$, Eq. 4.13 reduces to:

$$-t\delta p + (\tau_c - \tau_{BC})\delta x = \rho_m q_m \delta U_m + \rho_m \delta q_m U_m \tag{4.14}$$

77

Dividing both sides of the above equation by dx, and rearranging,

$$\tau_{BC} = \tau_C - t\frac{dp}{dx} - \rho_m q_m \frac{dU_m}{dx} - \rho_m U_m \frac{dq_m}{dx}$$

$$\qquad \text{I} \qquad \text{II} \qquad \text{III} \qquad \text{IV}$$

(4.15)

The above equation shows that the boundary shear stress, τ_{BC}, is derived from four components: (I) is the fluid induced shear stress from the main stream of flow above a dune, τ_C; (II) is the pressure gradient acting on the thickness of the carpet, always a positive contribution since pressure gradient in a contracting flow is negative; (III) is the rate of change of momentum in the flow direction; and (IV) is related to the entrainment of sediment from a dune.

It should be noted that the pressure gradient in Eq. 4.15 is produced by: 1) frictional resistance and 2) convective acceleration due to the bedform. The pressure drop between two sections is the sum total of the frictional pressure drop and the kinetic energy change based on the mean velocity. Alternatively, this pressure drop can be estimated from Eq. 4.12.

Eq. 4.15 is applicable to the general case of a non-uniform flow of water over a non-uniform flow of sediment. Special cases with practical significance may be identified as follows:

4.4.2.1 Stationary bedform

For a stationary bedwave, the sediment transport is constant along the bedwave, as is discussed later in this chapter where details concerning sediment continuity and the effect of sediment concentration on a bedwave are given.

Therefore for this stationary bedform situation, $dq_s/dx = 0$ and $dU_s/dx = 0$ as derived in kinematic section 4.3.1 and is given by Eq. 4.5. However, the water flow is non-uniform, so that the bedform induces a convective acceleration on the flow which in turn produces a pressure gradient. For such a case, Eq. 4.15 simplifies as follows:

$$\tau_{BC} = \tau_C - \delta_s \frac{dp}{dx} \qquad (4.16)$$

where δ_s = thickness of the carpet layer above the stationary bedform. As Eq. 4.16 indicates, the additional driving force for the sediments, apart form the fluid induced shear stress, is the total pressure gradient, dp/dx.

4.4.2.2   Open channel flow in the upper flow regime

For open channel flow in which the shear stress is high enough to wash away bedforms, the water and sediments flows are uniform. Under such a condition, there is no pressure gradient along the direction of flow, for the depth of flow is uniform. The driving force for the sediments is effectively the fluid induced shear stress at the mobile boundary and a small gravitational body force along the channel slope. For this case, provided the thickness of the carpet is negligible compared to the hydraulic radius of a conduit, Eq. 4.15 becomes, as assumed by Bagnold (1966),

$$\tau_{BC} = \tau_C \qquad (4.17)$$

4.4.2.3   **Effect of suspended load**

In Eq. 4.15 the last two terms on the right hand side are related to the entrainment of sediment from the dune surface. The boundary shear stress and the mean velocity increases towards the crest of a dune, with the effect of increasing the rate of sediment transport. This entrainment of sediment draws momentum from the flow. But when a suspended load exists and settles to join the carpet layer from the main body of flow, it introduces an additional momentum flux. Since suspended load has a higher velocity of flow compared to bedload, the influx of suspended load to the bedload gives an additional momentum to the carpet which can entrain more sediments as bedload. For the present experiments there was negligible suspended load.

4.5   Carpet Flow with Pressure Gradient

Carpet flow analysis for a plane bed and uniform flow is given in Chapter 3. This section builds on the analysis given in Chapter 3 and includes the additional forces due to pressure gradient created by a convective acceleration.

As discussed in section 4.3.2, a negative pressure gradient is induced by friction in a closed conduit or by non-uniform convective acceleration in either a closed conduit or an open channel. This pressure gradient creates an additional force on the carpet layer and acts directly on the sediment to produce a pressure force which increases the momentum of the moving particles, which, in turn, produces an additional shear stress within the sediment carpet, as expressed by term II in Eq. 4.15.

As explained earlier, the effect of this pressure gradient is similar to a buoyancy force for submerged objects. Therefore, the total pressure force is equivalent to the product of the pressure gradient along the direction of flow and the volume of sediments. Pressure forces on sediments are balanced by the shearing stresses. At a given level, y, from the top boundary, the shear stress due to pressure forces can be written as follows:

$$\tau_p = \frac{dp}{dx}\frac{C}{2}y \qquad (4.18)$$

where τ_p = shear stress due to pressure forces. In the above equation, the volume of sediments is obtained by taking the average concentration value, $C/2$.

Because this pressure force is directly proportional to the sediment concentration, Eq. 3.16, the induced shear stress is exactly proportional to the required upwards supporting stress necessary to allow the sediment to move. Therefore, Eq. 3.15 can be extended directly to include the pressure induced shear at the left hand side.

Therefore, combining the shear stress, τ_p, from Eq. 4.18, and the fluid induced shear stress on sediments, τ_{cs}, and equating with, τ, of Eq. 3.16, we have,

$$\tau = \tau_{cs} + \frac{dp}{dx}\frac{C}{2}y = \rho g(s_s - 1)\tan\phi\int_0^y C dy \qquad (4.19)$$

This equation will be used later in the analysis of carpet motion under pressure gradient.

4.6   Summary

This chapter considered the additional shear stress induced on a mobile boundary due to convective acceleration created by bedwaves.

Sediment bedwave kinematics was examined. For the stationary bedwave, the analysis shows that the sediment transport rate is constant and does not vary along the sloping wave. For a moving sediment bedwave of constant geometry, the analysis shows that the sediment transport rate increases linearly with bedwave height. Also for the moving bedwave, the sediment transport rate is equal to the dune height multiplied by the dune speed.

A control volume analysis of the flow shows the role of various force components and shows that the boundary shear stress can be calculated from pressure and velocity measurements. A control volume analysis of the carpet layer shows that in non-uniform flow the shear stress at the bottom of the carpet is greater than the fluid shear at the top of the carpet because of the effect of pressure gradient and sediment flux.

The effect of a pressure gradient on the sediment was investigated, showing that this pressure gradient is an efficient process for the transfer of stress to the particles, requiring no slip velocity.

These concepts and equations will be applied to the analysis of the experimental results.
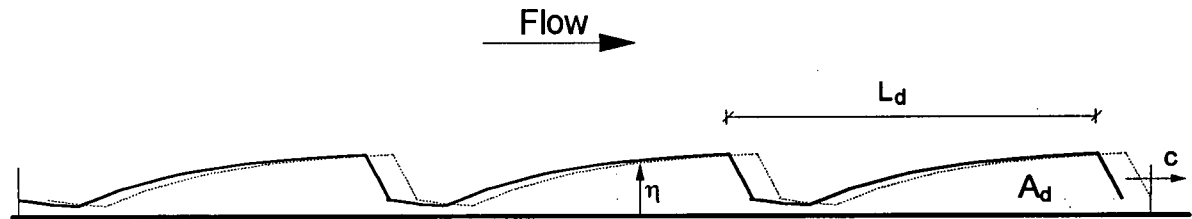
Figure 4.1. Definition sketch for a progressive constant shape sand wave
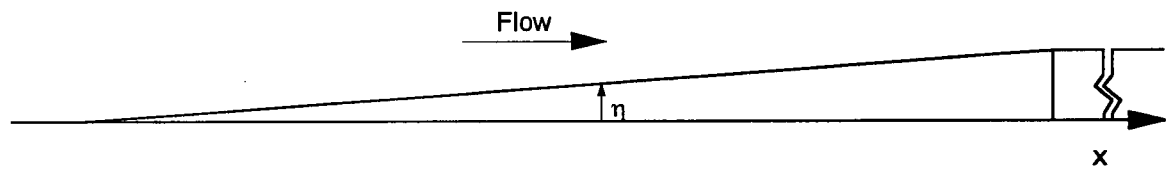
Figure 4.2. Definition sketch for a steady standing sand wave
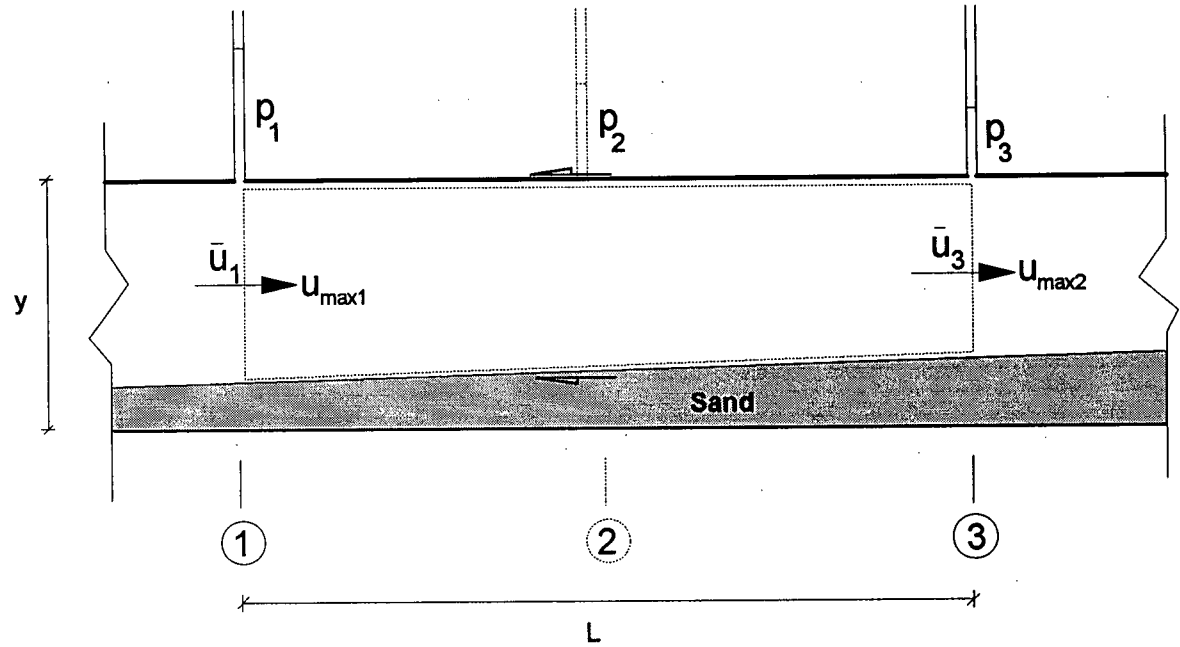
Figure 4.3. Schematic diagram of an inclined bedform
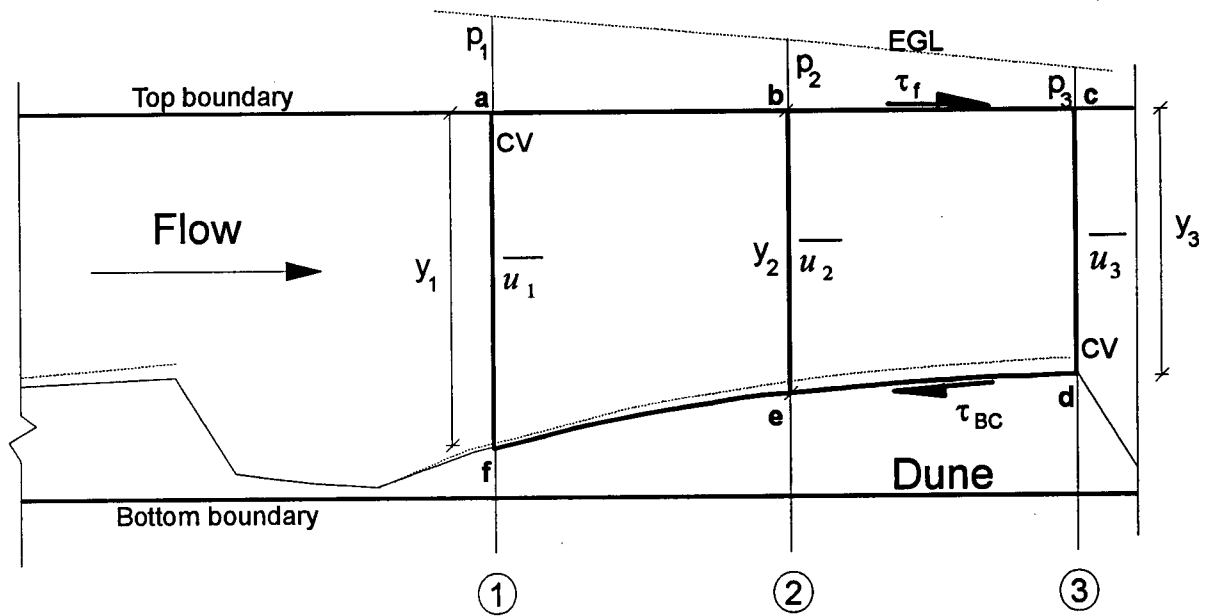
Figure 4.4. Schematic diagram for control volume over a dune
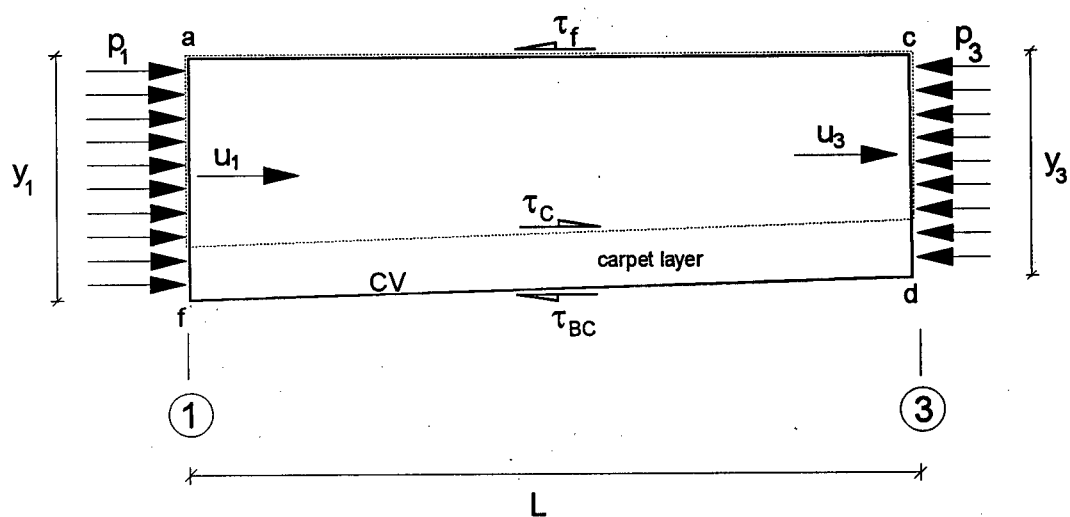
Figure 4.5. Control volume at the test section
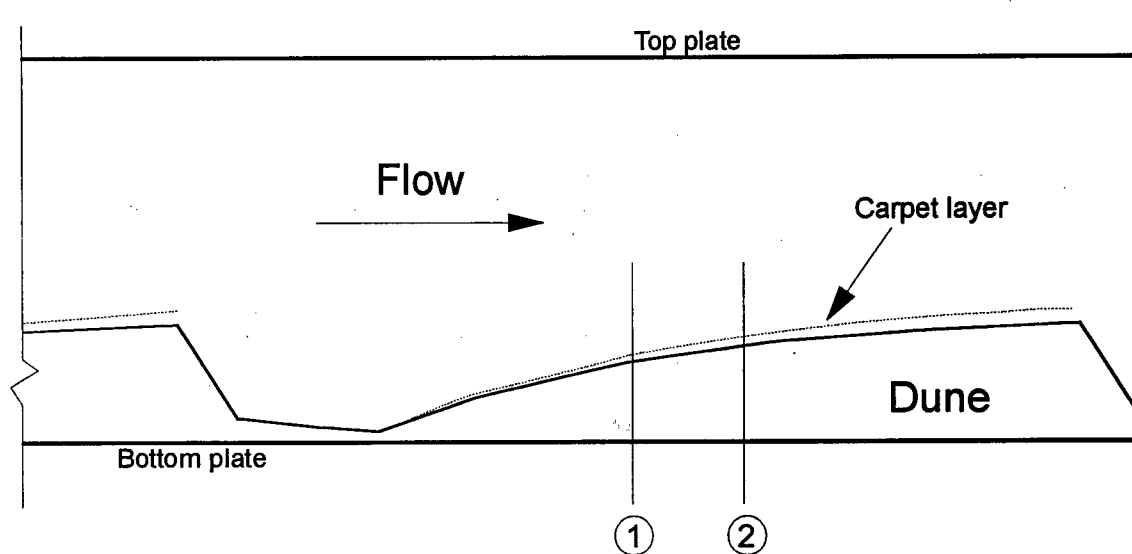
Figure 4.6. Schematic diagram of a dune in a closed conduit
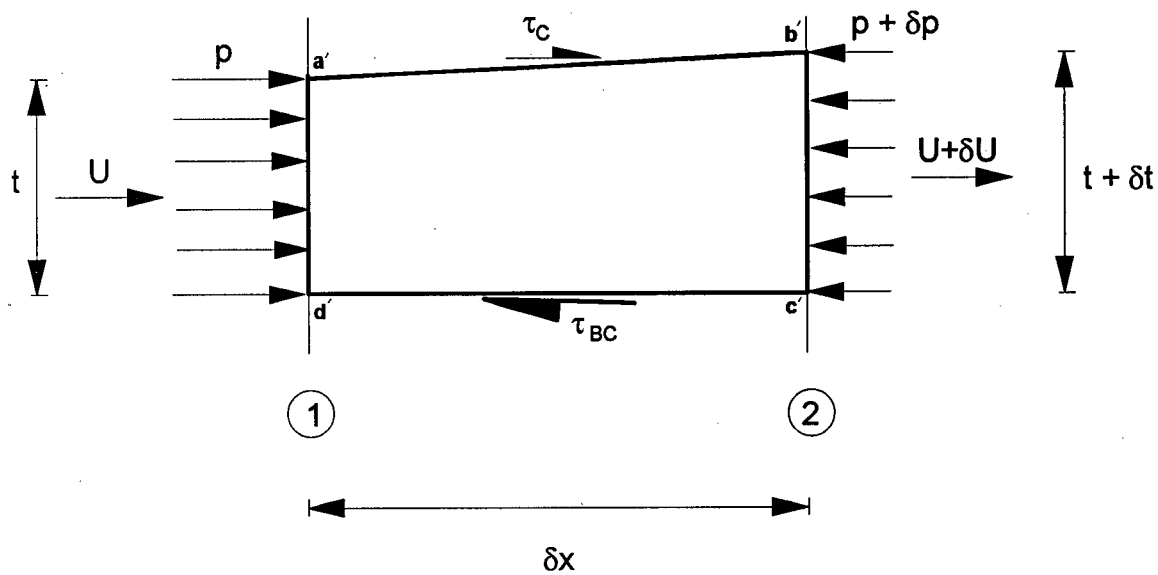
Figure 4.7. Elemental volume within carpet layer for the differential approach

CHAPTER 5

EXPERIMENTAL WORK

5.1   Introduction

The intention is to carry out experiments to check the theoretical relationships developed in Chapters 3 and 4. These experiments are for high bedload under non-uniform flow conditions produced by an adverse bed slope, and provide data to investigate the transfer of shear stress from the water flow to the moving sediment grains. The primary interest is to achieve a better understanding of intense bedload transport in an open channel with low bed slope and high depth, which combine to give a high shear stress, but little body force, or weight component, of the sediment in the flow direction. This flow induced transport is quite different to steep channel debris flows, where the streamwise body force of sediment and water mixture combine to drive the flow.

The high shear stress produced by the combination of low bed slope and high depth in the open channel situation cannot be modeled in the laboratory because of flow and size restrictions. Therefore, it was decided to use a closed conduit in which a pressure gradient could be used to create a high shear stress, but with zero bed slope. This method is not an exact model of the open channel situation, because it introduces a friction induced pressure gradient which is not present in a uniform open channel flow, and this is discussed fully in the theory sections, Chapters 3 and 4. Although the open channel case is free of pressure gradient, there is a body

force component due to the channel slope which has a slightly different effect than a pressure gradient. Details are given in Chapter 3.

In order to verify the theoretical/analytical model of grain motions in a flowing fluid (within the carpet thickness), it was necessary to make velocity measurements of the fluid and grains, and also the concentration profile of grains. The measurement of fluid velocity was carried out by using ADV (Acoustic Doppler Velocimeter), and not only was it possible to measure the fluid velocities, but also shear-stress variation within the fluid depth could be calculated from the turbulence measurements. The measurement of grain velocities and concentrations were made by employing a high speed camera and image processing software. The pressure variation within and across the test section was carried out by using piezometers and pressure transducers. The details of the experimental technique will be discussed in sections 5.4, 5.5 and 5.6.

5.2   Objectives of the Experiment

The aim of the these experiments was to measure the major factors involved in the carpet flow process so that the theoretical ideas presented in the previous chapters could be investigated experimentally. These factors are:

1. **A study of the fluid flow properties which are responsible for creating the carpet flow**
   These properties are:
   a) the pressure gradient;
   b) the flow velocity profile;
   c) the turbulent structure of the flow.

From these measurements, the flow rate, the Reynolds shear stresses, $\overline{\rho u'v'}$, and the boundary shear stresses were calculated.

2. A study of a carpet flow properties:

   a) the thickness of the carpet flow;

   b) the concentration of sediment grains in the carpet and the change of concentration with carpet depth;

   c) the velocity and direction of the carpet grains;

   d) the variation of carpet behavior in the flow direction;

5.3   Experimental Set-up

The experimental apparatus consists of a closed conduit loop, a pump capable of handling a sediment-water mixture, and a pump speed controller. This closed conduit is a closed sediment-water mixture re-circulating system. Sediment is fed into the system before the commencement of each experiment. For the experimental work, a fairly rounded filter sand was used which was closely graded between sieve sizes of 0.85 and 1.1 mm, giving it a mean size of about 1 mm.

5.3.1   Re-circulating conduit

In designing the system, the shear stress requirements for the given sediment size were estimated. Thus, based on economic considerations, which determined power and pump capacity, a suitable flow and pipe size was determined.

The test section was made of *Plexiglas*. It was 7.58 m long, 0.23 m wide and 0.2 m deep. It was found necessary to have a sufficient length of test section so that the boundary layer becomes fully developed. At the entrance to the test section, a 0.74 m long diffuser was installed to effect a smooth transition between the pipe and the rectangular section. There was a similar arrangement at the outlet end of the test section which converges so that the flow negotiates the transition smoothly from a rectangular to a circular section. Elbows with large radius-of-curvature were used to minimize frictional losses.

The lower section of the conduit and the rising and falling limbs were PVC pipes of 6 inch diameter, and the rising and falling limbs were 10 meters in length. The intention of the long vertical lengths was to measure the pressure drops in these legs in order to estimate the sediment transport rate. Additional length was also necessary to smooth the flow beyond bends and the pump delivery. Such a method was suggested and used by Einstein and Graf (1966), and Acaroglu and Graf (1968), among others. Measurements of the pressure drop along the rising and falling limbs of the conduit were made using pressure transducers.

The first set of experiments were carried out with a lesser test section length of 5.0 m. To give greater entry length for establishing the test flow conditions, this test section was increased to 7.58 m and the tests were repeated. The increased length gave similar dune behavior and therefore the entry length was considered satisfactory for both the 5.0 m and 7.28 m lengths.

5.3.2 Pump system and control

As indicated in Fig. 5.1, the sediment-water mixture was circulated using a centrifugal pump (*Weinman model 5G-4A-00P146*). The pump was driven by a 7.5 horsepower electric motor.

The pump was of cast iron construction with bronze casing wear ring, and graphite impregnated tephlon packing, with lantern rings and external flushing. The supply and delivery pipes were 6 inches in diameter. Valves were not installed to regulate the amount of discharge. Instead, the pump was controlled with a variable frequency drive to regulate the speed of the electric motor. The pump capacity and head-discharge characteristic was selected based on the design requirements of the experiments, namely the necessary discharge to mobilize the bed into a carpet mode, and the estimated frictional head losses throughout the system.

5.4 Flow Velocity Measurement Using ADV

5.4.1 General outline

The velocity measurement of flow was made by using a down-looking 3D acoustic Doppler velocimeter (ADV). The system consists of a probe; signal conditioning module; a high-frequency cable; and a processor. Fig. 5.2 shows the various components of the system. The probe has three receiver-arms attached to a stem which contains the transmitter. The three receiver arms are placed at 120° as shown in Fig. 5.3, a schematic diagram of the probe. The angle between the transmitter stem, the sampling volume and each receiver arms is 30°. The sampling volume is a vertical cylinder of 6 mm diameter. The height of the sampling cylinder can be made either 3 or 9 mm depending on the need. The sampling volume is located at 5 - 6 cm away from the transmitter-transducer.

Due to the high velocity of flow, which causes an intense vortex wake to be shed from the stem, the probe experienced high vibration. Therefore the initial turbulence measurements were erroneous because the movement of the probe due to vibration was superposed on the

turbulent velocity fluctuations. This difficulty was circumvented by attaching a streamlined sleeve to the stem. Such an arrangement reduced the vibration significantly so that reasonable velocity measurement was possible.

5.4.2   Operation technique

In brief summary, the acoustic doppler operation was as follows. The transmitter-transducer produces short period acoustic pulses of known frequency, in the vertical direction. The echo from ambient scatterers such us suspended sediments and seeding material within the sampling volume is received by the three receiver-transducers. The frequency of the echo is Doppler-shifted depending on the motion of the scatterers and it is assumed that the scatterers travel at the same velocity as the fluid they are suspended in. The signal received from the scatterers is amplified in the conditioning module and is then digitized and analyzed in the processing board, which is connected to a standard PC with a 386-processor for real-time plotting and data logging. The orthogonal components of the flow velocity are obtained from the geometry of the transmitted and received beams. Velocity measurements and associated values are then displayed on the screen on a real-time basis. The interfacing software provides menus to change the range of velocity, sampling time, sampling frequency, and other variables. All the real-time measurements were logged on a computer hard-drive for further data analysis.

5.4.3   Operation range

The ADV can measure velocities up to 300 cm/s, but for the present experiments more accurate and precise measurements were obtained by setting the maximum range to 250 cm/s. The measurement resolution is 0.1 mm/s over the velocity measurement range of 0 to 250

cm/s. An accuracy better than ± 0.25% or ± 0.25 cm/s, whichever is greater, can be obtained. The frequency of the signal, which in effect is the frequency of sampling, can be varied up to 25 Hz. In order to obtain refined data, and also, for more precise turbulence measurement, the maximum sampling frequency was used.

The closest the center of the sampling volume can get to the boundary is either 1.5 mm or 4.5 mm for the sampling cylinder heights of 3 mm and 9 mm, respectively. Except at the boundaries, where small sized sampling volume is desirable to get more representative measurements, the use of the small sized sampling volume is not recommended because of a loss of accuracy.

Since measurements employing the ADV were made in a sediment laden flow, it was not found necessary to add seeding to increase the strength of the echo/scatter. The strength of the echo is quantified in terms of a "signal-to-noise ratio" (SNR), expressed in dB. During the experiments the SNR was above 20 dB, the recommended value required to obtain accurate measurement.

5.4.4   Measurement procedure

For insertion of the ADV probe, several access holes, 15 cm in diameter, were cut in the top portion of the test section. PVC pipes of 3 inch were installed, as shown in Fig. 5.4. The height of the pipes was chosen so that the water level is below the rim. Fig. 5.5 gives the detail. In order to move the probe freely, i.e. in the vertical direction, the ADV signal conditioning module-casing was inserted and attached to a PVC pipe sleeve. The outer diameter of the pipe-sleeve was slightly less than the inner diameter of the installed pipe, and such an arrangement

allowed the movement of the sleeve within the installed pipe. Once the probe was located at a desired location, the sleeve was clamped to the installed vertical pipe with a screw threaded through the thickness of the installed pipe and bearing against the outer wall of the sleeve.

The provision of the stand pipes also allowed the measurement of flow velocities near the top boundary. In such cases, the probe was physically outside the flow, but the sampling volume remained within the flow.

As a first step in making measurements, the probe had to be oriented properly so that the horizontal velocity measurement direction matches with the direction of flow. This was done by adjusting the probe until minimum readings were obtained for the vertical and transverse velocity measurements at a low longitudinal flow. Once the orientation of the probe was completed, the distance of the sampling volume to the bottom *Plexiglas* boundary was ascertained. Since the *Plexiglas* bottom plate of the conduit gets covered with sediment under running conditions, the relative distance between the bottom boundary and the sampling volume was determined first with no sediment present.

5.4.5   Velocity measurements

For all the measurements, a minimum of 30 seconds of recording, at 25 Hz, was allowed in order to get a reliable average for the velocity and shear stresses and also to exceed the time scales of flow fluctuations involved in turbulent flow. Figs. 5.6 and 5.7 show the instantaneous horizontal velocities and the values of the moving averages. As indicated in the figures, the average values after 30 seconds are reasonably stable. Moreover, sufficient data to estimate the

different scales of turbulence is also captured. The figures also show that during the recording time span, the flow was similar and can be considered "quasi-steady".

5.5   Grain Velocity and Concentration

5.5.1   General

Grain velocity and concentration within the moving carpet layer was measured by using a high-speed camera and motion analyzer, Kodak, *EktaPro 1000, Motion Analyzer*. The system consisted of a camera, spot lights, connecting cable, motion analyzer, cassette conditioner and a monitor. For the experimental carpet flow conditions, the positions of spot lights and the camera were adjusted to obtain a clear and sharp image on the monitor. In order to freeze the motion of the grains and also facilitate easy tracking of individual particles within a carpet layer, the speed of the camera exposure was set at 1000 frames/second. Because of the high velocity of the moving grains, it was only necessary to run the camera for a few seconds to capture an adequate set of data.

Recording of the particles' movement was only possible at the side wall. Observation of the dune motion showed that the dune crest had a uniform height across the flume and the dune crest was almost straight, indicating that sediment motion was essentially uniform across the flow, even near the wall. Therefore it was considered reasonable to assume that such measurements at the side wall are reasonably representative of the dune motion.

5.5.2   Grain velocity measurement

The images recorded by the motion analyzer on a specialized magnetic tape were transferred on to a high resolution VCR video-tape so that the images are digitized and transferred to a PC for further image-processing. *Imager*, version 1.57, an image processing software from NIH (National Health Institute, USA), was used both to capture frames from a VCR video-tape and also for the actual processing. Each time, close to ten frames were selected which had time spacing of one-thousandth of a second. For each frame displayed on the screen, the coordinate system was kept the same so that each image was compared under the same reference. The horizontal and vertical scales were obtained from a known measurement that was included during recording. At a given level, the velocity of a particular grain was determined by comparing its horizontal and vertical positions in two different frames of known time spacing.

5.5.2.1   Verification of method

In order to verify the accuracy and also the repeatability of the technique applied, different measurements were analyzed. The first test was to check how far the average velocity changed with the time span selected. For this purpose the "moving averages" method was used. Fig. 5.8 shows the variation of the average velocity with time span (window) for two locations within the carpet layer. As shown in the figure, at sufficiently long periods of time, the average velocity becomes stable indicating that the span of time chosen to determine the average velocity of the grains is reasonably sufficient. The fluctuation of the average velocities, as seen in the figures, is due to both experimental error and also randomness introduced by the turbulent motion of the sediments.

In the other verification scheme, the average velocity between successive frames spaced with different time spans and also at different locations were obtained and compared. This helped to eliminate any inconsistency that may arise due to a choice of a particular segment of the recording. The averaging of the grain velocities was made for successive time spans of 0.001, 0.002, and 0.003 second. Fig. 5.9 gives the detail.

5.5.3 Grain concentration estimation

The *Imager* software has the capability of grading the brightness of a pixel for a given image. Moreover, for a specified rectangular area, it could give the brightness of pixels averaged for each horizontal line. Therefore for a rectangular section chosen, it is possible to obtain a profile of pixel brightness.

Each pixel is coded on a brightness grade of 0 to 255 depending. To obtain grain concentration, the assumption was made that the average level of brightness of the pixels at a given level depends on the concentration of sediment at that level. Where sediments were not present, namely above the carpet layer, the pixels were darker, and this level of darkness was used as a reference for "zero sediment concentration." On the other hand, the brightness of the region where sediments are not in motion was used as a reference for "maximum sediment concentration." These references were used for calibration purposes based on the assumption of linear variation of brightness between the two extreme values of "no sediment region" and "maximum sediment concentration region." Therefore, it was possible to determine the concentration of grains at intermediate levels, within the carpet layer.

5.6   Pressure Measurements

The measurement of pressure along the test-section was necessary for the comparison of the experimental results with the theoretical analysis of carpet flow. Two different approaches were used in measuring pressure gradients for the transitional regime and dunes, simple manometers and pressure transducers.

In the first approach, simple manometers were used to measure the pressure levels. As shown in Fig. 5.5, three pressure tapping points at 50 cm interval were employed. To dampen the pressure fluctuations, a manometer with 18 mm diameter was used.

For the moving dunes, pressure varied with time and therefore pressures were measured by using pressure transducers that were connected to a data-logging computer. The transducers were placed at intervals of 25 cm as shown in. Fig. 5.1a.

5.6.1   Pressure transducers

Pressure gradients over a dune length were obtained by employing eight pressure transducers; model *PX139-001D4V* from OMEGA® of differential type with operation range of ±1 PSI and common mode pressure of 50 PSI. The transducers use micromachined silicon pressure sensors in conjunction with stress-free packaging techniques to provide accurate and temperature-compensated measurements. The transducers operate from a regulated 5 volt DC power source, with a calibrated output of 4 volt in the range of 0.5 to 4.5 volts. Pressure was measured to the precision of ±1.0 mm.

Before the transducers were used to measure pressures, they were calibrated against known pressures which confirmed their linearity. To make sure that consistent sets of pressure measurements were obtained, the calibration was done before each experiment, but because linearity had already been proved, only two pressure measurements, a high and a low value, were needed.

The real time pressure measurements, over a dune length, of the eight transducers were logged by a computer for analysis. This made it was possible to construct the hydraulic grade line, for a given set of flow parameters.

Figs. 5.10, 5.11 and 5.12 give details of the pressure measurements obtained by using pressure transducers. The troughs on the graphs correspond to the crest of a dune where the pressure is expected to reach its minimum value for a given point measurement. And, accordingly, the crest of the graphs correspond to the point of reattachment where the flow velocity is at its minimum and the pressure at its maximum value. The cyclic nature of the graphs corresponds to the periodic behavior of the dunes.

5.6.1.1   Sediment discharge measurement using the loop-system

An attempt was made to measure flow and sediment discharge by using the loop system as outlined by Graf (1962) and Einstein (1966). In their method, the flow and sediment discharges are estimated indirectly by measuring the pressure drop along a known length of vertical pipe by using the principle of continuity of water and sediment phases, together with the concept that head drop in a sediment-water mixture flow is a sum total of the clear-water flow and

sediment. As will be explained, this method did not work for the present experiments because of the unsteady nature of the sediment flow.

Expressions that related the pressure drop to flow and sediment discharge in the vertical pipe of the re-circulating system were obtained by Einstein (1966) as follows:

$$\left(\frac{(\delta h_u)_m + (\delta h_d)_m}{2L}\right) = (S_s - 1)\Delta + \Theta[1 + (S_s - 1)C] \tag{5.1}$$

and

$$\left(\frac{(\delta h_u)_m - (\delta h_d)_m}{2L}\right) = (S_s - 1)(C + \Delta\Theta) \tag{5.2}$$

where δh_u = head drop in riser pipe; δh_d = head drop in the down pipe; L = length of pipe along which pressure drop is measured;

$$\Delta = \frac{\omega_0 A}{Q}C(1-C)^2 \quad and \quad \Theta = \frac{f}{D}\left(\frac{Q_m}{A}\right)\frac{1}{2g} \tag{5.3}$$

where ω_0 = the settling velocity of particles; A = crossectional are of the vertical pipes; C = concentration of sediments; Q = clear-water discharge; Q_m = sediment-water discharge; D = diameter of the vertical pipes; f = friction factor; and g = gravitational acceleration.

The loop system and theory was developed for measuring uniform and steady sediment transport rates where the concentration of sediment is constant and steady along the riser and down pipes. When it comes to measuring sediment transport rate for dunes, neither uniform

nor steady flow assumption can be made. For a flow with a dune bedform, three complications arise in the measurement procedure: 1) the concentration level in the vertical riser and down pipes is not the same nor constant, so that comparison can not be made; 2) even within each vertical pipe, the level of concentration is not the same for two given points (due to time lag); and 3) a dune gets washed out before entering the down pipe, with the effect of at least doubling the rate of sediment transport. Measurements have shown that the maximum sediment transport rate to be about double the sediment transport rate at a dune crest, which also agrees with theory. Therefore, the loop-system method is not suitable for measuring sediment transport rate when bed forms with varying sediment discharge exist.

5.7   Error Range

Each measurement has a range of error associated with it. The ranges are given under this section for the different measurements that were carried out during the experiments.

The fluid velocity measurements that were carried out using the ADV had an error margin of $\pm$ 0.62 cm/s, for the velocity ranges that were used during the experimentation. Subsequently, the Reynolds stresses that were obtained from the instantaneous velocity measurements had an error margin of $\pm$ 0.04 N/m^2.

For grain velocity measurements obtained by using an image processor, the error margin was less than $\pm$ 1.0 mm/s. The scatter from the average grain velocity was less than $\pm$ 1 cm/s. And the measured concentration values had an error margin of less than $\pm$ 1.0 % and scatter of about 5 %.

The pressure measurements that were made both with the pressure transducers and with the manometers had an error range of ± 1.0 mm head of water. The standard error of the pressure measurements was less than 3.5 mm head of water. The pressure measurement fluctuation from the average value is partly due to the turbulence in the flow.

The wave length of the dunes varied within the range of ± 3 cm. The speed of the dunes was measured by timing the amount of time taken for a dune crest to travel a know distance. The speed had a variation in the order of ± 0.2 cm/s. The dune height measurement at the different sections had a variation range of ± 0.25 cm.

5.8   Experimental Procedure

In order to check the performance of the pump and the closed-conduit circuit, the system was run without sediment inside. Once the performance was found satisfactory, sufficient amount of sediment was added into the system. Before the commencement of any experiment, it was always necessary to check and get rid of trapped air bubbles and this was done by letting the air bubbles escape through a vertical pipe opening, 15 cm in diameter, installed at the downstream end of the test-section. The details are shown in Fig. 5.5 shows the detail.

During the experiments, periodic temperature readings were made for two reasons: 1) to calibrate the ADV system, and 2) to keep the temperature range of water-sediment mixture consistent. Since velocity measurements for a single run take considerable amount of time, the temperature could rise by about two degrees Celsius during the period of experimentation. Since the flow was highly turbulent and the sediment particles are of the order of 1.0 mm, the

slight change of viscosity, and density, associated with the small change of temperature is not of much significance.

Near the sediment carpet layer and near the top plate, velocity measurements were made at vertical intervals of 1.0 mm to obtain enough detail of the velocity variation. In the regions farther away from the boundaries, the intervals were increased since the rate of change of velocity with the vertical was less in magnitude and sensitivity.

Upon the completion of an experiment, the pumping rate was reduced gradually and the sediments allowed to settle in the top section of the closed-conduit circuit in order to avoid the deposition of sediments within the pump casing. This is especially necessary since the sediments in the vertical pipe, at the delivery side of the pump, could all settle down on the pump casing. This would make restarting the pump difficult, if not impossible and damage the pump. Therefore, at the end of an experiment, the speed of the pump, and hence the discharge, was lowered in such a say that most of the sediments settled and accumulated in the horizontal section of the circuit. This had a double advantage: 1) the pump would not be jammed with sediments; and 2) it makes it easier to remove the whole sediment out of the system by just opening the removable top plate.

5.9   Summary

A re-circulating closed conduit experimental apparatus was built to investigate the shear stress transfer of fluid to moving sediments for bedwaves under intense bedload transport condition. The use of this closed conduit apparatus eliminated the surface wave effects associated with

open channels, and it was possible to produce high shear stresses necessary for intense bedload transport of the test section.

A high speed camera was used together with an image grabbing and processing software to measure the grain concentration and velocity within the carpet layer. Recording of particles movement was only possible at the side wall. Observation of the dune motion showed that the dune crest had a uniform height across the flume and the dune crest was almost straight. Therefore it was considered reasonable to assume that such measurements at the side wall are representative of the dune motion.

Although this study is mainly theoretical, experiments were used to verify the theories presented. However, some of the theories were developed to explain experimental results that were not expected at the outset. The findings of both the theory and the experiment are reported together in Chapter 6.
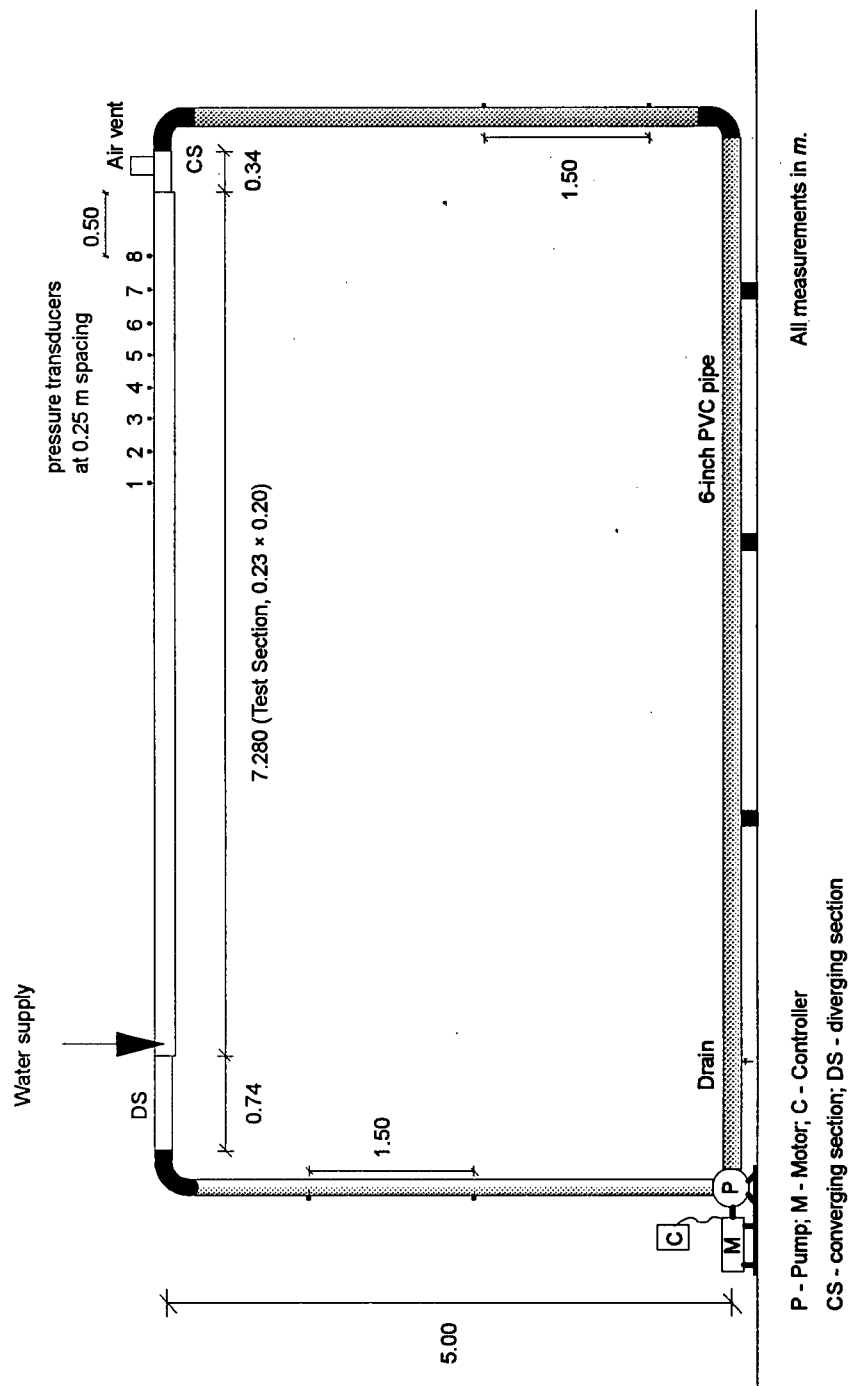
Figure 5.1. Schematic diagram of the re-circulating conduit
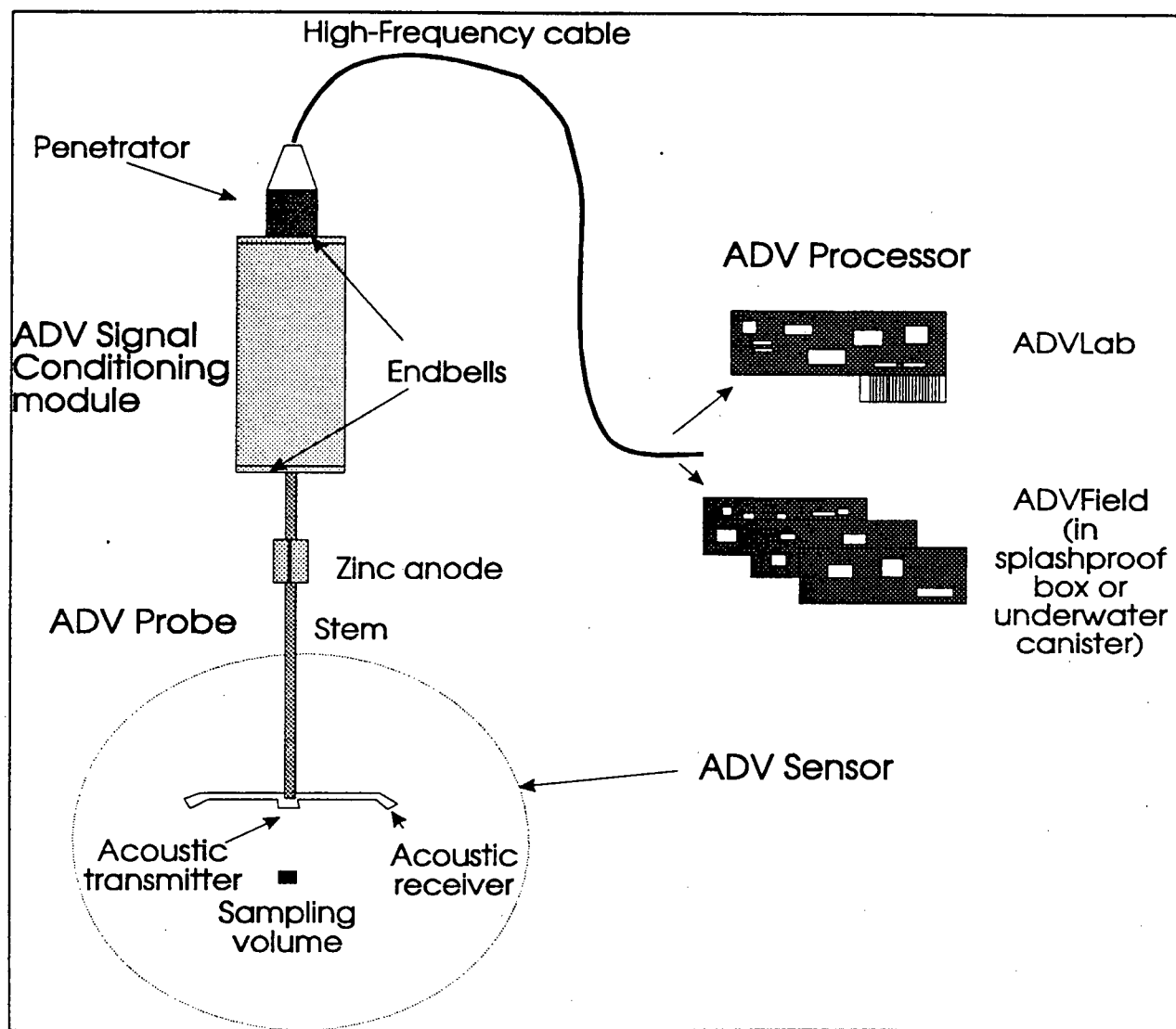
Figure 5.2. Schematic diagram of the ADV components
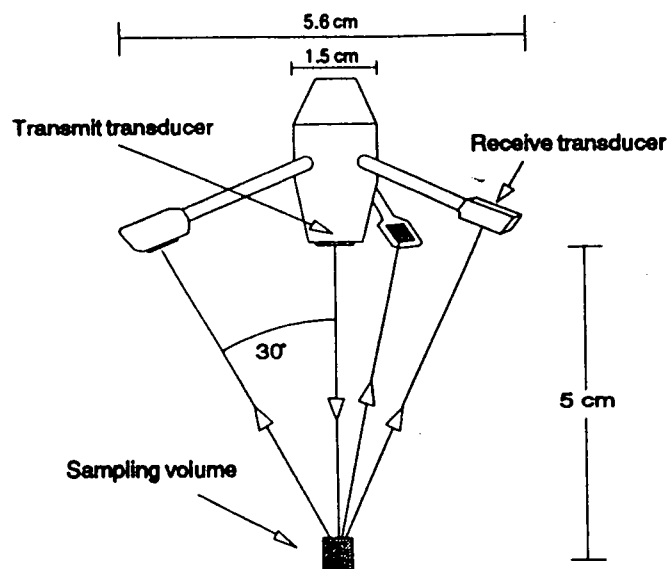
Figure 5.3. Measurement-probe configuration
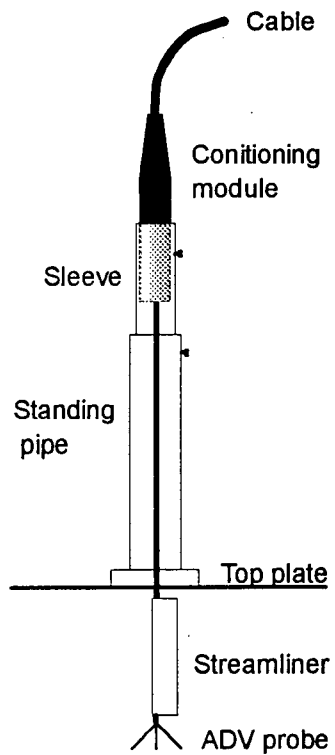
Figure 5.4. Installation of the ADV

Figure 5.5. Details of the test section

a)
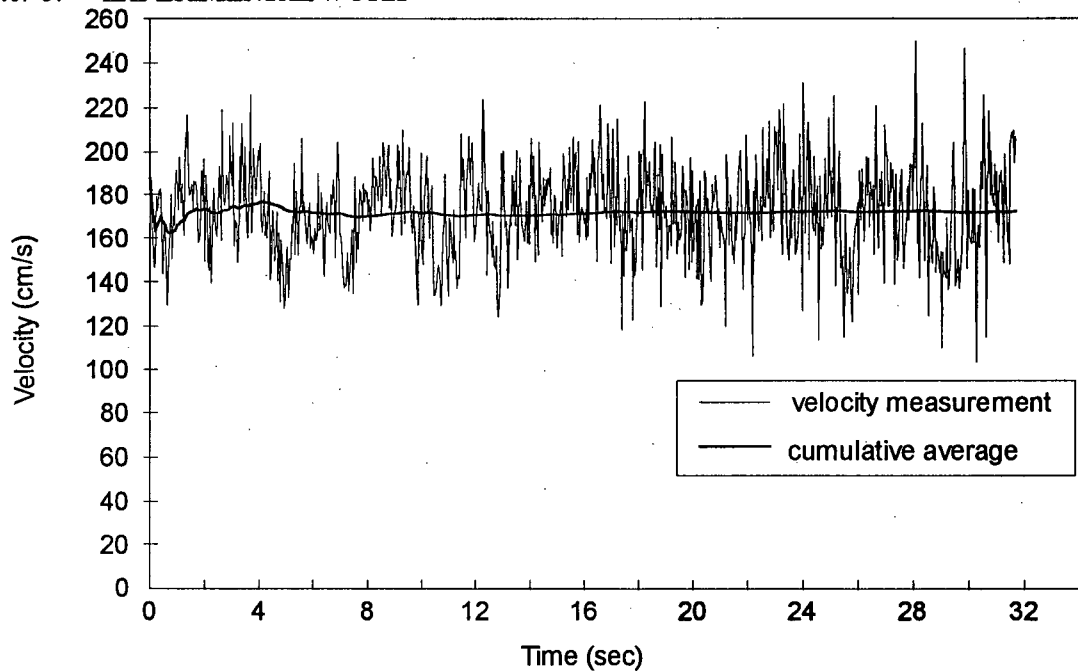
b)
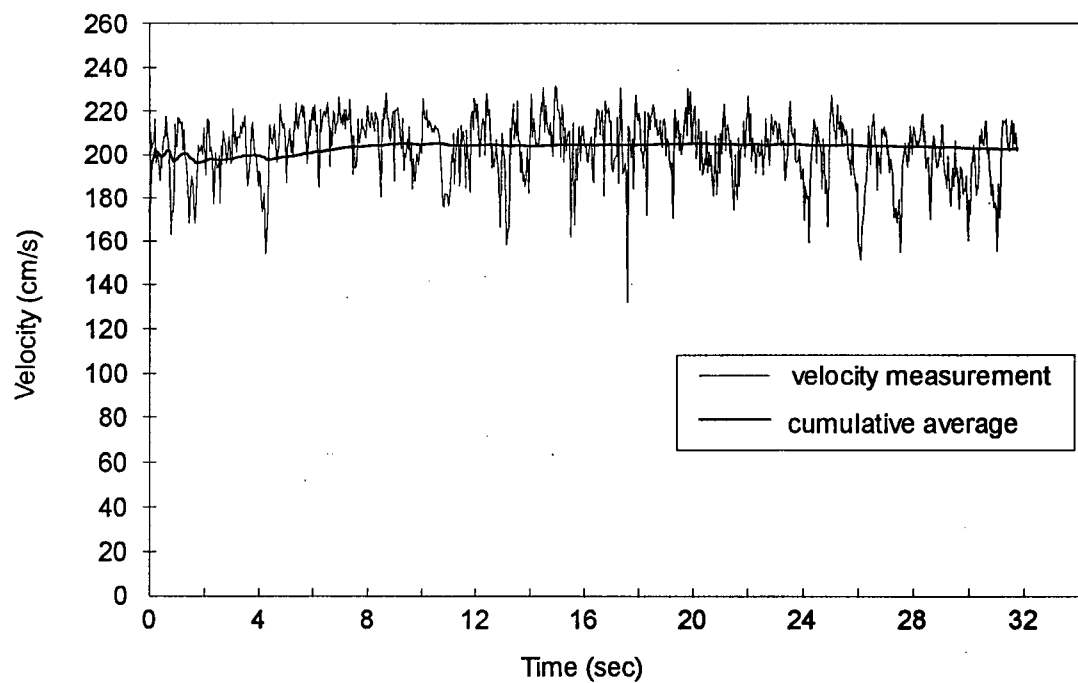
Figure 5.6. Velocity data and average velocity values for: a) 80 mm above the bottom boundary; and b) 100 mm above the bottom boundary, at section 3
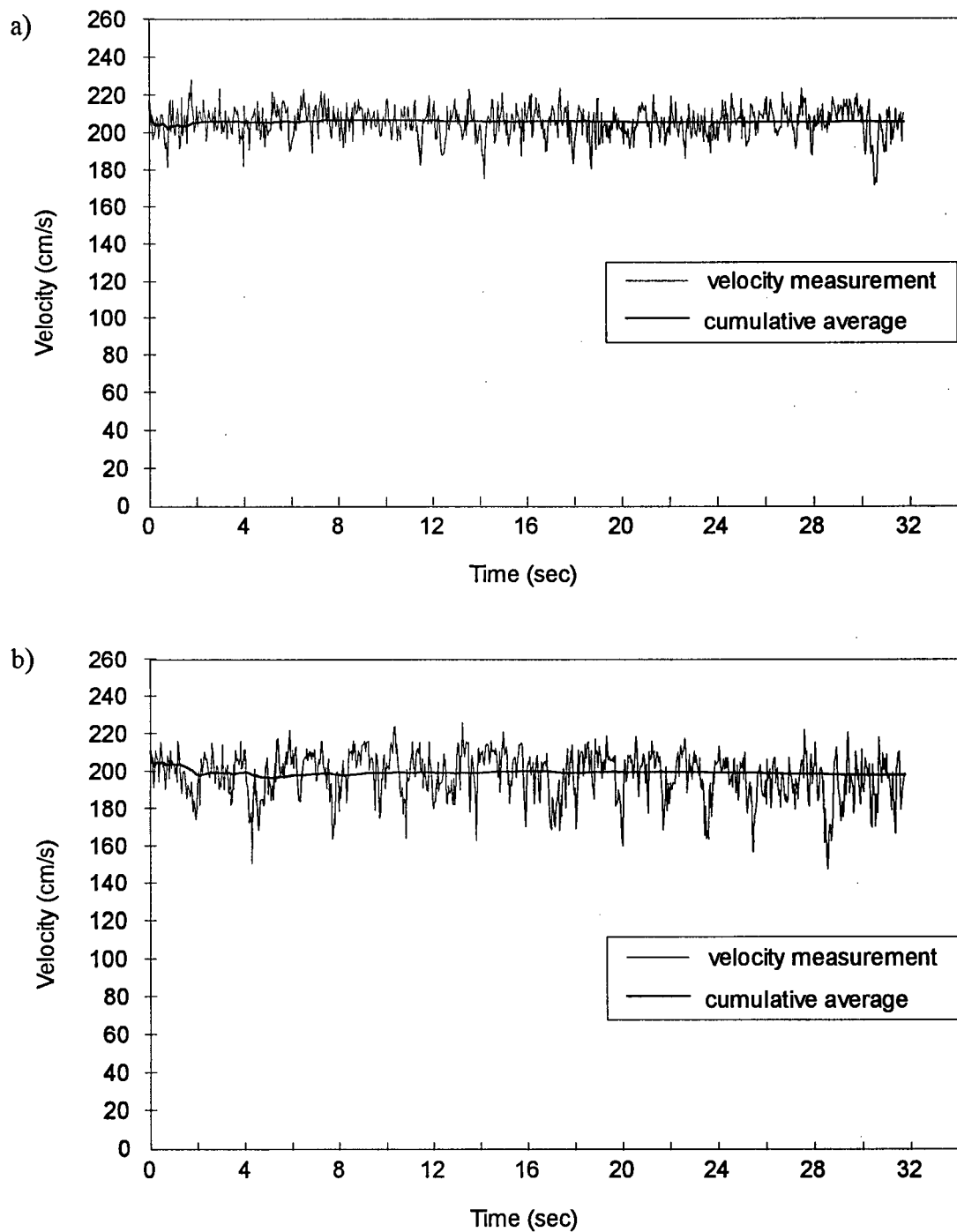
Figure 5.7. Velocity data and average velocity values for: a) 140 mm above the bottom boundary; and b) 180 mm above the bottom boundary, at section 3

a)
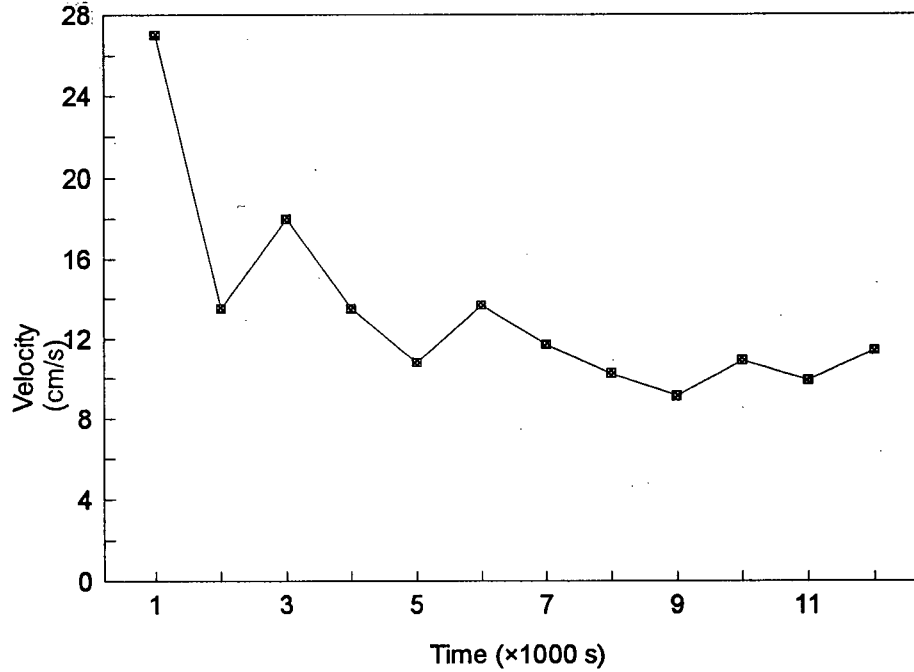
b)
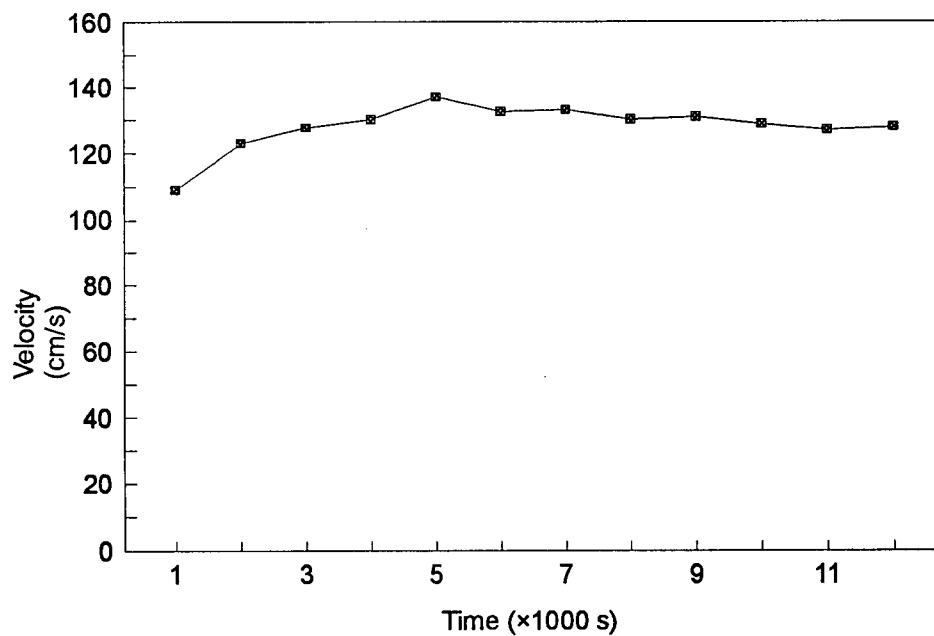
Figure 5.8. Variation of average grain velocity with time at: a) 2 mm from the stationary boundary; and b) at the top of carpet, at section 3
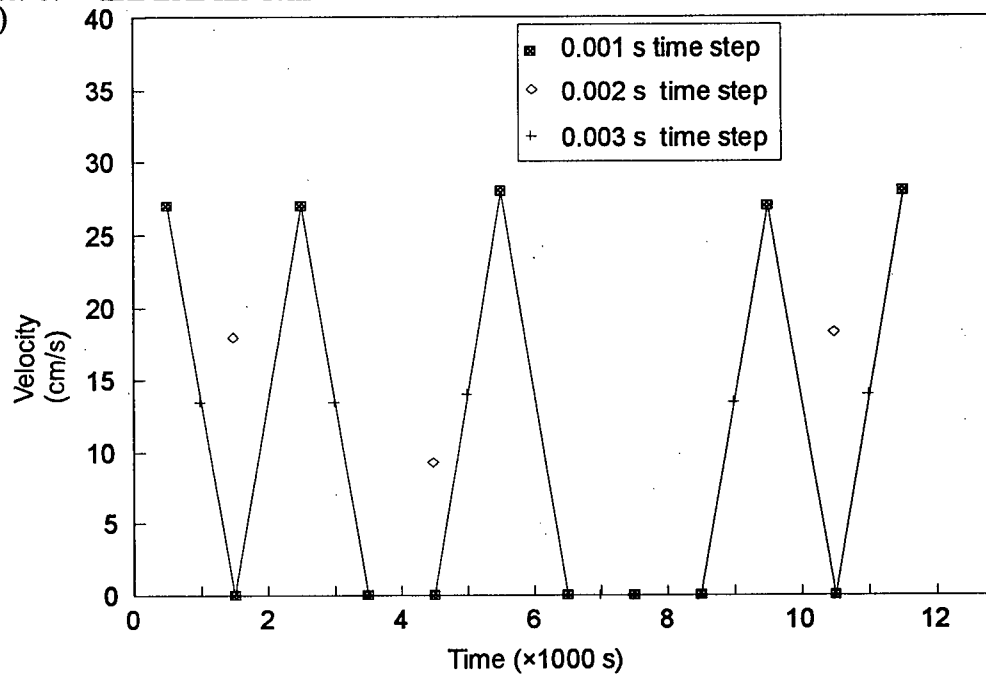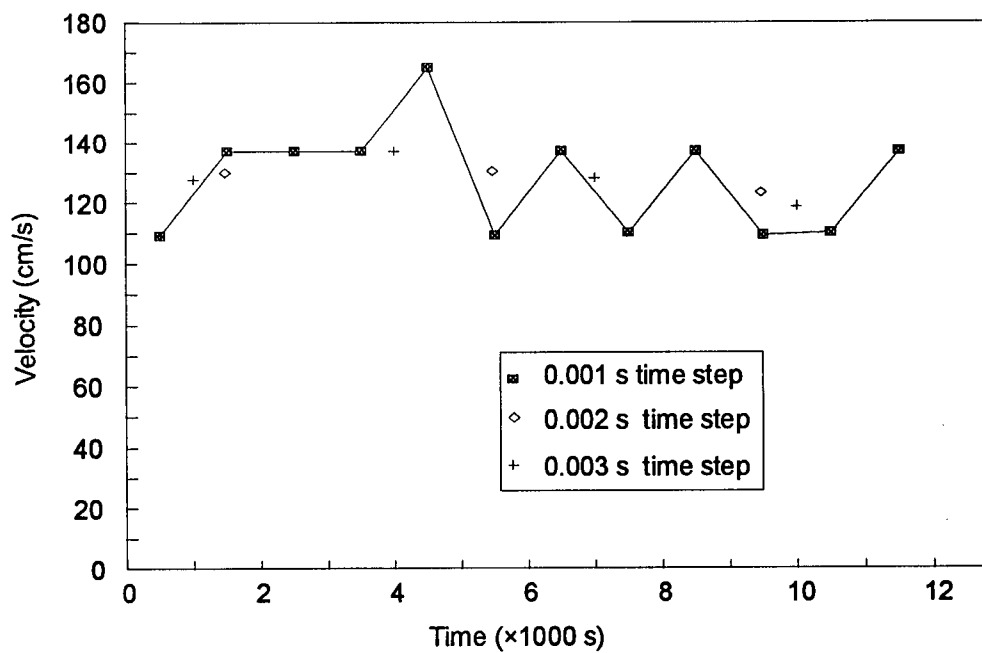
Figure 5.9. Variation of sediment average velocity with different averaging time for: a) 2 mm above the stationary boundary, and b) at the top of carpet, at section 3
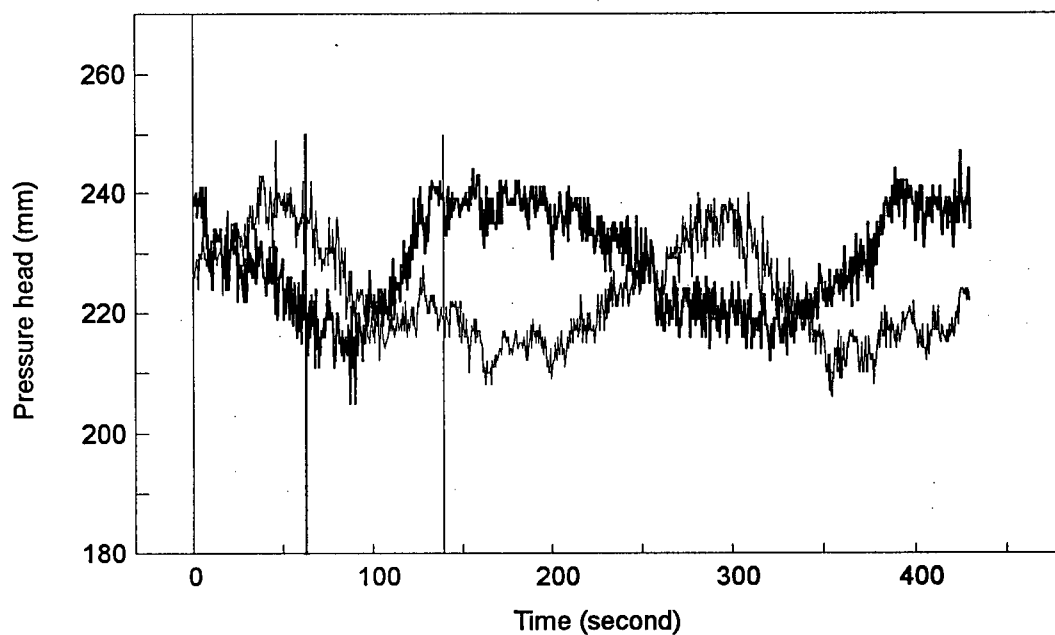
Figure 5.10 Pressure variation over a dune for two points 50 cm apart
(transducers 8 and 6, Fig. 5.1)
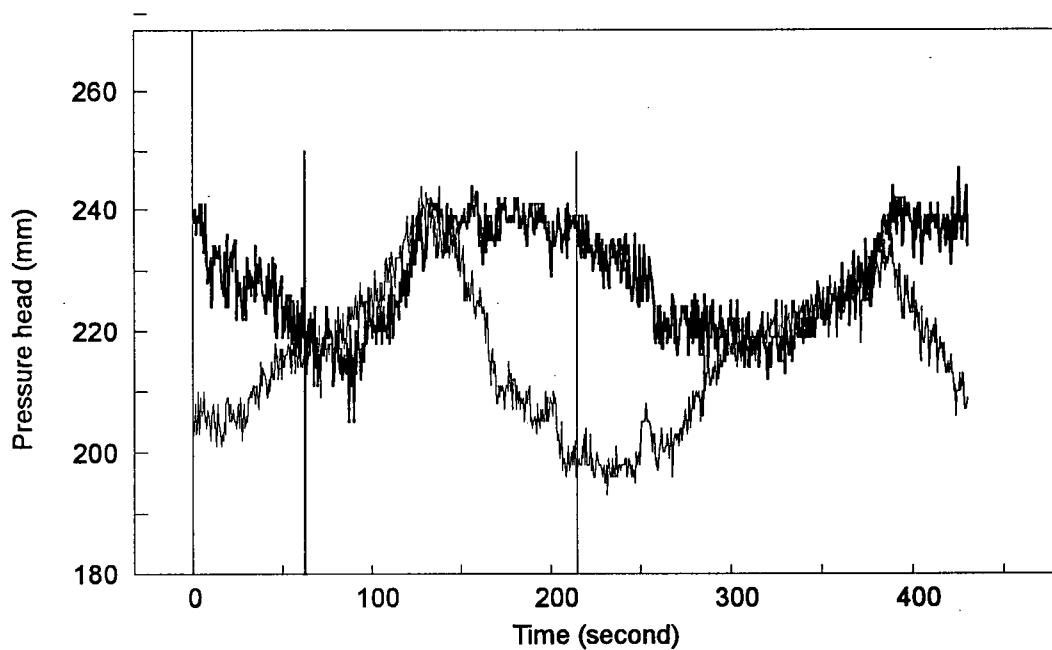
Figure 5.11 Pressure variation over a dune for two points 100 cm apart
(transducers 8 and 4, Fig. 5.1)
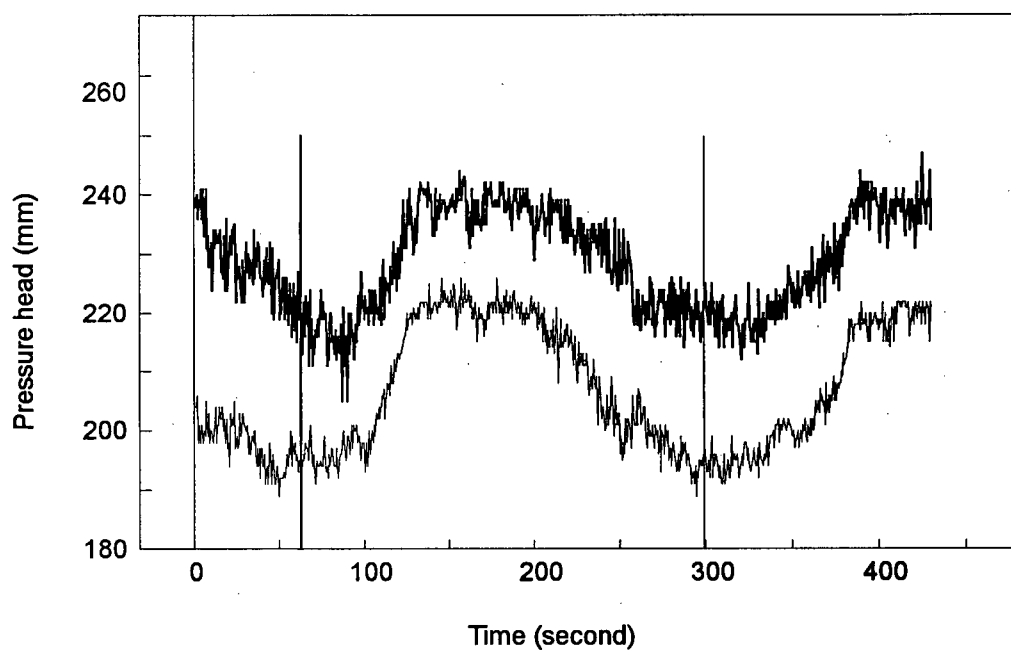
Figure 5.12 Pressure variation between points that are dune-length apart
(transducers 8 and 2, Fig. 5.1)

CHAPTER 6

RESULTS AND DISCUSSION

6.1   Carpet Flow Dynamics

This thesis deals with the study of intense bedload transport associated with sediment bedforms. The work has focused on the following factors: the dynamics of flow inside a carpet layer of sediment, the power requirements, the efficiency values, the frictional resistance, and the effect of convective acceleration on bedforms.

For this study, two flow regimes of bed configurations have been considered, firstly, the transitional regime, where the bedform is lengthening and flattening towards plane-bed, and secondly dunes, in the lower-flow-regime, were considered. This transitional flow regime, is a long shallow stationary bed slope. For both bed configurations, the pressure gradient induced by the convective acceleration due to bedforms was an additional factor compared to the plane-bed flow condition.

Previous work has confirmed the theory proposed by Bagnold that, for the plane bed carpet flow condition, shear stress from the main body of flow is transferred gradually through the depth of the moving-sediment layer to the stationary interface. The total shear stress from the flowing body of fluid exerted on the carpet is partly carried by the sediments and partly by the interstitial fluid. Under such a condition, the sediment shear stress is mainly due to intergranular collisions. It has been shown by Reynolds (1885) that when a layer of grains is subjected to a

shearing stress, the layer of grains tend to dilate. Bagnold (1956) extended this static analysis to the dynamic collision of sediment particles which creates a stress vector in space, and may be resolved into horizontal and vertical components. The horizontal component corresponds to the applied shear stress and hence to the resistance offered. The vertical component, which corresponds to the dilation, is a pressure which is balanced by the weight of the overlaying sediments: so that, unlike suspended load that is supported by the vertical component of the fluid turbulence, grains in a carpet flow are supported by inter-granular collisions, Bagnold (1956).

The purpose of this study was to examine the flow of sediment in bedwaves in which non-uniform fluid flow plays an important role. Theory has been developed which explores the additional shear stress induced in a moving carpet of sediment by the convectively accelerating fluid flow field. It has been argued that shear stress arises in two ways: 1) turbulence induced fluid shear stress; and 2) shear stress induced by the convective pressure gradient.

The resulting carpet flow requires transfer of the fluid shear stress to the moving sediments, as argued by Bagnold (1956, 1966), and the process is inefficient because the shear stress requires a slip velocity between the carpet grains and the fluid. However, in the present work, it is argued that the additional shear stress resulting from the convective pressure gradient is transferred to the sediments more efficiently, because the pressure acts directly on the sediment grain particles, as defined in the theory sections, Chapters 3 and 4. However, this additional pressure gradient force gives rise to additional carpet shearing and therefore also creates power loss within the carpet because of the intergranular collisions which creates the dispersive pressure needed to support the weight of carpet, exactly as defined by Bagnold. This total

dispersive pressure therefore matches the total weight of carpet, where the total shear stress arises from the two sources defined earlier.

The theory developed indicates that the sediment carpet process should be more efficient for bedwaves, because of the effect of the convective acceleration. Experiments were carried out to check this theory and to measure this increase in efficiency.

6.2   Theoretical Solutions

The physical processes of carpet flow were examined by considering the analytical solution of the problem and then by carrying out experiments to verify the conclusions. An analytical solution was obtained in Chapter 3 for the dynamics of carpet flow based on the empirical-theoretical formulation given by Bagnold (1954, 1956). There have been various studies by different researchers, mostly of a theoretical nature, but Bagnold's result is physically based and has been verified extensively by experiment.

Bagnold's (1954) results, based on his classic drum experiments, related shear and normal stresses with the grain and fluid properties. The shear stress and the corresponding dilation stress are related to the weight of supported sediment and the grain velocity gradient and concentration. For the present study, the grain velocity gradient and hence the velocity of the grains was computed from known stresses and stationary boundary condition. For the range of stresses and concentration values that were outside the limits given by Bagnold's experiments, modifications and extrapolations were made. This was necessary for the transition region between inertia and viscous behaviour, where a formulation was not given.

117

Bagnold identified three regions of grain flows: micro-viscous, grain-inertia, and the transition between the two. The classification is based on a non-dimensional number, the Bagnold number, B, similar to Reynolds number, which is a ratio between inertial and viscous stresses. The micro-viscous region is where the viscosity of the fluid dominates the flow property with respect to inertia of the grains where the presence of the grains has mostly the effect of modifying the fluid viscosity. Analytical results indicated that such a flow occurs either when the grain velocity is very low near the stationary boundary or at the interface of the main fluid body and the carpet, where the shear stress taken by the sediments is comparatively small. The rest of the carpet layer, which constitutes the major section, is dominated by the grain-inertia and the transitional region. Since a definite relationship was not given for the transitional region, it was found necessary to interpolate between the micro-viscous and grain-inertia, depending on the non-dimensional value, G.

Moreover, Bagnold's results were given for λ values up to 17. But in the present work, the linear concentration limit, λ, considered for a carpet flow, where interlocking of grains takes place at the interface with the stationary boundary, has been assumed to be 22. The value of $\lambda = 22$ was obtained from the interlocking condition given by Bagnold. Therefore, it was necessary to extrapolate for the missing range.

Bagnold used neutral density lead stearate particles for his experiments. The dynamic coefficient of friction he obtained for his particles was 0.32. But, as he also indicated (Bagnold, 1973), the dynamic coefficient of friction for sand has to be about equal to the static value. Therefore, this modification was also incorporated in adopting Bagnold's results.

Obtaining an exact closed-form mathematical solution of the governing equations for a carpet flow was not possible, mainly because the three flow regions outlined by Bagnold (micro-viscous, transitional and grain-inertia) were encountered within the carpet depth. Therefore, it was necessary to obtain a numerical solution that could allow for the change of regime within the carpet. It order to find a closed numerical solution to the governing equations, it was found necessary to approximate the concentration profile of sediments within the carpet. Uniform, linear (Wilson, 1984) and non-linear (Nnadi and Wilson, 1992) were tried. The non-linear proposed by Nnadi and Wilson was also verified by experiment. The results are shown in Fig. 6.1. The following are the main conclusions:

1) Based on the results, the uniform-concentration profile was discarded because it does not give realistic results, because the calculated slip velocity was found to be negative, as discussed in Chapter 3.

2) The linear concentration profile gave satisfactory results and agreed well with the experimental measurements of the grain concentration and velocity. The slip velocity condition also was satisfied.

3) The non-linear profile analysis also agreed well with the experimental measurements of the grain concentration and velocity. The non-linear profile was found to give very similar results as the linear profile.

A full discussion and results of the theoretical approach are shown in Chapter 3. It was verified mathematically that a carpet flow is feasible. Moreover, a slip velocity between the sediments and fluid was also clearly indicated. Both the linear and the non-linear sediment concentration

profiles gave feasible solutions and the difference between the two is not significant. Results are given by Figs. 3.8, 3.9, 3.10, and 3.12. Also the experiments supported the assumption of a linear or near linear sediment concentration variation as described below.

6.3   Experimental Results for the Non-Uniform Flow

Experiments were conducted to investigate the behavior of a carpet flow as it exists in non-uniform flow. Details of the experimental set-up and procedures are given in Chapter 5. The experiments studied the non-uniform and mildly unsteady behaviour of a moving sediment dune. The experiments also studied the non-uniform "transitional-flow-regime" between the plane bed and dunes where a stationary bedform existed in the channel.

The experimental set-up utilized a closed-conduit and a high flow rate, because much higher shear stresses can be generated in a closed conduit than is possible in a laboratory scale open channel. The experimental measurements included the pressure gradient, ADV measurement of fluid velocity and turbulence, and sediment particle motion and concentration. High speed video and an image grabbing and processing techniques were used to determine the velocity and relative concentration of sediments within the carpet. This study therefore examines the theoretical requirements of a carpet flow and then reports on some of the preliminary experiments which examine these theoretical factors. These experiments have proved to be difficult, but provide evidence to support the theory.

Of the various measurements and calculations made, the following are considered to be the most reliable, given in descending order.

1) Values of sediment unit discharge, q_s, obtained from wave speed, k, and wave height, η. The values of k and η are not difficult to measure, and therefore the sediment discharge can be accurately determined.

2) Pressure variation on bedwaves. The pressure sensors and pressure transducers utilized were able to make precise measurements within a 1.0 mm head of water. Therefore, the hydraulic grade lines obtained for the different bedwaves are accurate and representative. Also the time varying nature of the pressures at several locations could be accurately recorded by computer.

3) Boundary shear stress for the smooth wall was estimated using boundary layer power law calculations based on the mean velocity profiles. These estimates are considered approximate, and were checked against equivalent steady uniform pipe flow calculations.

4) The weight of a carpet layer and the corresponding necessary shear stress can be estimated reasonable, although it is sensitive to the carpet thickness measurement and the maximum concentration of particles at the base of the carpet.

5) The unit sediment discharge, q_s, obtained from the carpet measurements depends on the grain velocity measurement and thickness of carpet. This value compares well with the unit sediment discharge obtained from wave speed and wave height measurements, and was therefore independently checked.

6) The hypothetical shear stress required to transfer a given carpet load was obtained from Bagnold's stream-power equation. This shear stress, obtained by back-calculating from known

sediment discharge and flow velocity measurements, was used to calculate the overall transport efficiency value for a dune length

7) The least accurate estimates were the carpet stresses calculated using the control volume, which is very sensitive to measurements of bed level height and to velocity profile measurements, and which therefore gives sensitive changes in the momentum flux term. Since differencing of large values is involved, a slight change in the flow parameters introduces a significant difference. But generally the calculations indicate a high shear stress for the carpet. This gives at least an approximate confirmation of carpet stress values calculated from carpet weight estimation.

6.3.1   Results for the transitional-flow-regime: The stationary bedform

6.3.1.1   Experimental observation

Sediment transport occurs in different modes. Although there are different ways of categorizing the mode of sediment transport, two regimes may be identified readily: the lower-regime with ripples and dunes; and the upper-regime with plane-bed and antidunes. Observation and measurement of the transitional flow regime and dunes was made in a circulating closed-conduit system. Chapter 5 gives the details of the experiments and the apparatus used.

At low discharges, dunes were observed, but, were washed away as the flow rate was increased. As a consequence, a stationary shallow dune-like bed configuration resulted. In the first set of the experiments the flow was increased to its maximum value in an attempt to produce flat bed and carpet flow conditions. However, the stress level was not high enough so

that the dunes began to wash out but the final regime consisted of a shallow dune-like bedform which became stationary in the channel. As discussed in the theory sections, Chapters 3 and 4, this stationary shallow bedform proved to be very useful because the resulting non-uniform fluid flow was steady and could be studied at length, unlike the unsteady moving bedform situation. This study was an excellent preparation for the later experiments on unsteady moving dune behaviour, because the steady flow is much easy to measure.

6.3.1.2   Concentration and velocity of sediments

The following discussion is given for the transitional flow regime where a shallow stationary dune is considered. Once the reliability of the image grabbing technique was established, further analysis of the data was carried out to obtain the concentration and velocity profiles. The details of the concentration profile is given by Fig. 6.1 and Fig. 6.2 shows the velocity data points for the three sections of the test reach. To check repeatability of the experimental results, two sets of measurements were made at each section for comparison.

As indicated in Fig. 6.2, for this stationary bedform, the sediment velocity profiles for the three sections are very similar, save for some inherent experimental errors. Moreover, the thickness of the carpet was also similar for the three sections. This establishes that there was no acceleration of the sediments as they moved in a carpet flow: which means, a steady state was achieved for the moving sediments. This important conclusion was used in Chapter 4 in the analysis of the convective acceleration of the fluid.

A regression analysis was carried out to obtain a relationship between the grain velocity and height from the stationary interface (base of carpet). From a dimensional analysis point of view

and also by theoretical reasoning, the grain velocity can be made non-dimensional with respect to the shear velocity. Also, the location of the sediment from the stationary interface is made non-dimensional with respect to the thickness of carpet. Fig. 6.3 shows the data points from experiment and the best-fit line for the velocity profile. The best-fit line that approximates the grain velocity with respect to relative height is as follows:

$$\frac{U}{u_*} = 20\left(\frac{y}{\delta_s}\right) \tag{6.1}$$

where U = grain velocity and δ_s = thickness of carpet.

The coefficient and exponent of the right hand side of Eq. 6.1 is different from previous results given by Wang and Qian (1987) and that of Sumer et al. (1996). Eq. 6.1 is different from the ones mentioned earlier in that it incorporates the effect of pressure gradient on sediment carpet flow.

Grain velocity measurements from the experimental results were compared with the theoretical model that was developed in Chapter 3. The results, in graphical form, are given by Fig. 6.4. Grain concentration variation along a vertical has the effect of modifying grain velocity gradient. A correction to the grain velocity gradient was made by multiplying the un-corrected velocity gradient by the quantity $(1 + \alpha Ri)$; where Ri is Richardson number, and α is a numerical constant close to 5 as given by Webb (1970) and Turner (1973). Although the theoretical results match reasonably well when $\alpha = 5$, a much closer result is obtained when the value of α is set equal to 3. Near the stationary boundary of the carpet layer, the matching between the experimental and the theoretical results is very close. But near the top of the carpet, the difference between the two results gets larger. Moreover, the theoretical grain

velocity profile shows an abrupt change near the top of the carpet where the sediment concentration suddenly becomes zero.

6.3.1.3   Effect of convective acceleration on stationary bedwave

The velocity measurements at the three test sections of the test reach shown on Fig. 6.5 indicated that there existed an acceleration of the flow caused by the sloping of the bed. By Bernoulli, this increase in velocity is compensated by a decrease in pressure. Therefore, the drop in pressure observed along the test section is the sum total of pressure drop due to frictional resistance and due to convective acceleration and these pressures are shown in Table 6.2. The pressure gradient associated with the convective acceleration contributes to an increase in the frictional boundary shear stress at the top surface of the carpet. In addition, the pressure gradient also acts directly on the carpet to create an additional drag force on the particles.

Velocity and pressure measurements were made at cross-section 3, of the test-section. Details of the experiments are given in Chapter 5, and Figs. 5.1 and 5.5 give details of the test-section. Velocity and Reynolds stresses measurements are indicated by Figs. 6.5 and 6.6, respectively, and the boundary Reynolds stresses are determined from Fig. 5.6. Table 6.1 shows a summary of the velocity measurements at the three sections. These values are used in the control volume analysis to obtain the total boundary shear stress.

To compare with these measured pressures and velocities, the following calculation was made.

The maximum velocities at each cross-section occur at a region of near zero shear stress, and therefore along the line of maximum velocities energy should be conserved. Therefore, Eq. 4.3 which is based on Bernoulli's principle is used to relate maximum velocities between two sections to a corresponding drop in pressure.

The maximum velocity values for sections 1 and 3 are given on Table 6.1. Therefore, by substituting the corresponding values of the maximum velocities in to Eq. 4.3, the following is obtained:

$$\frac{P_1 - P_3}{\gamma} = \frac{2.133^2 - 1.989^2}{2 \times 9.81} = 0.030 \, m \qquad (6.2)$$

The above result is almost the same as the pressure change measured by the manometer as indicated on Table 6.2, which confirms the relationship between the flow acceleration of the maximum velocities and the convective pressure decrease, specifically as given by Eq. 4.3.

The experimental results were used to give two estimates of the boundary shear stress, using the theory developed in Chapter 4.

The boundary shear stress was obtained by using two different approaches and a comparison was made between them: The boundary shear stress was first calculated from the balance of force and momentum flux of the flow. Eq. 4.1 from Chapter 4 is used in conjunction with the control volume given by Fig. 4.4. The different flow and geometrical parameters are given on Tables 6.1 and 6.2. The smooth wall boundary shear stress was obtained from the graphical representation of Reynolds stress with depth as given by Fig. 6.6. The Reynolds stress values were extrapolated towards the upper smooth wall boundary from values measured in the cross-

section. Accordingly, a value of $\tau_f = 3.0 \, N/m^2$ was estimated. Therefore, substituting the corresponding values into Eq. 4.1, the boundary shear stress, $\tau_{BC} = 19.0 \, N/m^2$.

Secondly, the boundary shear stress was calculated by relating the weight of transported sediment to the corresponding shear stress.

Eq. 4.2 is used to obtain the necessary shear stress required to mobilize the measured carpet thickness of 0.010 m. Substituting the corresponding values, $\tau_{BC} = 22.0 \, N/m^2$.

The values for the boundary shear stress obtained from the two approaches discussed above are close given the sensitivity of the momentum flux terms in the control volume analysis.

6.3.1.4   Slip velocity between sediments and fluid

The velocity measurements of the fluid made within the sediment carpet are not considered reliable because some of the measurements obtained were not realistic. The major problem for the ADV instrument is the interference from the moving sediments. Although a small amount of sediment concentration, known as seeding, is necessary to obtain flow measurements, but when there is a large amount of sediment, the behavior of the instrument becomes unpredictable. This was confirmed from personal communication with the support group of the ADV manufacturers. However, although the measurements taken within the carpet layer are not accurate, some of the measurements are in the expected range.

The theoretical results have shown that a slip velocity between the sediments and fluid is required for the transfer of shear stress. Not withstanding the shortcoming mentioned above, a

comparison of the sediment and fluid velocity measurements was made and Fig. 6.7 gives the detail. As indicated in the figure, a slip velocity does appear to exist. However, the fluid measurements near the stationary boundary are not realistic, since close to negligible velocity should have been recorded.

6.3.2 Results from dune experiments

During the experiments, it was observed that four dunes were present in the conduit at a given time and three of them were reasonably uniform. This confirms that the entry length of the experimental test length was adequate to achieve satisfactory flow conditions. Moreover, even for the first set of experiments which were carried out with less working length of only 5.0 m, the dunes were essentially very similar to the dunes obtained with the increased entry length. Fig. 6.8 gives the comparison between the two sets of dunes.

6.3.2.1   Actual dune kinematics

The theoretical model, Eq. 4.13, developed in Chapter 4, assumes all flow of sediment to occur in the downstream direction. The experiments showed that some reverse flow of sediment occurred and therefore the actual kinematics are slightly different as will now be discussed.

A Flow over a dune consists of two portions: the flow over the stoss side and the flow over the separation zone past the lee side of a dune. As Eq. 4.13 indicates, the rate of sediment transport on the stoss side increases with η, the dune height. Close to the point of reattachment, the rate of sediment transport is negligible, but increases towards the crest where it reaches its maximum value. Due to the high level of turbulence, characterized by a bursting phenomena,

that is generated near the separation zone, sediments are suspended for a short period of time before they settle and are transported as a bedload.

Within the separation zone a reverse roller produces a sediment movement that is in the opposite direction of the overall flow and dune movement so that the lee side of the dune not only gets filled with the sediment that "spills" from the crest, but also with sediment that is moved by the reverse roller. This situation is shown diagramatically in Fig. 6.9. Therefore, the effective dune height at the crest, η_e, that is associated with the sediment transport over the stoss side is less than the maximum dune height, η_{max}. This is shown on Fig. 6.10.

It should therefore be possible to define an effective dune height, η_e, based on actual sediment transport rate by using Eq. 4.19. The value of η_e is less than η_{max} and is probably approximated by the dune height above the flow reattachment point. The relative comparison between η_e and η_{max} and other dune measurements are summarized on Table 6.3.

The difference between the dune heights, η_e and η_{max}, as given by Eqs. 4.13 and 4.18, respectively, is attributed to the scouring of sediment at the lee side of a dune created by the reversal of flow within the separation zone. Close to 13% of the sediment transport is estimated to be contributed by the scouring of sediment from the trough of the downstream dune.

6.3.2.2   Boundary shear stress results

In order to obtain boundary shear stress values from the control volume analysis, complete flow and pressure measurements were made for two sets of unit discharges of $0.115\,m^2/s$ and $0.136\,m^2/s$. Flow velocity measurement results are given by Figs. 6.11a and 6.11b, respectively. And the corresponding flow parameters are given on Tables 6.4 and 6.5.

The substitution of the corresponding values into Eq. 4.1 yields average boundary shear stresses of $\tau_{BC} = 7.3\,N/m^2$ and $\tau_{BC} = 10.2\,N/m^2$ for the unit discharges of $0.115\,m^2/s$ and $0.136\,m^2/s$, respectively. The boundary shear stress for the unit discharge rate of $0.136\,m^2/s$ from sediment submerged weight consideration, as given by Eq. 4.2, is $\tau_{BC} = 15.5\,N/m^2$. The difference between the shear stress values obtained from the control volume analysis and the submerged weight of sediments is mainly due to the sensitivity of the momentum flux terms to small changes of velocity measurements. Therefore the shear stress values obtained from the sediment weight estimates are considered more reliable.

These shear stress values have been compared with the theoretical values derived by Bagnold (1966) who developed theoretical relationship for the onset of carpet flow and for the threshold of sediment suspension. For the purpose of this study, the criterion for the threshold of carpet flow as given by Bagnold (1966) was superimposed on Bagnold's modifies Shields diagram. Note that Bagnold modified the Shields diagram by replacing the abscissa with particle size. Fig. 6.12 shows the three threshold criteria of flow over a mobile bed; namely, initiation of motion, carpet flow, and suspension. The region between the *onset of carpet flow* and *suspension criterion* is characterized as carpet flow mode of bedload with negligible suspended load. Dunes with intense bedload fall under this category.

The results from the two flow discharges are indicated and plotted on Fig. 6.12. As the figure shows, the value for the unit discharge of 0.136 m^2/s and the stationary bedform plot above the curve for suspension criterion, and yet in these experiments the observed suspended load was negligible. This result would appear to confirm that the additional shear stress created by the convective acceleration is not directly associated with the turbulence of the flow, because the transport of suspended load depends on the level of turbulence. As previously argued, the total shear stress, τ_{BC}, is made up of two components, a fluid turbulent induced value and a convective acceleration induced value. The experimental measurements indicate that the shear stress caused by fluid turbulence is below the value required for suspension. Therefore, the additional shear stress induced by the convective pressure gradient can produce more intense bedload motion, but without inducing any suspension. It therefore appears that it may be possible for sediment bedwaves to induce stronger total shear stress in the carpet layer which can exceed the magnitude of the normal, fluid induced, turbulent shear stress required for full suspension, and yet the flow will continue to be a carpet bedload of even greater intensity. This conclusion is an interesting possibility which requires further testing.

6.3.2.3 Behaviour of dunes for a range of discharge

A quite unexpected result occurred when it was found that an almost exactly similar dune or bedform shape occurred for different flow rates and for different sediment discharge rates. It had been expected that when the water flow rate was increased, a longer bedwave would form with a corresponding increase in sediment discharge rate. This increased flow rate would be associated with higher shear stress and higher convective accelerations. However, as stated above, the bedwave geometry was unchanged, even though the shear stress and the convective

pressure gradient was higher. But, at the same time, the rate of sediment transport and the speed at which the dunes moved were different. Table 6.3 gives the summary of the results obtained. These surprising results are presented below and the theoretical implications are discussed.

A summary of the experimental results is presented on Table 6.6. It can be seen that q varied from 0.115 to 0.149 m^2/s and the corresponding q_s, which relates to the wave speed k, varied significantly from 1.51 to 3.45 cm^2/s. Experiments were carried out to examine how large a range of flow conditions could produce a similar shape of bedwaves. Above and below this range of flow condition the bedwave geometry changed. For the lower flows the bedwaves had smaller wave length and dune height, and for higher flows, the bedwaves tended to be irregular in shape and size until they started to get washed out at significantly higher flow.

However, within the range of flows given above, the shape remained similar with the dune height and dune length varying less than 3 %. The average measured dune geometry is given by Fig. 6.13.

6.3.2.3.1   Dune celerity and flow velocity

From the analysis of the data it was found that the dune celerity varies linearly with the cube of the average flow velocity, as shown in Fig. 6.14. Since dune celerity is directly proportional to the sediment discharge, for a given dune geometry, and tractive shear stress is proportional to the square of average velocity, the linear relationship between dune celerity and the cube of average velocity indicates that the sediment discharge, q_s, varies with the stream power.

6.3.2.3.2   Similarity of dune shape

The following is an investigation of how the three dunes can have the same shape and yet satisfy the different sediment and flow conditions. This examination of these bedwaves included consideration of: 1) the kinematic requirements; 2) the shear stress requirements; and 3) the convective pressure gradient requirement.

As described earlier, the total shear stress acting on sediment bedwaves has two components: 1) fluid shear stress (Reynolds stress); and 2) additional shear stress from the pressure gradient induced by convective acceleration.

The fluid shear stress may be given as follows:

$$\tau_f = C_f \rho \overline{u}^2 \tag{6.3}$$

where τ_f = fluid induced shear stress; C_f = coefficient of friction; ρ = density of fluid; and $\overline{u}$ = average velocity of flow. The shear stress is at its minimum at the point of reattachment and reaches a maximum value at the crest. The rate of sediment transport also varies accordingly.

Similarly, the pressure gradient in the fluid induces an additional shear stress that acts on the sediments of a carpet layer. The pressure induced shear stress at the interface of a carpet layer and a stationary boundary is given as follows from component II of Eq. 4.6:

$$\tau_p = \frac{\delta p}{\delta x} t \Rightarrow \rho \overline{u} \frac{-\delta \overline{u}}{\delta x} t \tag{6.4}$$

where τ_p = pressure induced shear stress; p = pressure; x = coordinate in the horizontal direction.

But, the increment of velocity, $\delta\bar{u}$, can be written as follows:

$$\delta\bar{u} = \bar{u}(y_1/y_2 - 1)$$ (6.5)

where y_1 and y_2 are depth of fluid flows at two sections of a dune, δx apart.

Substituting Eq. 6.5 into Eq. 6.4,

$$\tau_p = \rho\bar{u}^2 \frac{(y_1/y_2 - 1)}{\delta x} t$$ (6.6)

Therefore, the total shear stress, the sum of the fluid and pressure induced shear stresses, is given by combining Eqs. 6.3 and 6.6:

$$\tau_T = C_f\rho\bar{u}^2 + \rho\bar{u}^2 \frac{(y_1/y_2 - 1)}{\delta x} t$$ (6.7)

where τ_T = the total shear stress.

In the above equation, for a given geometry of a bedwave, the total shear stress would be purely a function of $\bar{u}^2$ if the carpet layer thickness, t, is constant. However the following argument indicates that t should vary.

Previously it has been shown in section 6.3.2.3.1 that,

$$q_s \propto \bar{u}^3 \tag{6.8}$$

Also it is reasonable to expect that the average grain velocity should be proportional to the flow velocity, i.e. :

$$\bar{U}_s \propto \bar{u} \tag{6.9}$$

where $\bar{U}_s$ = average grain velocity.

Combining Eqs. 6.8 and 6.9,

$$\bar{U}_s \propto (q_s)^{\frac{1}{3}} \tag{6.10}$$

Now the sediment discharge is the product of thickness, t, mean grain velocity $\bar{U}_s$, and carpet sediment concentration $\bar{C}$,

$$q_s \propto t\bar{U}_s\bar{C} \tag{6.11}$$

However, the sediment concentration $\bar{C}$ should be constant, so that combining Eqs. 6.10 and 6.11,

$$t \propto (q_s)^{\frac{2}{3}} \tag{6.12}$$

For the experiments, q_s varied from 1.51 to 3.45 cm^2 / s. Therefore,

$$\frac{t_1}{t_3} = \left(\frac{q_{s1}}{q_{s3}}\right)^{\frac{2}{3}} \approx 0.6 \qquad\qquad (6.13)$$

The above is a simplified argument and there may be other factors which help to reduce the variation in *t*. However the experiments indicate that for a significant range of flow, the stresses appear to scale so that the dune geometry could be maintained. Clearly more work is needed to clarify this interesting aspect of the work.

The above result indicates that the carpet tractive forces, both the fluid and pressure shear stresses, scale approximately with the square of flow velocity. This has important implication both for 1) flow and sediment dynamics over a dune of a given size; and 2) different flow condition over a similar dune shape. As has been observed in the present experiments, a similar dune size can exist for different sediment and flow rates. Therefor, it does appear that, for a limited range of sediment transport, the shear stresses can scale, with $\bar{u}^2$, as demanded by the similarity considered above. However, it leaves unanswered the question of what actually determines this dune size. Perhaps it is determined by the scale of the experiments.

6.3.2.4 EGL and HGL over a dune

The unsteady flow over a moving dune can be considered to be essentially non-uniform steady flow, because the unsteady motion of the dune with time is slow compared with the fluid flow and sediment velocities. On the stoss side of a dune, the flow keeps accelerating until it reaches the crest and the head loss is mainly due to frictional resistance from the boundary. Immediately after the crest, the flow experiences an expansion loss that is associated with re-circulation induced by the lee side of a dune. But, at the same time, a certain amount of pressure is recovered as the flow velocity decreases within the expansion zone.

136

Figs. 6.15 and 6.16 show the plotting of the EGL and HGL over a dune length for the unit discharges of $0.115 \, m^2/s$ and $0.136 \, m^2/s$, respectively. The overall EGLs and HGLs are indicated on Fig. 6.17. The figure shows how the EGL and HGL vary as dunes move in progression. It can be seen from the figure that the average slope of the EGL is fairly close to the actual pattern of the EGL variation, so that the energy loss from the dunes is almost uniform. As will be discussed later in section 6.5, for sediment transport over a dune, only that portion of a dune where sediments move has to be considered, because the portion of the separation zone of a dune is not effective in the overall transport of sediment.

The expansion loss due to an abrupt change of cross-section between the crest and the reattachment point has been estimated from the usual expression for an abrupt expansion; i.e.

$$h_e = \frac{\left(\bar{u}_3 - \bar{u}_1\right)^2}{2g} \qquad (6.14)$$

where h_e = head loss due to sudden expansion; $\bar{u}_3$ = average velocity at the crest; $\bar{u}_1$ = average velocity at the reattachment point; and g = acceleration due to gravity. This expansion head loss for the unit discharges of $0.115 \, m^2/s$ and $0.136 \, m^2/s$ calculated from Eq. 6.14 are 5.3 mm and 6.0 mm, respectively. However the measured head losses from the experiments are 15.3 mm and 16.9 mm, respectively, so that the measured head losses are higher than the calculated values suggesting an additional head loss associated with frictional loss of the conduit.

6.4   Frictional Resistance in Grain-inertia Region

A frictional resistance equation for intense bedload in the grain-inertia region was obtained in Chapter 3 as follows:

$$\frac{k}{D} = 2.5\tau_*$$

(3.44)

The above relationship for determining the friction factor of an intense bedload was found to give a better match to experimental results obtained by other investigators. Fig. 6.18 gives the graphical representation of the results obtained by different researchers. As the figure shows, the proposed frictional relationship given by Eq. 3.44 is applicable up to $\tau_* \cong 2$. For higher values of Shields parameter, τ_*, it is possible that the presence of suspension, and hence the modification of concentration profile, requires reformulation of the assumption on which Eq 6.9 was derived.

As Eq 6.9 shows clearly, the relative roughness depends on the value of the non-dimensional shear stress. For a straight channel with rough surface and clear water, the relative roughness depends mainly on the grain size. Although there are many different and conflicting relationships for the relative roughness of a clear water flow, the following will be used (Yalin, 1977):

$$\frac{k}{D} = 2$$

(6.15)

The above is basically a resistance equation for a clear water flow. Comparison of Eq. 3.44 for intense bedload and Eq. 6.15 for clear water indicates that the relative roughness will be equal for both cases when the non-dimensional shear stress is close to 0.8. Above this value, flow with intense bedload, as in carpet flow, will have higher flow resistance than an equivalent rough-bed clear water flow. On the other hand, a flow with an intense bedload, but with lower non-dimensional shear stress will exhibit lower flow resistance. Therefore, these equations indicate that the resistance to flow with intense bedload depends on the Shields parameter, and

could be higher than the clear water case for values of the Shields parameter greater than 0.8, but the resistance could be less than clear water at low values of the Shields parameter. This conclusion is preliminary at this stage, but might explain some of the conflicting evidence of increase or decrease of resistance.

6.5   Efficiency of Intense Bedload

Under this section the power transfer efficiency factors involved in transporting sediment in both the flat bed and non-uniform flow will be given. The uniform flow condition is compared with the non-uniform results.

6.5.1   Efficiency of intense bedload transport for flat bed condition

In a channel or closed conduit flow, a carpet layer draws power from the main body of flow and hence there is an efficiency factor involved in the power transfer process as first put forward by Bagnold (1966). Firstly, there is a dissipation of power in the transfer of power between the main body of fluid and a carpet layer as a whole. Secondly, there is dissipation of power in the transfer of power from the interstitial fluid within the carpet to the grains. Ultimately, all the power dissipated is lost to heat through viscosity in the case of fluid flow, and through intergranular collisional friction for the grains.

Theoretical calculations from Chapter 3 show that close to 20 % of power is transferred to the carpet. According to Bagnold (1966), the power transferred to the carpet is close to one third of the available stream power. Bagnold's result gives a higher efficiency because the carpet is

modeled as a moving "belt," whereas in reality it is a dispersed group of grains. Also Bagnold (1966) used an approximation of the fluid and grain velocities within a carpet layer.

Within the carpet, the same theoretical results also show that close to 25 % of the power is effective in moving the sediment within the carpet layer. Therefore, the overall efficiency of sediment transport for a carpet layer of sediments is estimated to be about 5 %, which is the product of the two power transfer processes, 20 % and 25 %. Bagnold (1966), estimated this value to be close to 10 %. Therefore, the difference between the results of his analysis and this appears to depend, at least partly, on his simplifying assumptions.

6.5.2   Efficiency of intense bedload transport for the non-uniform flow condition

When bedforms exist, the flow is forced to accelerate and decelerate as it moves over the dunes. This flow acceleration produces pressure changes which modify the flow field as discussed in Chapter 4.

In this non-uniform flow, the pressure gradient due to the convective acceleration is also felt and absorbed by a carpet layer of a bedform. The additional pressure gradient induces an additional direct driving force on the grains so that the total shear stress in the carpet is the sum of the fluid induced shear stress and the pressure induced shear stress. The effect of the pressure gradient is analogous to a buoyancy force on an immersed object. This additional transfer of force to the grains without a corresponding loss of power increases the efficiency factor of power transfer to the carpet from the main body of fluid. But this additional pressure force induces additional shearing within the carpet which causes an additional power dissipation

within the carpet. Part of this pressure induced shear does not require a slip velocity between the fluid and the grains because it acts directly on the grains themselves.

Within the carpet layer there is both water and grains. Therefore, the pressure force accelerates both water and grains. The water accelerates more because of its lower mass, so that the pressure force induces an additional slip velocity between water and grains. The pressure force therefore accelerates the grains in two ways, by direct action which is very efficient, and by additional fluid shear induced by the faster moving water. The overall efficiency of these processes is very difficult and complex, but it can be seen to be more efficient than the effect of fluid shearing alone.

However, although the sediment transport process on the accelerating stoss side of the dune is more efficient, there is also an additional power loss when the flow re-expands after the crest, and so the question is whether the added efficiency of convective pressure transfer is greater than this expansion loss.

The overall bedload efficiency of a dune can be obtained from a known sediment transport rate and power dissipation. The average sediment transport rate can be obtained from the geometry and kinematics of a dune as discussed in Chapter 4. Therefore Fig. 4.6 may be used to give

$$q_s = \frac{A_d C_b}{(L_d/c)} \tag{6.16}$$

where q_s = unit sediment discharge; A_d = sidewise area of the mobile part of a dune; C_b = sand concentration under loose condition; c = celerity of dune; and L_d = wave length of a dune.

Therefore, the immersed weight sediment transport rate based on Eq. 6.16 is:

$$i_s = q_s \gamma (s_s - 1) \qquad (6.17)$$

where γ = unit weight of water; and s_s = specific gravity of sand.

The pressure difference between two successive crests is the overall head loss over a dune, because the velocity head at each crest of the dunes is constant. Therefore the power dissipation over a single dune length can be obtained from the pressure measurements between dune crests and the flow discharge rate. The total head loss includes the loss due to sudden expansion downstream of the crest, the frictional loss of the side walls, and the loss to sediment transport of the dune. But in finding the overall bedload efficiency, the frictional loss due to the side walls will be subtracted from the total head loss over one cycle of dune. The frictional head loss from the side walls is obtained by assuming an equivalent pipe flow and using the Moody diagram to obtain the equivalent friction factor. Since the test section was constructed from a Plexiglas, a smooth-wall approximation was used.

Therefore, the stream power can be calculated as follows:

$$\omega = q\gamma S_{fd} \qquad (6.18)$$

where q = unit flow discharge, and S_{fd} = energy slope of the dune. The overall energy slope of a dune was obtained by considering the pressure drop between successive dune crests.

Based on Bagnold's stream-power approach, Eqs. 6.17 and 6.18 may be combined to give bedload efficiency values. Therefore,

$$e_b = \frac{i_b \tan \phi'}{\omega}$$

(6.19)

where ϕ' = internal angle of friction.

In the above analysis, the overall head loss over the entire dune was considered in evaluating the stream power. But, in the region between the crest and the reattachment point, an expansion head loss occurs that does not contribute to the streamwise sediment transport rate. The effective region of sediment movement is the stoss side of the dune where the effect of convective acceleration is significant. Therefore, the power available for transport over the stoss region is even lower, so that the transport efficiency in the stoss region is higher than the overall value which can be calculated from Eq. 6.19.

The results for the three dune cases studied are tabulated on Table 6.7. In summary, these results show that the sediment transport efficiency over the stoss side of a dune to be about double the value for the overall bedload efficiency factor a whole dune length. The overall bedload efficiency factor for dunes is similar to that given by Bagnold (1966) for flat bed condition. This result is supported by the river data compiled by Bagnold (1966) where the sediment transport efficiency factors for rivers, which presumably contained dunes and ripples, was about 10 %, close to Bagnold's flat bed value.

Table 6.1. Measurements of fluid average velocities at the test-section

for the stationary bedwave

	Section 1	Section 2	Section 3
Maximum vel. (*m/s*)	1.989	2.072	2.133
Average vel. (*m/s*)	1.874	1.927	1.961
Depth of flow (*m*)	0.133	0.130	0.128

Table 6.2. Measurement summary for sections 1 and 3 of the stationary bedwave

Section	Depth of flow (*m*)	Vel., avg. (*m/s*)	Pressure head (*m*)	$\rho \sum u^2 dA$ (*N*)
1 - including carpet (57-67mm)	0.143	1.792	0.323	98.21
3 - including carpet (62-72mm)	0.138	1.878	0.293	101.8

Table 6.3 Dune kinematics measurements and results ($k = 1.13$ *cm/s*)

Dune height (*cm*)	Distance from crest (*cm*)	Measured unit sediment discharge (cm^2/s)	Unit sed. disc. from kinematics (cm^2/s)	Estmat. of effective dune height (*cm*)
7.1	0.0	4.25	4.90	6.2
5.6	55.0	3.62	3.86	5.2

Table 6.4. Flow parameters of dune for unit discharge of 0.115 m^2/s

	Section 1	Section 2	Section 3 (crest)
$\overline{u}$ (m/s)	0.722	0.898	1.045
$\overline{p}/\gamma$ (cm)	23.7	21.8	19.5
$\overline{y}$ (m)	0.160	0.120 ± 0.003	0.105 ± 0.003
A (m^2)	0.037	0.028	0.024
α	1.263	1.113	1.178
β	1.099	1.047	1.052
Distance between sections 1 and 2, and between sections 2 and 3 is 0.5 m.			
Pressure drop between sections 1 and 2 is 2.0 cm, and between sections 2 and 3 is 2.3 cm.			

Table 6.5. Flow parameters of dune for unit discharge of 0.136 m^2/s

	Section 1	Section 2	Section 3 (crest)
$\overline{u}$ (m/s)	0.837	1.04	1.170
$\overline{p}/\gamma$ (cm)	23.9	21.3	18.8
$\overline{y}$ (m)	0.160	0.125 ± 0.003	0.110 ± 0.003
A (m^2)	0.037	0.029	0.025
t (mm)	2.5	6.8	8.0
α	1.105	1.069	1.145
β	1.28	1.027	1.061
Distance between sections 1 and 2, and between sections 2 and 3 is 0.5 m.			
Pressure drop between sections 1 and 2 is 2.6 cm, and between sections 2 and 3 is 2.5 cm.			

145

Table 6.6. Head loss and dune speed for different unit discharges and pump speeds

Pump speed (RPM)	Unit discharge (m^2/s)	Dune speed (cm/s)	Head loss per dune length (mm)	Expansion loss (mm)
30	0.115	0.625	26	15.3
35	0.136	1.130	30	16.9
37	0.149	1.430	40	22.0

Table 6.7. Dune bedload transport efficiency factors

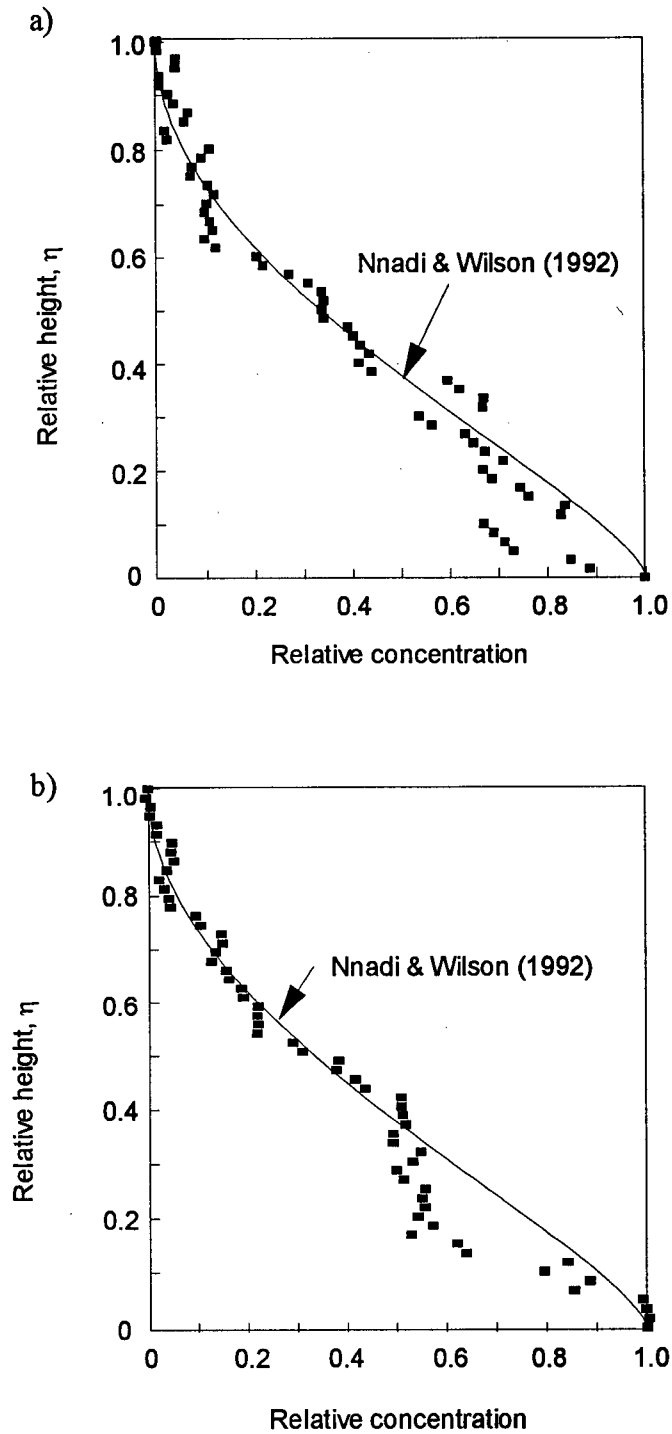| Pump speed (RPM)	Unit discharge (m^2/s)	Sed. transport (cm^2/s)	Overall efficiency factor (%)	Effic. factor over stoss side (%)
30	0.115	1.510	9.7	20.0
35	0.136	2.778	12.7	19.3
37	0.149	3.450	11.5	24.0

Figure 6.1. Variation of concentration with height within the carpet
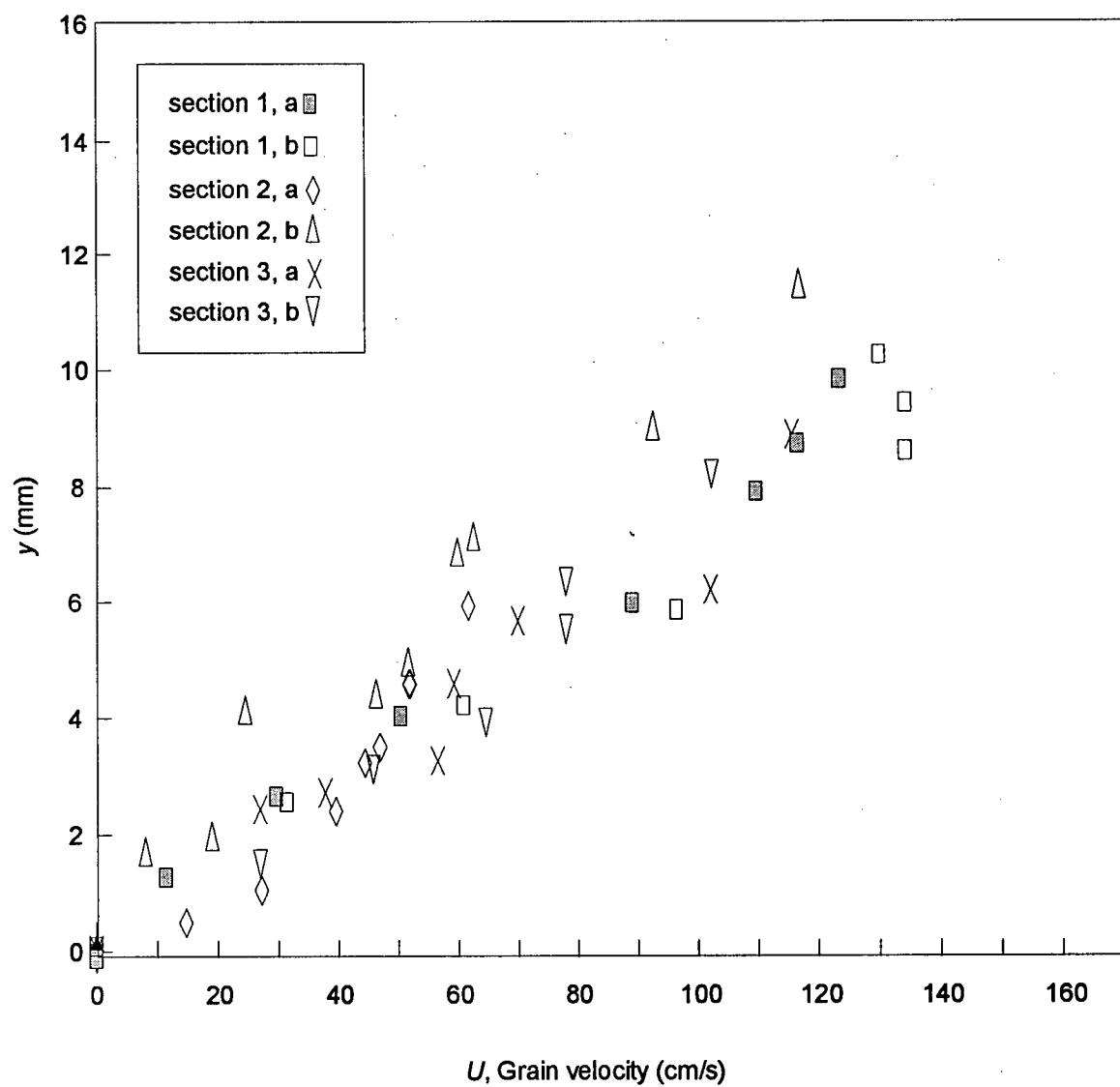layer for data taken at two different times

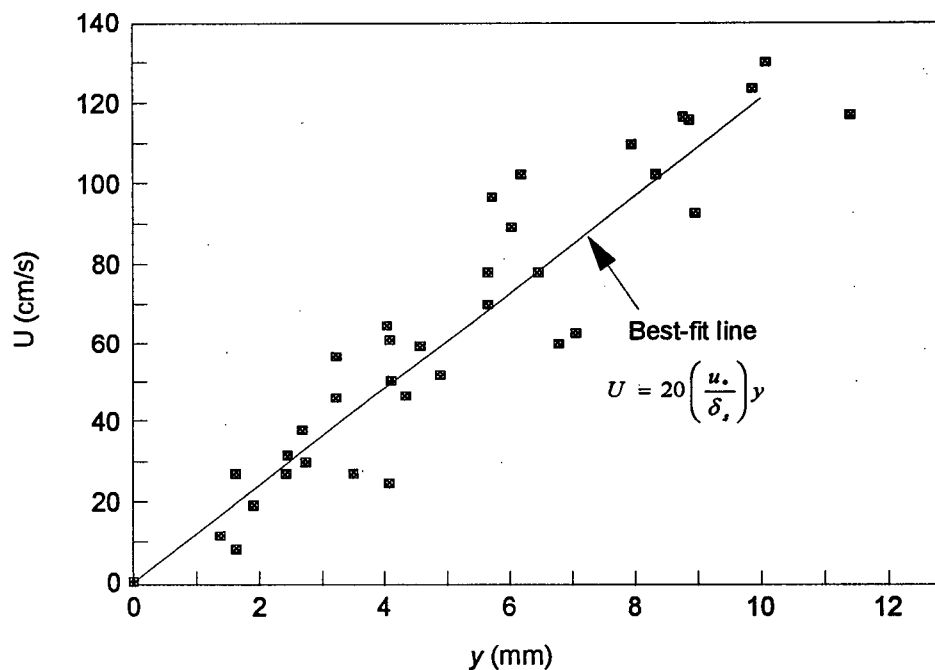Figure 6.2. Grain velocity data points for the three sections (Fig. 5.5)

Figure 6.3. Grain velocity data points and best-fit line for the stationary bedwave
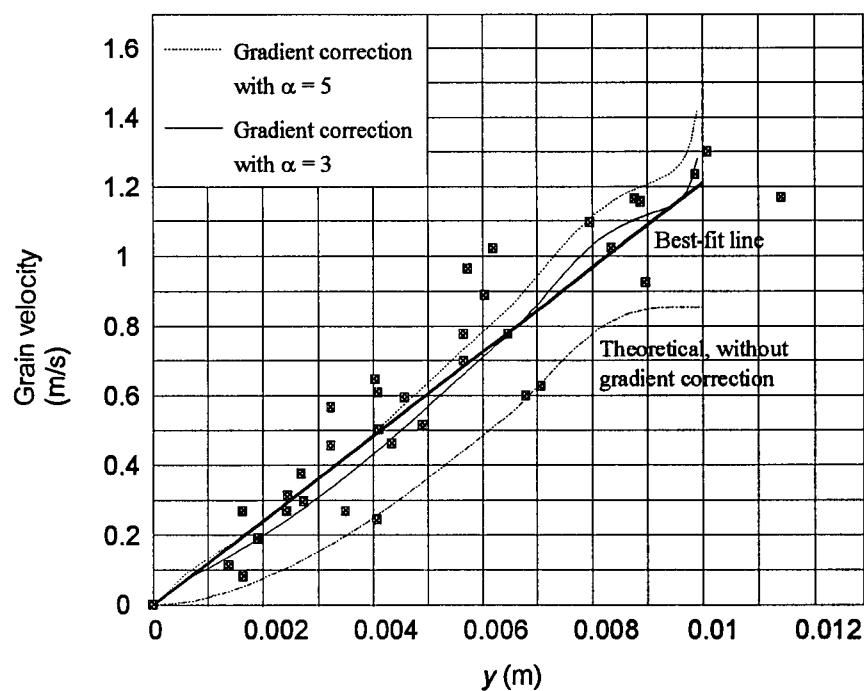

Figure 6.4. Theoretical and experimental grain velocity profiles for the stationary bedwave
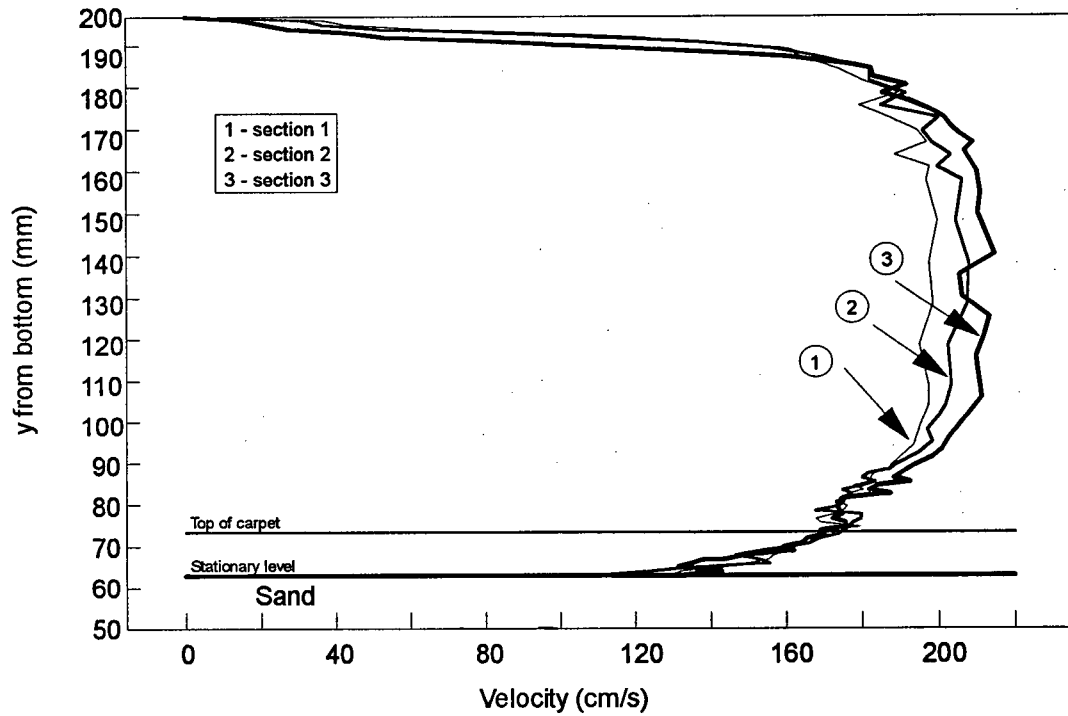
Figure 6.5. Velocity measurements at three sections of the stationary bedwave (Fig. 5.5)
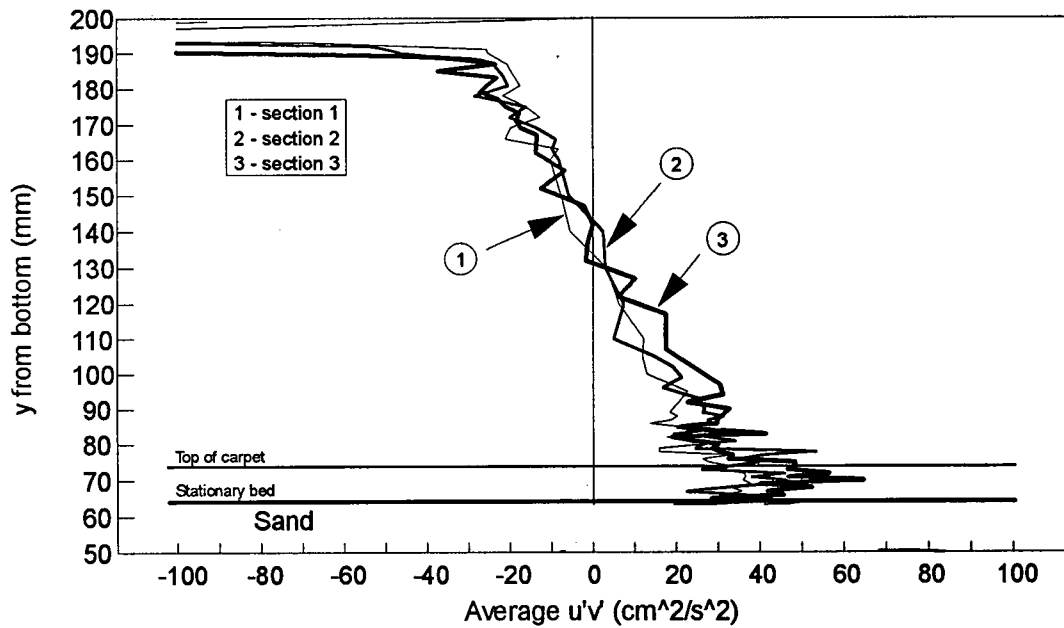
Figure 6.6. Reynolds stresses for the three sections of the stationary bedwave (Fig. 5.5)
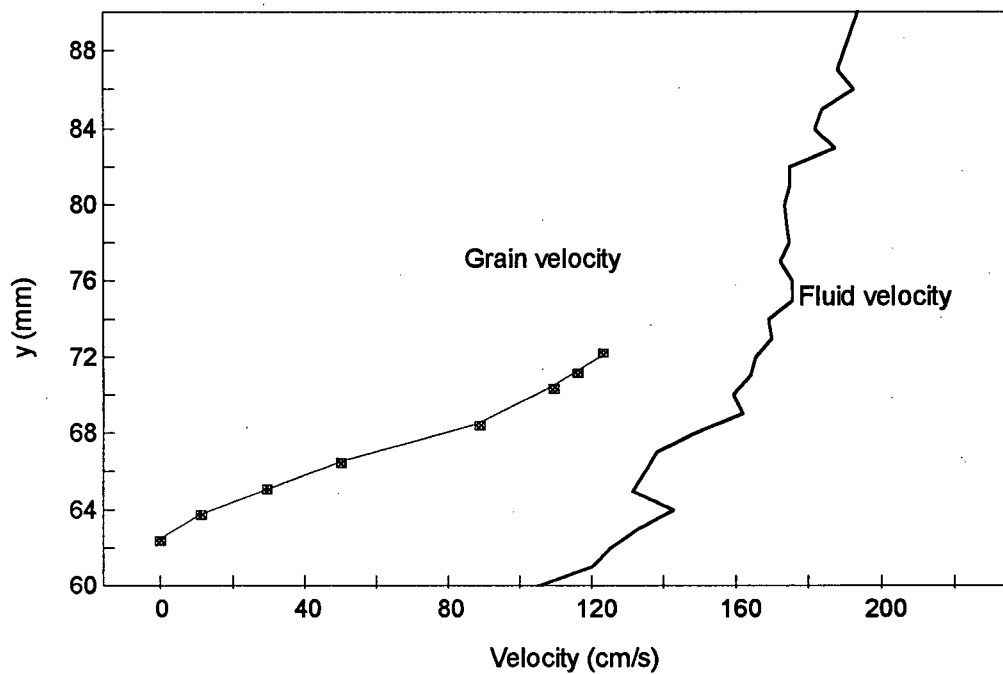
Figure 6.7. Grain and fluid velocity measurements at section 3, Fig. 5.5
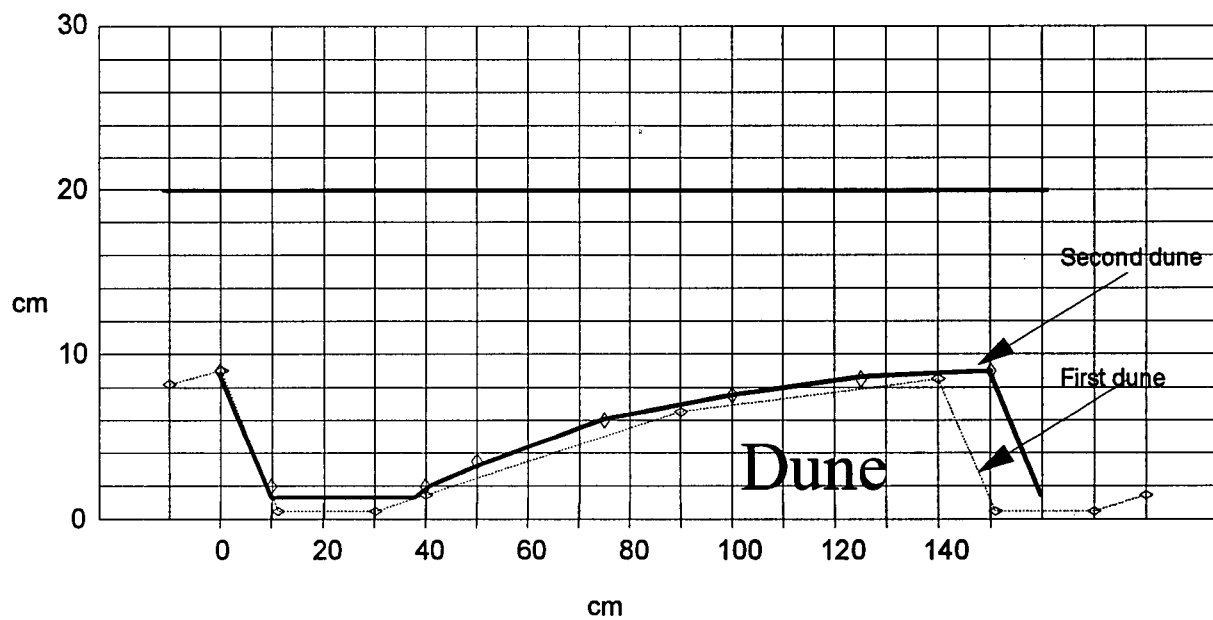
Figure 6.8. Comparison between the first and second dune geomerty
with and without the extended entry length
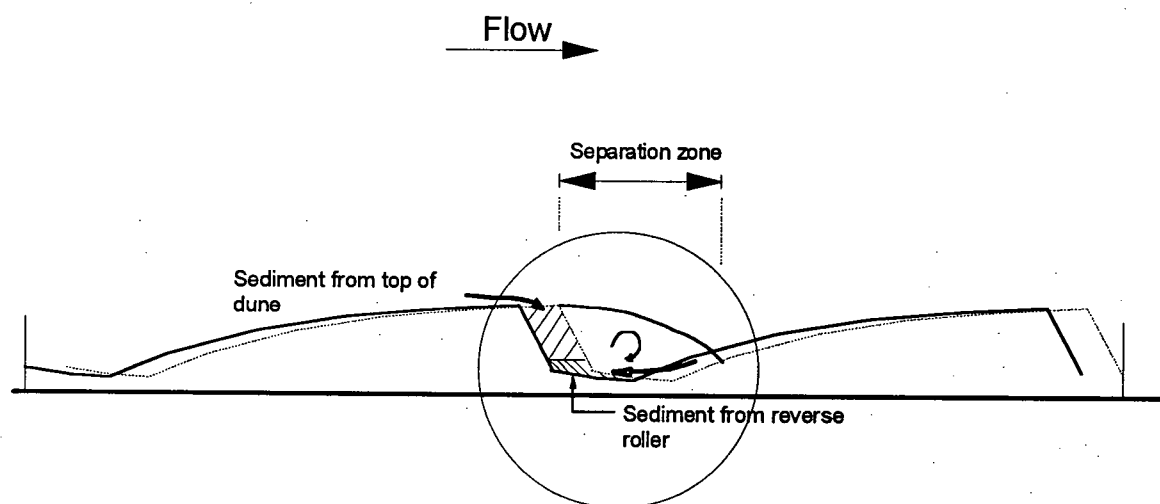
Flow

Figure 6.9. Flow over a dune
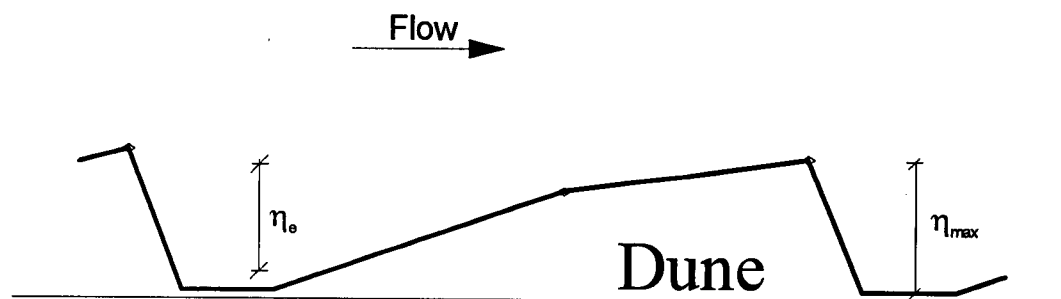
Flow

Figure 6.10. Definition schetch for a dune
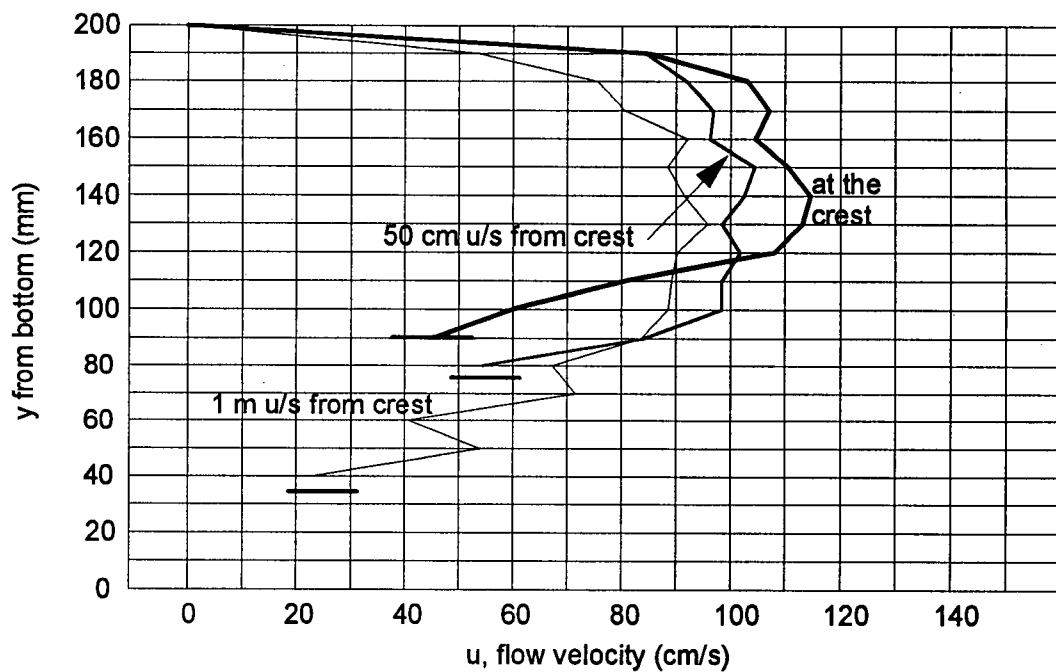
Figure 6.11a. Velocity profile over a dune with q = 0.115 m²/s, Fig. 4.2
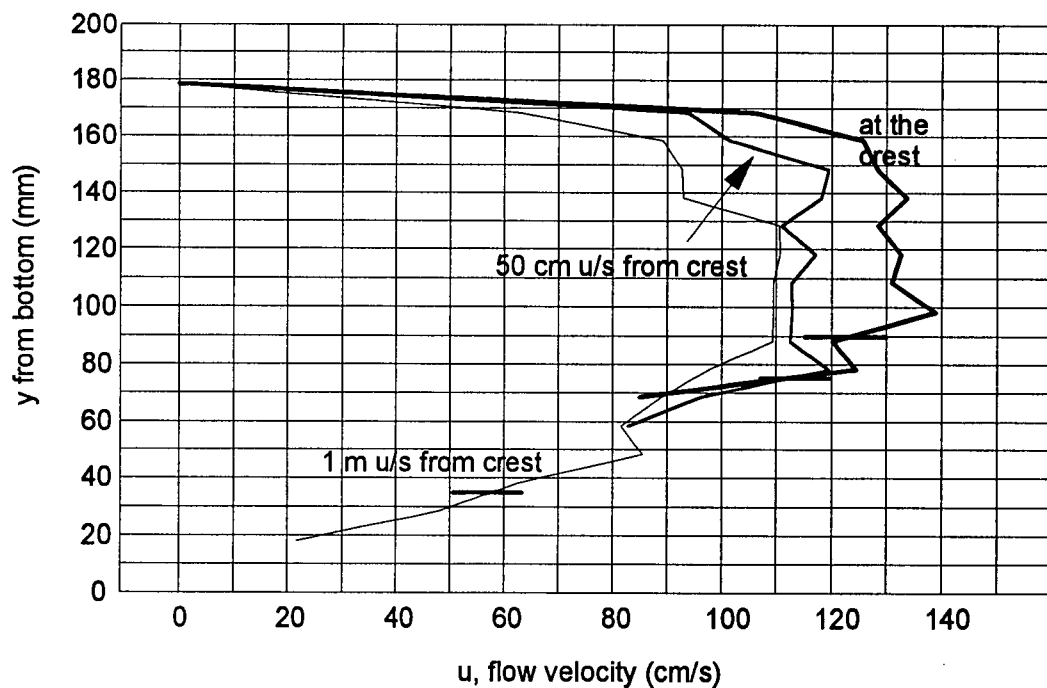
Figure 6.11b. Velocity profile over a dune with q = 0.136 m²/s, Fig. 4.2
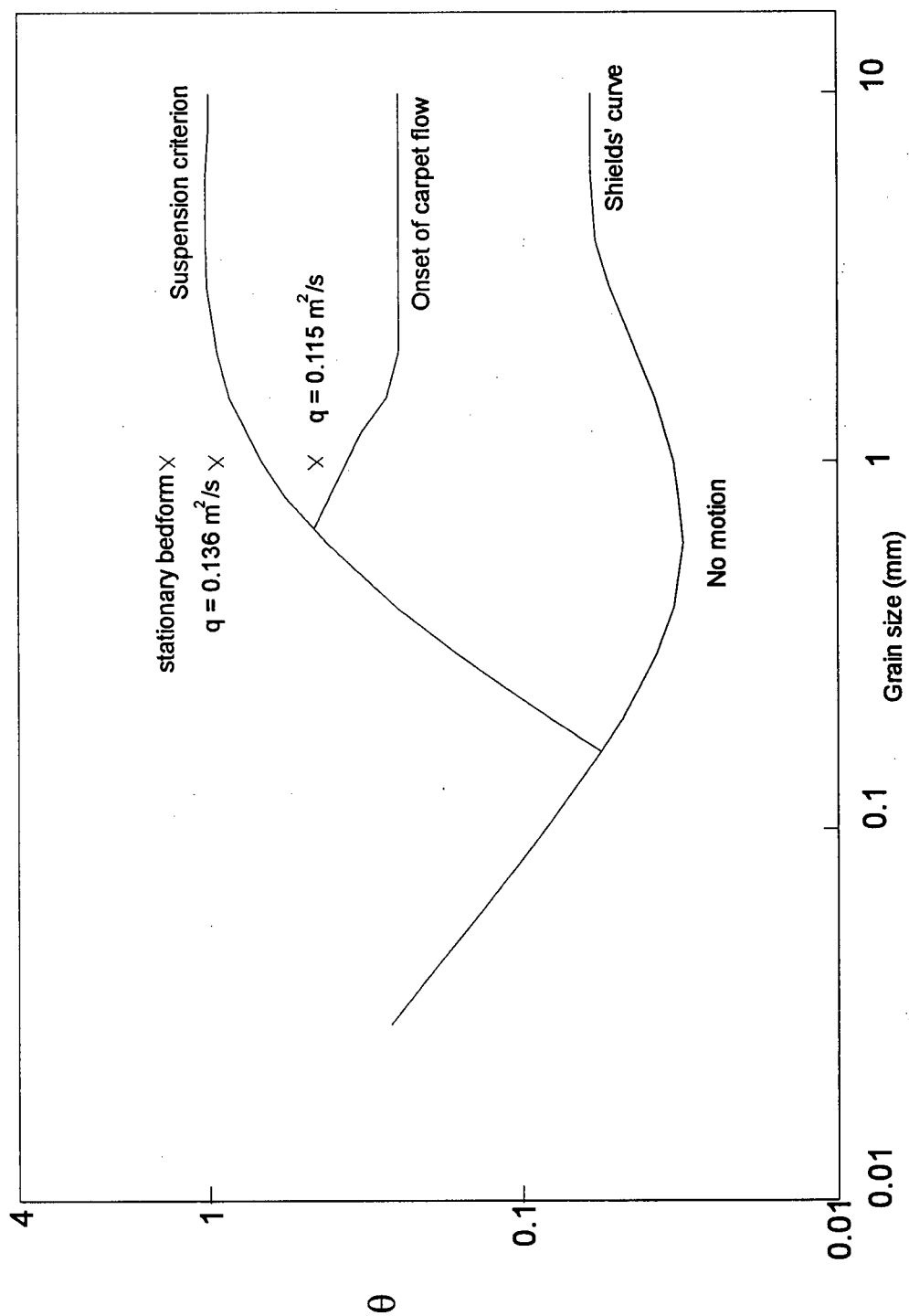
Figure 6.12. Suspension and no-motion criteria for a carpet flow
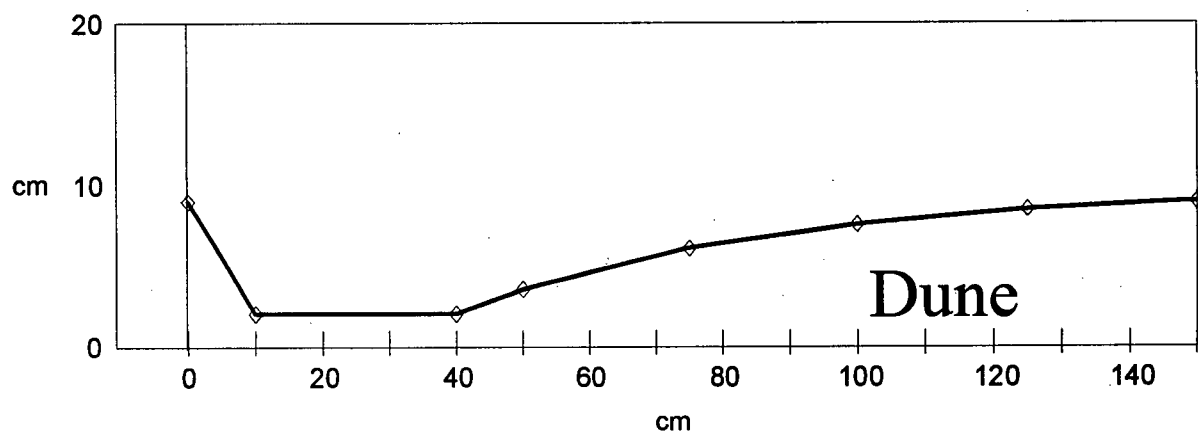
Figure 6.13 Average dune geometry for different flow discharges
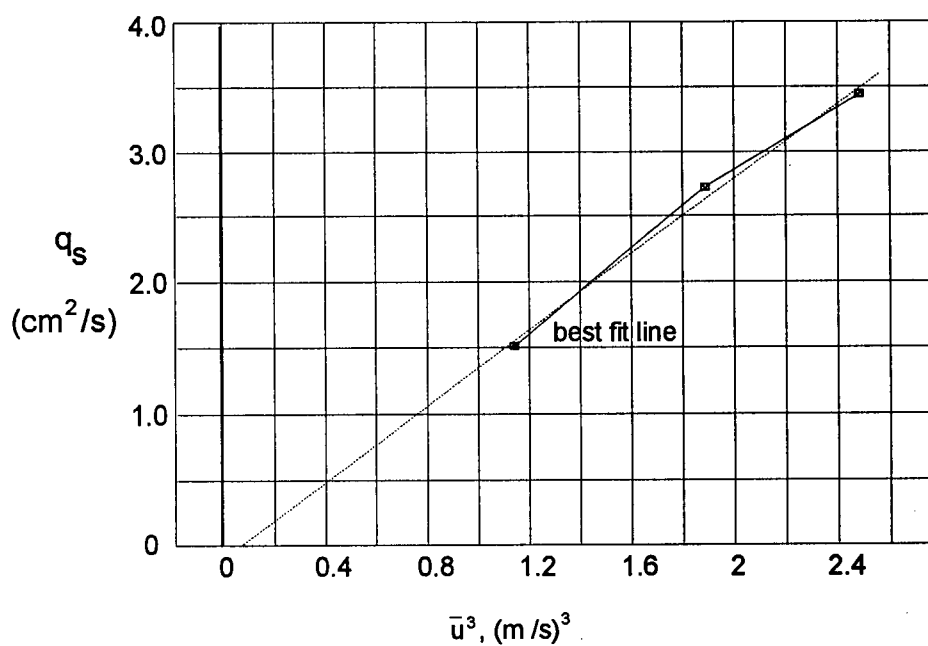
Figure 6.14 Variation of $\bar{u}^3$ related to the stream power, with sediment discharge
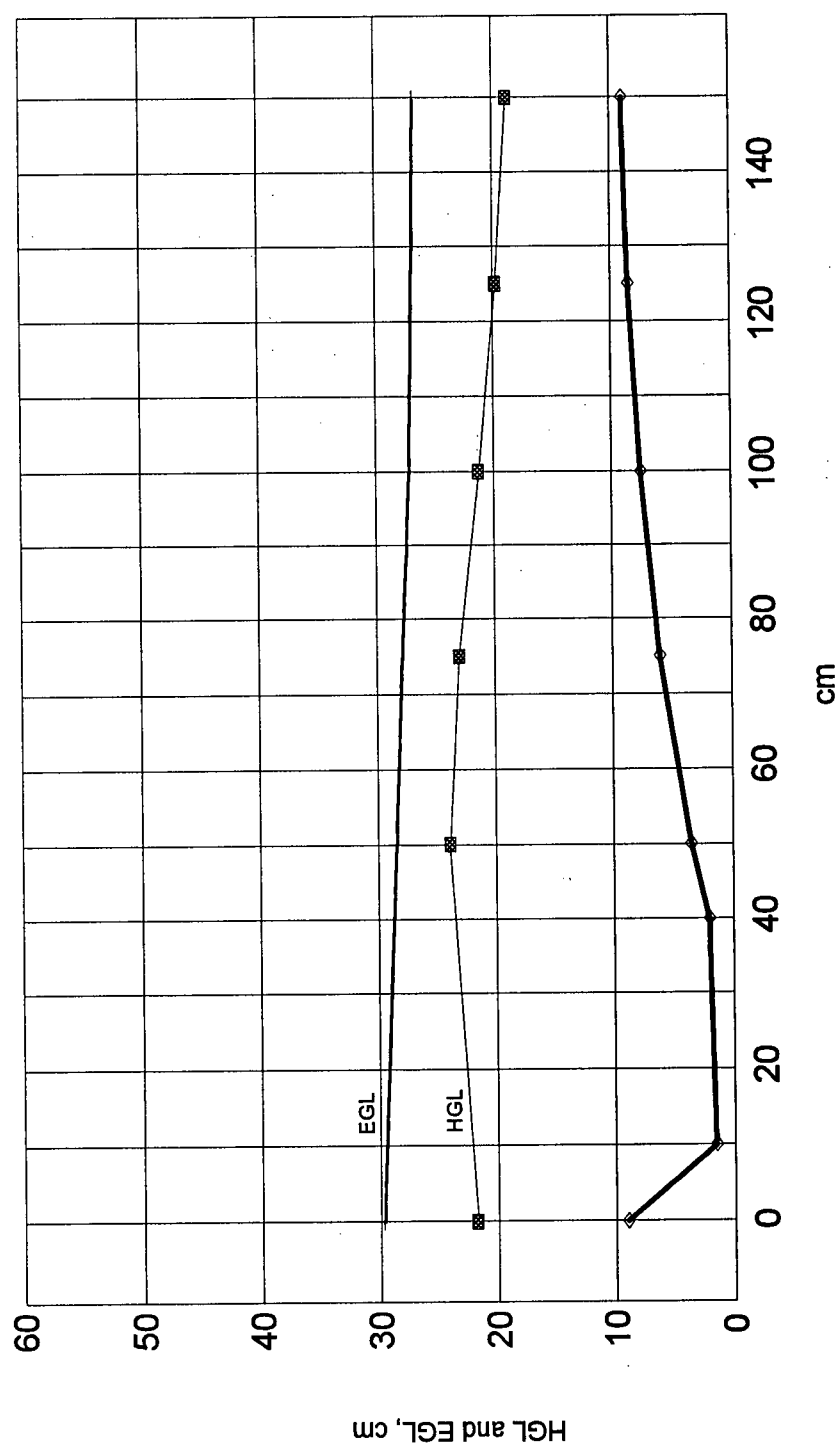
Figure 6.15. HGL and EGL over the dune with q = 0.136 m²/s
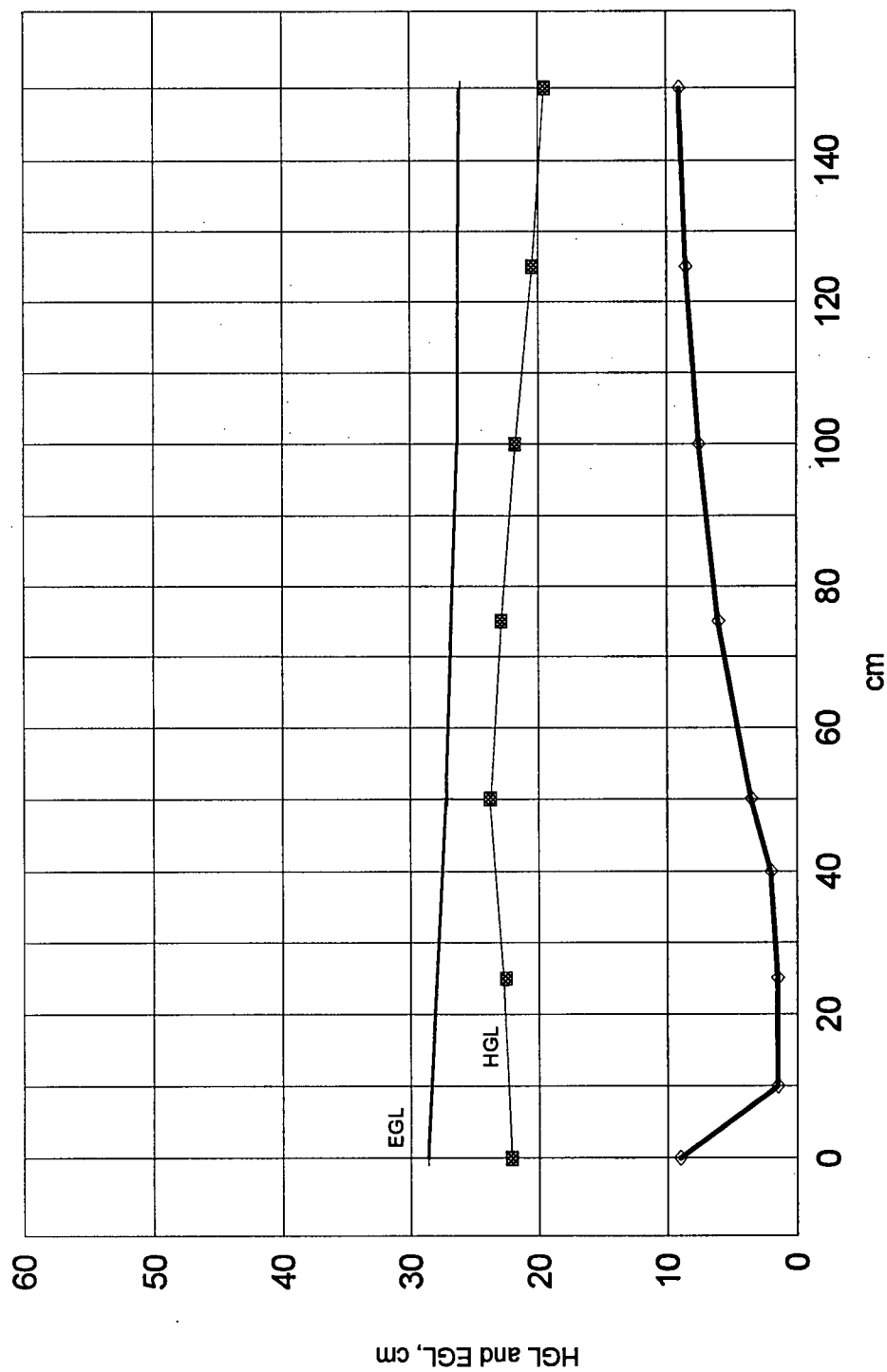
Figure 6.16. HGL and EGL over the dune with q = 0.115 m^2/s
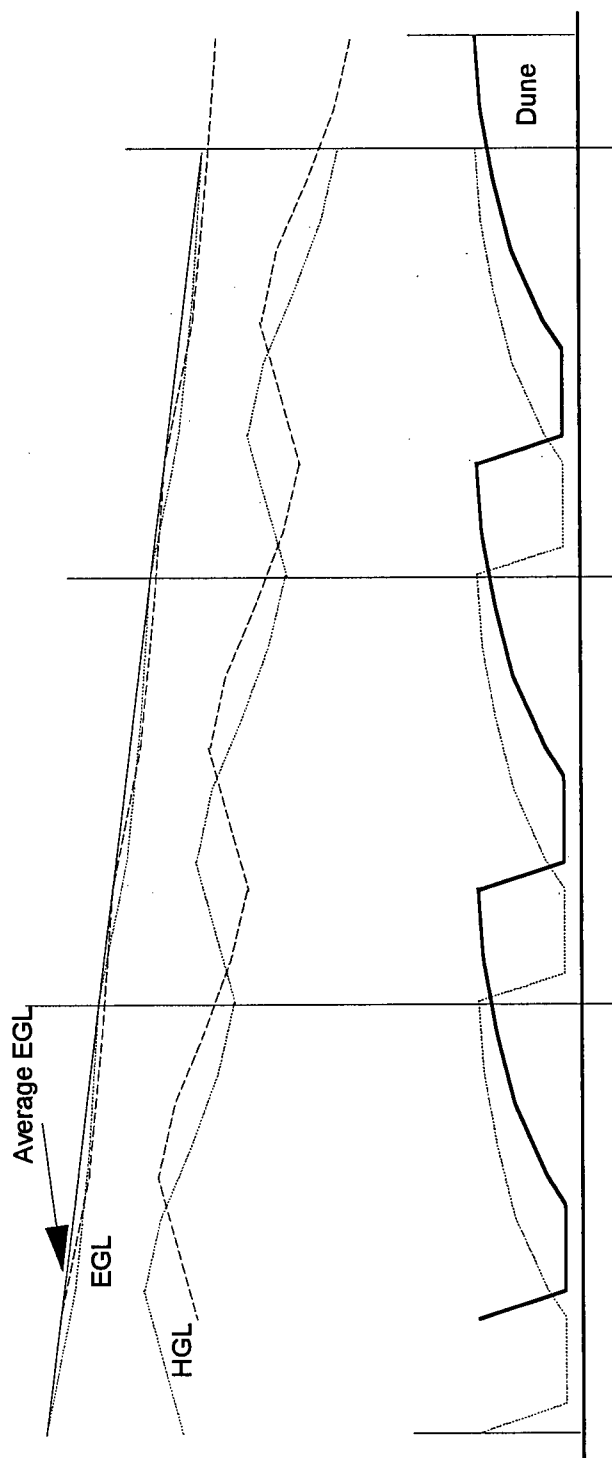
Figure 6.17. Overall HGL and EGL pattern over several dunes
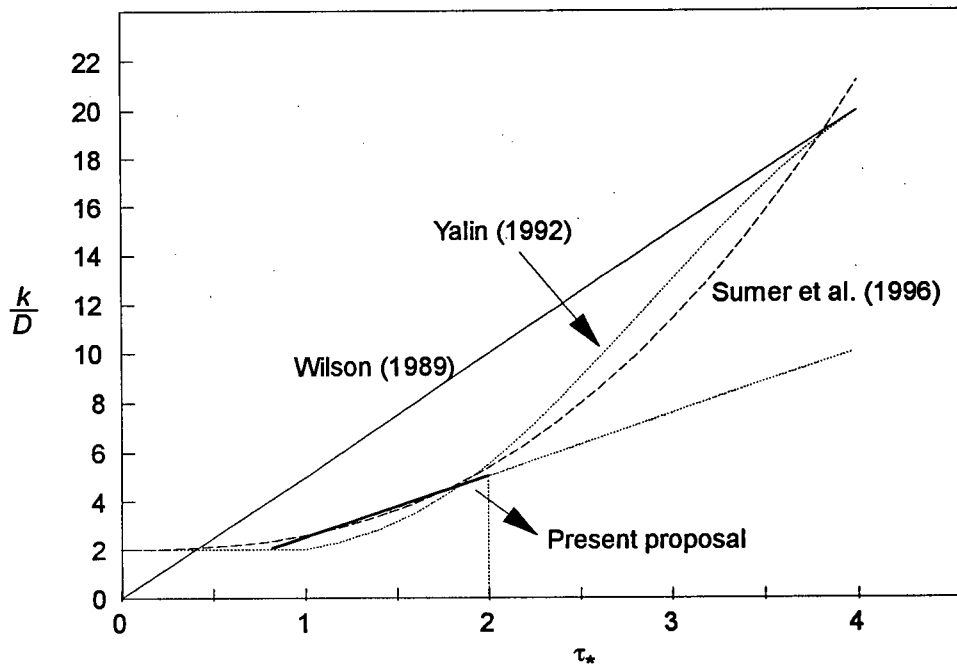
Figure 6.18. Variation of relative roughness, *k/D*, with Shields parameter, τ_*

CHAPTER 7

CONCLUSIONS AND RECOMMENDATIONS

7.1   Conclusions

This study is concerned with intense bedload transport under non-uniform flow conditions, which occur when sediment bedwaves are formed. The study has been mainly theoretical, but with some supporting experimental work to test the theoretical ideas. Theory has been developed for a convectively accelerating flow and it is argued that the strong pressure gradient produced by the fluid acceleration causes additional transporting stress on the moving sediment carpet. The theory indicates that an additional stress arises from the convective pressure gradient which acts directly on the individual sediment grains. This direct force is like a buoyancy force on an immersed object, because it is caused by a pressure gradient.

Bagnold's dispersive pressure concept is considered to be fundamentally true, so that the fluid shear force and the additional direct pressure force on the particles create a total shear stress within the carpet, and a corresponding dispersive pressure must match the weight of the sediments in motion. Using these concepts, a control volume analysis of flow over a bedwave was carried out and the various governing factors were identified.

The control volume analysis indicates that the convective acceleration produces a significant pressure gradient which can increase the shear stress on a carpet layer. A significant part of this additional shear stress is caused by the direct pressure gradient acting on the sediment particles.

This analysis indicates that the transfer of stress from the fluid to the grains can be more efficient because of this pressure gradient term. The additional pressure acts across the whole cross-section on both the fluid and the grains. This is quite different to the fluid shear stress which must be gradually transferred to the grains, and which requires a slip velocity between the fluid and the grains. This shear transfer process produces loss in energy. In contrast, the pressure gradient is transmitted directly with no associated slip velocity loss. However, within the carpet, this pressure term produces additional shear stress and the resulting shearing involves energy loss within the carpet, as described by Bagnold. This analysis indicated that the sediment transport process could be more efficient than for the flat bed case because of the effect of the convective acceleration.

Experiments were carried out to check the theory and to determine the relative importance of the various terms involved in defining a carpet flow. The experiments included measurements of fluid velocity, pressure, bedwave geometry and speed, grain velocity and concentration. From this basic velocity data calculations were made to estimate the Reynolds stresses and the momentum flux, which are required for the control volume analysis. The main conclusions from these theoretical analyses and supporting experiments are given below.

The preliminary analysis of carpet flow under flat bed, uniform flow showed that a linear increase of particle concentration with depth gave a feasible solution of the governing equations and matches with the experimental measurements (Chapter 3). This theoretical study of carpet flow was made by employing Bagnold's (1954) semi-theoretical relationships that were based on his rotating-drum experiments. This theory considers the grain shear stress, coupled with the equilibrium of the submerged weight of sediments and the normal dispersive pressure. The theoretical results were compared with the experimental findings. Comparison was made for the

velocity profile of grains within the carpet layer, and the experimental grain velocity profile approximated a linear variation with depth. The theoretical results showed a reasonable fit with the experimental results except for some deviation near the top interface of the carpet, where the sediment concentration goes to zero.

Conclusions given below are for the non-uniform flow.

1) For the non-uniform flow over a dune, the shear stress level at the base of the carpet was calculated to be significantly higher than the fluid turbulent shear. This is established from the high speed video measurements of the carpet flow grain velocities and relative concentrations from which the weight of moving sediment was estimated. Further confirmation of the weight of moving sediment was given by the measurement of the bedwave speed and geometry. The transport rate was calculated from kinematic considerations.

2) The measurements of sediment transport correlated linearly with the cube of the mean velocity at the crest cross-section, confirming that sediment transport is a function of stream power.

3) The stream power for a total bedwave was calculated from the various measurements. Also the average sediment transport rate for the dune was calculated from the bedwave kinematics. The efficiency of sediment carpet flow was then calculated using these stream power and sediment transport values. The average efficiency for a complete dune wavelength was found to be very close to the flat bed value estimated theoretically by Bagnold (1966) of about 10 %.

However, the above estimate includes the expansion loss downstream of the crest, which is not attributable to the transport on the dune stoss. Therefore, a further calculation was made of the energy loss associated with the transporting region of the bedwave. For this part of the process, the average efficiency of the sediment transport was found to be about twice the overall efficiency, about 20 %, which confirms the higher efficiency produced by convective acceleration.

4) Identical bedwaves under different flow conditions were observed during the experiments. For a given flow range, they had almost identical geometry but different sediment transport rates. A theoretical analysis showed that the total shear stress is approximately a function of the average velocity squared for a given geometry of bedwave. Therefore, it indicates that the carpet tractive forces, both the fluid and pressure shear stresses, scale almost with the square of flow velocity for a limited range of flow. However, it leaves unanswered the question whether the dune size is influenced by the scale of the experiments.

5) The effective bedwave height obtained from the measured sediment transport rate was found to be less than the total bedwave height obtained from the geometry of a dune. A reverse roller at the re-circulation zone produces a reverse flow of sediment that contributes to the build up of sediment at the lee side of a dune. The value of the effective dune height is determined by observing the height of a dune above the flow reattachment point.

6) The expansion losses for the dunes between the crest and the flow reattachment point were estimated by comparing the total energy which was obtained from velocity and pressure measurements. This expansion loss for the dunes was found to be higher than the usual abrupt-expansion loss. It is possible that the frictional loss within the re-circulation zone is significant.

The overall summary of this study is that sediment bedwaves produce a convective flow field which causes an additional pressure gradient term. This pressure gradient causes extra shear stress within the moving sediment carpet. Also this pressure force is transferred to the carpet without the power loss associated with fluid shear stress transfer; and therefore the efficiency of transport is higher. However, this extra efficiency is partly offset by the expansion loss downstream of the dune crest, so that the overall efficiency of bedwave transport appears to be similar to the flat bed efficiency. A direct comparison of bedwave and flat bed transport is difficult, because each requires different flow conditions.

7.2   Recommendations

The present study was conducted with uniform grain sizes. This was done to avoid the possible complication that may arise from the use of graded grains. It is not clear how a mixture of sediments of different size would behave under intense bedload condition. The intergranular collisional strain-stress relationship for graded grains has to be defined theoretically and confirmed by experiments. Moreover, experiments have to conducted with different grain sizes, from fine to coarse sand.

Velocity measurement of the fluid was made by using the acoustic doppler technique. Due to the limitations of the instrument, the measurements of the fluid velocity within the carpet layer were not reliable. A measurement technique has to be devised to improve these measurements, and to check the validity of Prandtl's mixing-length concept within the carpet layer.

Finally, the geometric similarity of dunes for a given range of flow discharge needs further investigation to derive an explanation of the factors which control dune size.

REFERENCES

Acaroglu, E. R., and Graf, W. H. (1968). "Sediment transport in conveyance systems, Part 2." *Bull., International Association of Scientific Hydrology*, XIII(3), 123-135.

Ackermann, N. L., and Shen, H (1982). "Stresses in rapidly sheared fluid-solid mixtures." *Journal of the Engineering Mechanics Division*, ASCE, 108, 95-113.

Ackers, P., and White, W. R. (1973). "Sediment transport: new approach and analysis." *Journal of the Hydraulics Division*, ASCE, 99(11), 2041-2060.

Albertson, M. L., Simons, D. B., and Richardson, E. V. (1958). "Discussion of 'Mechanics of sediment ripple formation,' by H. K. Lui." *Journal of Hydraulic Division*, ASCE, 84(1), 23-31.

Babic and Shen (1989). "A simple mean free path theory for the stresses in a rapidly deforming granular material." *Journal of Engineering Mechanics*, ASCE, 115, 1262-1282.

Bagnold, R. A. (1954). 'Experiments in a gravity-free dispersion of large solid spheres in a Newtonian fluid under shear." *Proc., Royal Society of London*, A 225, 49-63.

Bagnold, R. A. (1956). 'The flow of cohesionless grains in fluids." *Phil. Trans., Royal Society of London*, A 249, 235-297.

Bagnold, R. A. (1966). "An approach to the sediment transport problem from general physics." *Physiographic and Hydraulic Studies*, Geological Survey Professional Paper 422-I, U.S. Geological Survey, Washington, D.C., USA.

Bagnold, R. A. (1973). 'The nature of saltation and "bedload" transport in water." *Phil. Trans., Royal Society of London*, A 332, 473-504.

Bailard, J. A. (1981). "An energetics total load transport model for a plane sloping beach." *Journal of Geophysical Research*, 86C, 10938-10954.

Bailard, J. A. and Inman, D. L. (1981). "An energetics total load transport model for a plane sloping beach: local transport." *Journal of Geophysical Research*, 86C, 2035-2043.

Barnes, Jr., H. H., (1967). *Roughness Characteristics and Natural Channels*, Geological Survey Water-Supply Paper 1849, U. S. Geological Survey, Washington, D.C., USA.

REFERENCES

Bogardi, J. (1959). "Hydraulic similarity of river models with mobile bed." *Acta Technica*, Hungary, Vol. 24.

Brownlie, W. R. (1981). *Prediction of Flow Depth and Sediment Discharge in Open Channels*, Report No. KH-R-43A, W. M. Keck Laboratory, Caltech, USA.

Chen, G., and Yang, Y. (1989). "Flow structure and bed load transport on the plane movable bed." *Proc., Fourth International Symposium on River Sedimentation* (IRTCES, editor), China Ocean Press, Beijing, China, 1, 474-481.

Chow, V. T. (1959). *Open-Channel Hydraulics*. McGraw-Hill, Inc., New York, USA.

Cook, H. L. (1935). "Outline of the energetics of stream-transportation of solids." *Proc., American Geophysical Union*, Reports and Papers, Hydrology -- 1935, 456-463.

Coulomb, C. A. (1773). "Essai sur une application des regles de maximis et minimus a quelque problems de statique relatifs a l'architecture." *Acad. R. Sci. Mem. Math. Phys.*, 7, 343-382.

Cowan, W. L. (1956). "Estimating hydraulic roughness coefficients." *Agricultural Engineering*, 37(7), 473-475.

Daily, J. W., and Harleman, D. R. F. (1966). *Fluid Dynamics*. Addison-Wesley, Inc., Massachusetts, USA.

du Boys, M. P. (1879). "Études du regime et l'action exercée par les eaux sur un lit à fond de graviers indefiniment affouilable." *Annales de Ponts et Chaussés*, 5(18), 141-195.

Einstein, H. A., and Graf, W. H. (1966). "Loop system for measuring sand-water mixtures." *Journal of the Hydraulics Division*, ASCE, 92(1), 1-12.

Einstein, H. A. and Barbarossa, N. L., (1952). "River channel roughness." *Transactions, ASCE*, 117, 1121-1132.

Engelund, F. (1966). "Hydraulic resistance of alluvial streams." *Journal of the Hydraulics Division*, ASCE, 92(2), 315-326.

Engelund, F. (1981). "Transport of bed load at high shear stress." *Progress Report 53*, Institute of Hydrodynamics and Hydraulic Engineering, Technical University of Denmark, 31-35.

Engelund, F. and Hansen, E. (1967). *A monograph on sediment transport in alluvial streams*, Teknisk Forlag, Copenhagen.

REFERENCES

Eshagira, S., and Ashida, K. (1992). "Unified view of the mechanics of debris flow and bed-load." *Advances in Micromechanics of Granular Materials* (Shen, H. H., et al., editors), 391-400.

Eshagira, S., and Ashida, K., Yajima, H., and Takahama, J. (1989). "Constitutive equation of debris flow." *Annuals, Disaster Prevention Research Institute*, Kyoto University, 32(B-2), (in Japanese).

Garde, R. J., and Ranga Raju, K. G. (1963). "Regime criteria for alluvial streams." *Journal of the Hydraulics Division*, ASCE, 89(6), 153-164.

Garde, R. J. and Ranga Raju, K. G. (1970). "Discussion of 'Friction-factors for flat-bed flows in sand channel' by F. Lovera and J. F. Kennedy." *Journal of the Hydraulics Division*, ASCE, 96(4), 1052-1056.

Garde, R. J. and Ranga Raju, K. G. (1985). *Mechanics of sediment transportation and alluvial stream problems*. 2nd edition, Wiley Western Limited, India.

Graf, W. H. (1971). *Hydraulics of Sediment Transport*, McGraw-Hill, Inc., New York, USA.

Graf, W. H., and Weisman, R. N. (1969). "Continuous measurement of water-sand mixtures." *22nd International Navigation Congress, Section 2 Ocean Navigation*, 17-26.

Griffiths, G. A. (1993). "Comment on 'Flow resistance under conditions of intense gravel transport' by J. Pitlick." *Water Resources Research*, 29(7), 2457-2458.

Gust, G., and Southard, J. (1983). "Effects of weak bed load on the universal law of the wall." *Journal of Geophysical Research*, 88(10), 5939-5952.

Hanes, D. M. (1984). "Flow resistance due to intense bedload transport." *Proc., 19th International Coastal Engineering Conference*, ASCE, Chapter 89, 1306-1310.

Hanes, D. M. (1986). "Grain flows and bed-load sediment transport: Review and extension." *Acta Mechanica*, 63, 131-142.

Hanes, D. M., and Bowen, A. J. (1985). "A granular-fluid model for steady intense bed-load transport." *Journal of Geophysical Research*, 90(C5), 9149-9158.

Hanes, D. M., and Inman, D. L. (1985a). "Experimental evaluation of a dynamic yield criterion for granular fluid flows." *Journal of Geophysical Research*, 90(B5), 3670-3674.

Hanes, D. M., and Inman, D. L. (1985b). "Observations of rapidly flowing granular-fluid materials." *Journal of Fluid Mechanics*, 150, 357-380.

REFERENCES

Hetsroni, G. (1993). "The effect of particles on turbulence in a boundary layer." *Particulate Two-Phase Flow* (Roco, M. C., editor), Butterworth-Heinemann Series in Chemical Engineering, Storeham, Massachusetts, USA, 244-261.

Hiscott, R. N. (1994). "Traction carpet stratification in turbidites--fact or fiction?" Journal of Sedimentary Research, A64(2), 204-208.

Iverson R. M., and Denlinger, R. P. (1987). "The physics of debris flows -- a conceptual assessment." *Erosion and Sedimentation in the Pacific Rim*, Proceedings of the Corvallis Symposium, IAHS Publication No. 165, 155-165.

Jenkins, J. T., and Savage, S. B. (1983). "A theory for the rapid flow of identical, smooth, nearly elastic, spherical particles." *Journal of Fluid Mechanics*, 130, 187-202.

Johnson, P. C., and Jackson, R. (1987). "Frictional-collisional constitutive relations for granular materials, with application to plane shearing." *Journal of Fluid Mechanics*, 176, 67-93.

Keluegan, G. H. (1938). "Laws of turbulent flow in open channels." *Journal of Research*, National Bureau of Standards, Washington, D.C., Research Paper 1151, 21, 707-741.

Kinfu, Y., and Quick, M. C. (1994). "Carpet flow analysis." *Proc., 1994 ASCE National Conference on Hydraulic Engineering*, Buffalo, New York, USA, 1961-1965.

Kirkgöz, M. H. (1989). "Turbulent velocity profiles for smooth and rough open channel flow." *Journal of Hydraulic Engineering*, ASCE, 115(11), 1543-1561.

Kraus, N. C., Lohrmann, A., and Cabrera, R. (1994). "New acoustic meter for measuring 3D laboratory flows." *Journal of Hydraulic Engineering*, ASCE, 120(3), 406-412.

Lamberti, A., Montefusco, L., and Valiani, A. (1991). "A granular-fluid of the stress transfer from the fluid to the bed." *Proc., Euromech 262 Colloquium on Sand Transport in Rivers, Estuaries and the Sea* (Soulsby , R. and Bettess R., editors), 209-214.

Langbein, W. B. (1942). "Hydraulic criteria for sand waves." *Transactions, American Geophysical Union*, 615-618.

Limerinos, J. T. (1970). "Determination of the Manning coefficient from measured bed roughness in natural channels." *Studies of Flow in Alluvial Channels*, Geological Survey Water-Supply Paper 1898-B, U. S. Geological Survey, Washington, D.C., USA.

Lovera, F. and Kennedy, J. F. (1969). "Friction-factors for flat-bed flows in sand channels." *Journal of the Hydraulics Division*, ASCE, 95(4), 1227-1234.

REFERENCES

Lun, C. K .K., Savage, S. B., Jeffrey, D. J., and Chepurniy, N. (1984). "Kinetic theories for granular flow: inelastic particles in Coutte flow slightly inelastic particles in a general flow flied." *Journal of Fluid Mechanics*, 140, 223-256.

Luque, F. R. and van Beek, R. (1976). "Erosion and transport of bedload sediment." *Journal of Hydraulic Research*, IAHR, 14(2), 127-144.

Lyn, D. A. (1991). "Resistance in flat-bed sediment-laden flows." *Journal of Hydraulic Engineering*, ASCE, 117(1), 94-114.

McDowell, D. M., (1989). "A general formula for estimation of the rate of transport of non-cohesive bed-load." *Journal of Hydraulic Research*, IAHR, 27(3), 355-361.

McLean, S. R., Nelson, J. M., and Wolfe, S. R. (1994). "Turbulence structure over two-dimensional bed forms: Implications for sediment transport." *Journal of Geophysical Research*, 99(C6), 12729-12747.

McTigue, D. F. (1978). "A model for stresses in shear flow of granular materials." *Proc., U.S.-Japan Seminar on Continuum Mechanical and Statistical Approaches in the Mechanics of Granular Materials* (Cowin, S. C., and Satake, M., editors), Gakujutsu Bunken, Fukyu-kai, Tokyo, Japan, 258-265.

Meyer-Peter, E. and Müller, R. (1948). "Formulas for bed load transport." *Proceedings, 3rd Meeting of IAHR*, 39-64.

Miyamoto, K. (1985). "Mechanics of grain flows in Newtonian fluid." Ph.D. Thesis (in Japanese), Ritsumeikan University, Japan.

Nelson, J. M., McLean, S. R., and Wolfe, S. R. (1993). "Mean flow and turbulence fields over two-dimensional bed forms." *Water Resources Research*, 29(12), 3935-3953.

Nnadi, F. N. and Wilson, K. C. (1992). "Motion of contact-load particles at high shear stress." *Journal of Hydraulic Engineering*, ASCE, 118(12), 1670-1683.

Nnadi, N. F., and Wilson, K. C. (1995). 'Bed-load motion at high shear stress: Dune washout and plane-bed flow." *Journal of Hydraulic Engineering*, ASCE, 121(3), 267-273.

Ogawa, S., Umemura, A., and Oshima, N. (1980). "On the equations of fully fluidized granular materials." *ZAMP*, 31, 483-493.

Owen, P. R., (1964). "Saltation of uniform grains in air." *Journal of Fluid Mechanics*, 20, 225-242.

REFERENCES

Pacheco-Ceballos, R., (1990). "Transport of sediments: Analytical solution." *Journal of Hydraulic Research*, IAHR, 27(4), 501-518.

Pitlick, J. (1992). "Flow resistance under conditions of intense gravel transport." *Water Resources Research*, 28(3), 891-903.

Prandtl, L. (1933). "Neuere Ergebnisse Turbulenzforschung." *Zeitsschift des Vereins Deutscher Ingenieure*, Berlin, Germany, 77(5), 105-114 (in German).

Prandtl, L. (1956). *Führer durch die Strömungslehre*, Vieweg Verlag, Braunschweig.

Quick M. C., (1978). *Sediment transport by ripples and dunes*. Dept. of Civil Engineering, University of British Columbia, Vancouver, Canada.

Quick, M. C. (1982). "Sand ripple motion under combined surface wave and current action." *Euromech 156: Mechanics of Sediment Transport*, 275-280.

Quick, M. C. (1991). 'Reliability of flood discharge estimates." *Canadian Journal of Civil Engineering*, 18(4), 624-630.

Rákóczi, L. (1967). "Experimental study of flume-bed roughness." *Proc., International Association of Hydraulic Research 12th Congress*, 1, 181-186.

Reynolds, A. J. (1974). *Turbulent flows in Engineering*. John Wiley & Sons Ltd., USA.

Reynolds, O. (1885). "On the dilatancy of media composed of rigid paticles in contanct." *Philos. Mag.*, 5th Series, Vol. 20, 469-489.

Richardson, E. V. and Simons, D. B. (1967). "Resistance to flow in sand channels." *Proc., International Association of Hydraulic Research 12th Congress*, 1,141-150.

Rubey, W. W. (1933). "Equilibrium-conditions in debris-laden streams." *Proc., American Geophysical Union*, Reports and Papers, Hydrology -- 1933, 497-507.

Savage, S. B., and Jeffrey, D. J. (1981). "The stress tensor in a granular flow at high shear rates." *Journal of Fluid Mechanics*, 110, 225-272.

Savage, S. B., and Sayed, M. (1984). "Stresses developed by dry cohesionless granular materials sheared in an annular shear cell." *Journal of Fluid Mechanics*, 142, 391-430.

REFERENCES

Savage, S. B., and McKeown, (1983). "Shear stresses developed during rapid shear of concentrated suspensions of large spherical particles between concentric cylinders." *Journal of Fluid Mechanics*, 127, 453-472.

Shen, H., and Ackerman, N. L. (1982). "Constitutive relationships for solid-fluid mixtures." *Journal of Engineering Mechanics Division*, ASCE, 108(5) , 748-763.

Silin, N. A., Vitoshkin, Y. K., Karasik, V. M., and Ocheretko, V. F. (1969). "Research of the solid-liquid flow with high consistence." *Proc., 13th Congress of International Association of Hydraulic Research*, 2, 147-156.

Simons, D. B., and Richardson, E. V. (1966). "Resistance to flow in alluvial channels." *Studies of Flow in Alluvial Channels*, Geological Survey Professional Paper 422-J, U. S. Geological Survey, Washington, D.C., USA.

Shook, C. A., Gillies, R., Haas, D. B., Husband, W. H. W., and Small, M.(1982). "Flow of coarse and fine sand slurries in pipelines." *Journal of Pipelines*, 3, 13-21.

Stonestreet, S. E., Copeland R. R., and McVan, D. C. (1994). "Bed load roughness in supercritical flow." *Streams above the line: Channel morphology and flood control*, Proc., the Corps of Engineers Workshop on Steep Steams, 27-29 October 1992, Seattle, Washington, USA, Section 6.

Sumer, B. M., Kozakiewicz, A., Fredsøe, J., and Deigaard, R. (1996). "Velocity and concentration profiles in sheet-flow layer of movable bed." *Journal of Hydraulic Engineering*, ASCE, 122(10), 549-558.

Takahashi, T. (1978). "Mechanical characteristics of debris flow." *Journal of the Hydraulics Division*, ASCE, 104(8), 1153-1169.

Takahashi, T. (1980). "Debris flow on prismatic open channel." *Journal of the Hydraulics Division*, ASCE, 106(3), 381-396.

Takahashi, T. (1981). "Debris flow." *Annual Review of Fluid Mechanics*, 13, 57-77.

Takahashi, T. (1991). *Debris flow*, IAHR Monograph Series, A.A. Balkema, Rotterdam, The Netherlands.

Townsend, A. A. (1976). The structure of turbulent shear flow, 2nd edition, Cambridge University Press, UK.

Tsubaki, T., Hashimoto, H., and Suetsugi, T. (1983). "Interparticle stresses and characteristics of debris flow." *Journal of Hydroscience and Hydraulic Engineering*, 1(2), 67-82.

REFERENCES

Turner, J. S. (1973). *Buoyancy effects in fluids*. Cambrige University Pess, Cambridge, UK.

Valiankov, M. A. (1954). "Principle of the gravitational theory of the movement of sediments." *Academy of Science Bulletin, USSR*, Geophysics, Series No. 4, 349-359 (GTS Translation No. 62-15004).

Vanoni, V. A., and Nomicos, G. N. (1960). "Resistance properties of sediment-laden streams." *Trans., American Society of Civil Engineers*, 125(3055), 1140-1175.

Wan, Z., and Wang, Z. (1994). *Hyperconcentrated flow*, IAHR Monograph Series, A.A. Balkema, Rotterdam, The Netherlands.

Wang, Z. and Larsen, P. (1994). "Turbulent structure of water and clay suspensions with bed load." *Journal of Hydraulic Engineering*, ASCE, 120(5), 577-600.

Wang, Z., and Qian, N. (Ning, C.) (1984). "Experiment study of two-phase turbulent flow with hyperconcentration of coarse particles." *Scientia Sinica*, Series A, 27(12), 1317-1327.

Wang, Z., and Qian, N. (Ning, C.) (1985). "Experimental study of motion of laminated load." *Scientia Sinica*, Series A, 28(1), 102-112.

Wang, Z., and Qian, N., (Ning, C.) (1987). "Laminated load: Its development and mechanism of motion." *International Journal of Sediment Research*, 1 (November), 102-124.

Wang, Z., Zeng, Q., and Zhang, X. (1990). "Experimental study of solid-non-Newtonian fluid two-phase flow." *Journal of a Sediment Research*, 3, 2-13 (in Chinese).

Webb, E. K. (1970). "Profile relationships: The log-linear range, and the extension to strong stability." *Quartely Journal of the Royal Meteriological Society*, 96, 67-90.

White, W. R., Paris, E., and Bettess, R. (1980). "The frictional charactersitics of alluvial steams: a new approach." *Proc., Institution of Civil Engineers*, Part 2, 69, 737-750.

White, W. R., Bettess, R., and Wang, S. (1987). "Frictional characterstics of alluvial steams in the lower and upper regimes." *Proc., Institution of Civil Engineers*, Part 2, 83, 685-700.

Whiting, P. J., and Dietrich, W. E. (1990). Boundary shear stress and roughness over mobile alluvial beds." *Journal of Hydraulic Engineering*, ASCE, 116(12), 1495-1511.

Wiberg, P. L., and Rubin, D. M. (1989). "Bed roughness produced by saltating sediments." *Journal of Geophysical Research*, 94(C4), 5011-5016.

REFERENCES

Williams, G. P. (1970). "Flume width and water depth effects in sediment transport experiments." *Geological Survey Professional Paper 562-H*, U. S. Geological Survey, Washington, D.C., USA.

Wilson, K. C. (1966). "Bed-load transport at high shear stress." *Journal of Hydraulic Division*, ASCE, 92(6), 49-59.

Wilson, K. C. (1984). "Analysis of contact-load distribution and application to deposition limit in horizontal pipes." *Journal of Pipelines*, 4(3), 171-176.

Wilson, K. C. (1987). "Analyses of bed-load motion at high shear stress." *Journal of Hydraulic Engineering*, ASCE, 113(1), 97-103.

Wilson, K. C. (1989). "Mobile-bed friction at high shear stress." *Journal of Hydraulic Engineering*, ASCE, 115(6), 825-830.

Wilson, K. C. and Pugh, F. J. (1988). "Dispersive force basis for concentration profiles." *Journal of Hydraulic Engineering*, ASCE, 114(7), 806-810.

Wilson, K. C. and Nnadi, F. N. (1990). "Behaviour of mobile beds at high shear stress." *Proc., 22nd Inter'l Conference on Coastal Engineering*, ASCE, New York, N.Y., 3, 2536-2541.

Yalin, M. S. (1977). *Mechanics of sediment transport*. 2nd edition, Pergamon Press, London, UK.

Yalin, M. S. (1992). *River Mechanics*. Pergamon Press, Inc., Tarrytown, New York, USA.

Yang, C. T. (1972). "Unit stream power and sediment transport." *Journal of the Hydraulics Division*, ASCE, 98(10), 1805-1826.

Yang, C. T., and Molinas, A. (1982). "Sediment transport and unit stream power function." *Journal of the Hydraulics Division*, ASCE, 108(6), 774-793.

Yano, K, and Daido, A. (1969). "The effect of bed-load movement on the velocity distribution of flow." *Proc., 13th Congress of International Association of Hydraulic Research*, 2, 325-332.

APPENDIX A

The following are notations used in the computer programs.

coo   = maximum possible concentration of sand

co   = concentration of sand where interlocking takes place

TAUT   = applied shear stress (*N/m*)

dels   = thickness of carpet (*mm*)

DPDX   = pressure gradient (N/m^3)

mu   = viscosity ($kg/m-s$)

D   = grain diameter (*m*)

TANPHI   = coefficient of dynamic friction

SIGMA   = grain weight per unit volume (N/m^3)

y   = vertical coordinate (*m*)

dely   = increment in y direction (*m*)

delc   = increment in concentration

TAU3   = shear stress (N/m^2)

P   = normal stress (N/m^2)

C   = concentration

G2   = G^2

NN   = N

DUDY   = grain strain rate ($1/s$)

LAMDA = λ

A.1   COMPUTER PROGRAM FOR CARPET FLOW ANALYSIS: NON-LINEAR CONCENTRATION PROFILE

```
       OPEN "RESUTL3.OUT" FOR OUTPUT AS #1
       OPEN "RES3-LOG.OUT" FOR OUTPUT AS #2
REM    NON-LINEAR CONCENTRATION PROFILE WITH CONVECTIVE
       ACCELERATION PRESSURE TERM INCLUDED
       DIM C(2000), CC(2000), y(2000), TAU3(2000), DUDY(2000),
       NN(2000), LAMDA(2000), G2(2000), P(2000), FS(2000)
       coo = .62
       co = .543
       D = 1 / 1000
REM    TAUT = 10
       dels = 10
REM    DPDX = (3 / 100) * 9810
       mu = .001
       TANPHI = .6
       TANPHI3 = .75
       PHI = ATN(TANPHI)
       SIGMA = 2650
       A = 1000 * 9.81 * (2.65 - 1)
REM    CARY = TAUT / ((A * ((TANPHI + TANPHI3) / 2) * .4 * co) -
       DPDX * .4 * co)
       CARY = dels / 1000
       delY = .0001
REM    delC = .0001
       C(0) = 0
       y(0) = 0
       TAU3(0) = 0
       i = 0
10     i = i + 1
       y(i) = y(i - 1) + delY
       ETA = (CARY - y(i)) / CARY
```

```
        IF ETA < 0 THEN GOTO 90
        C(i) = co * (1 - 4 * ETA ^ 1.5 + 3 * ETA ^ 2)
        N = 0
15      N = N + 1
        CC(i) = C(i)
REM     integration
20      SUMLL = 0
        FOR j = 1 TO i
          SUMLL = CC(j) + SUMLL
        NEXT j
        ESUMLL = (SUMLL - .5 * CC(i)) * delY
        P(i) = A * ESUMLL
        TAU3(i) = P(i) * (TANPHI + TANPHI3) / 2
        LAMDA = 1 / ((coo / C(i)) ^ (1 / 3) - 1)
        G2(i) = TAU3(i) * SIGMA * D ^ 2 / LAMDA / mu ^ 2
        LAMDA(i) = LAMDA
        IF G2(i) <= 100 THEN
          FS(i) = 1
          TAU3(i) = P(i) * TANPHI3
          DUDY(i) = TAU3(i) / (1 + LAMDA) / (1 + LAMDA / 2) / mu
          NN(i) = LAMDA ^ .5 * SIGMA * D ^ 2 * DUDY(i) / mu
          PRINT #2, "<=100 VISCOUS"
          PRINT #2, i; CARY - y(i); NN(i); G2(i)
        ELSE
          IF G2(i) >= 3000 THEN
          FS(i) = 3
          PRINT #2, ">=3,000 INERTIAL"
            IF LAMDA <= 14 THEN
              TAU3(i) = P(i) * TANPHI
              DUDY(i) = (TAU3(i) / (.042 * SIGMA * LAMDA ^ 2 * D ^ 2
                * SIN(PHI))) ^ .5
            ELSE
              TAU3(i) = P(i) * TANPHI
              cof = .04 + (LAMDA - 14) * (.427 - .04) / (22 - 14)
```

```
      DUDY(i) = ((TAU3(i) / TANPHI) / (cof * SIGMA * LAMDA ^
        2 * D ^ 2)) ^ .5
    END IF
    NN(i) = LAMDA ^ .5 * SIGMA * D ^ 2 * DUDY(i) / mu
    PRINT #2, i; NN(i); G2(i)
  ELSE
   TAU3(i) = P(i) * TANPHI3
   DUDYL = TAU3(i) / (1 + LAMDA) / (1 + LAMDA / 2) / mu
   IF LAMDA <= 14 THEN
     TAU3(i) = P(i) * TANPHI
     DUDYI = (TAU3(i) / (.042 * SIGMA * LAMDA ^ 2 * D ^ 2 *
       SIN(PHI))) ^ .5
   ELSE
     cof = .04 + (LAMDA - 14) * (.427 - .04) / (22 - 14)
     TAU3(i) = P(i) * TANPHI
     DUDYI = ((TAU3(i) / TANPHI) / (cof * SIGMA * LAMDA ^ 2
       * D ^ 2)) ^ .5
   END IF
   DUDY(i) = (3000 - G2(i)) / 2900 * DUDYL + (G2(i) - 100)
     / 2900 * DUDYI
   TAU3(i) = A * ESUMLL * (TANPHI + TANPHI3) / 2
   NN(i) = LAMDA ^ .5 * SIGMA * D ^ 2 * DUDY(i) / mu
   FS(i) = 2
   PRINT #2, "100<= TRANSITION <=3000"
   PRINT #2, i; NN(i); G2(i); DUDY(i); DUDYL; DUDYI
  END IF
 END IF
 PRINT i; C(i); y(i); delY; DUDY(i); LAMDA; NN(i)
 GOTO 10
90 FOR j = 0 TO i - 1
 k = i - 1 - j
 y(j) = y(i - 1) - y(k)
 PRINT #1, y(j); C(k); TAU3(k); P(k); DUDY(k); LAMDA(k); 0;
 FS(k)
```

```
       NEXT j
       PRINT #1, "        "
       PRINT #1, delC; "dely="; delY; co; TAUT; D; "cary(mm)=";
       CARY * 1000; DPDX
       CLOSE #1
       CLOSE #2
100    END
```

A.2   COMPUTER PROGRAM FOR CARPET FLOW ANALYSIS: LINEAR CONCENTRATION PROFILE

```
      OPEN "RESUTL2.OUT" FOR OUTPUT AS #1
      OPEN "RES2-LOG.OUT" FOR OUTPUT AS #2
REM   LINEAR CONCENTRATION PROFILE
      DIM C(2000), CC(2000), Y(2000), TAU2(2000), DUDY(2000),
      NN(2000), G2(2000), LAMDA(2000)
      Coo = .62
      Co = .543
      D = 1 / 1000
      mu = .001
      TANPHI = .53
      PHI = ATN(TANPHI)
      SIGMA = 2650
REM   TAUT = 9810 * R * S(9810 * 1 * .001)
      TAUT = 10
      A = 1000 * 9.81 * (2.65 - 1)
      k = 1000 * 9.81 * (2.65 - 1) * Co ^ 2 * TANPHI / TAUT
      DELY = .00005
      delC = .00005
      C(0) = 0
      Y(0) = 0
      TAU2(0) = 0
      i = 0
10    i = i + 1
      Y(i) = Y(i - 1) + DELY
      C(i) = 0
      N = 0
15    N = N + 1
      C(i) = (C(i) + delC)
      CC(i) = C(i)
REM   INTEGRATION
```

```
20    SUMLL = 0
      FOR j = 1 TO i
        SUMLL = CC(j) + SUMLL
      NEXT j
      ESUMLL = (SUMLL - .5 * CC(i)) * DELY
      IF N > 50000 THEN PRINT "N-HIGH": GOTO 100
      diffc = (k * ESUMLL - C(i) ^ 2) / (k * ESUMLL) * 100
      IF diffc > 0 THEN GOTO 15
        diffco = (Co - C(i)) / Co * 100
        IF (diffco) >= 0 THEN
        TAU2(i) = A * TANPHI * ESUMLL
        LAMDA = 1 / ((Coo / C(i)) ^ (1 / 3) - 1)
        G2(i) = TAU2(i) * SIGMA * D ^ 2 / LAMDA / mu ^ 2
        LAMDA(i) = LAMDA
        IF G2(i) <= 100 THEN
          DUDY(i) = TAU2(i) / (1 + LAMDA) / (1 + LAMDA / 2) / mu
          NN(i) = LAMDA ^ .5 * SIGMA * D ^ 2 * DUDY(i) / mu
          PRINT #2, i; NN(i); G2(i)
        ELSE
          IF G2(i) >= 3000 THEN
            IF LAMDA <= 15 THEN
              DUDY(i) = (TAU2(i) / (.042 * SIGMA * LAMDA ^ 2 * D ^ 2
                * SIN(PHI))) ^ .5
            ELSE
              cof = .042 + (LAMDA - 15) * (.22 - .042) / (22 - 15)
              DUDY(i) = (TAU2(i) / (cof * SIGMA * LAMDA ^ 2 * D ^ 2
                * SIN(PHI))) ^ .5
            END IF
          ELSE
          DUDYL = TAU2(i) / (1 + LAMDA) / (1 + LAMDA / 2) / mu
            IF LAMDA <= 15 THEN
              DUDYI = (TAU2(i) / (.042 * SIGMA * LAMDA ^ 2 * D ^ 2 *
                SIN(PHI))) ^ .5
            ELSE
```

```
         cof = .042 + (LAMDA - 15) * (.22 - .042) / (22 - 15)
         DUDYI = (TAU2(i) / (cof * SIGMA * LAMDA ^ 2 * D ^ 2 *
           SIN(PHI))) ^ .5
       END IF
      DUDY(i) = (3000 - G2(i)) / 2900 * DUDYL + (G2(i) - 100)
         / 2900 * DUDYI
      NN(i) = LAMDA ^ .5 * SIGMA * D ^ 2 * DUDY(i) / mu
      PRINT #2, "<=3000"
      PRINT #2, i; NN(i); G2(i); DUDY(i); DUDYL; DUDYI
      END IF
     END IF
     PRINT i; "  "; C(i); Y(i); "  "; DELY; "  "; diffco; " ";
         N
    GOTO 10
   ELSE
   END IF
   FOR j = 0 TO i - 1
    Y(j) = Y(i - 1) - Y(i - 1 - j)
    k = i - 1 - j
    PRINT #1, Y(j); C(k); TAU2(k); DUDY(k); LAMDA(k)
    PRINT #2, j; Y(j); G2(k)
   NEXT j
   PRINT #1, delC; DELY; TANPHI; Co; TAUT; D
   CLOSE #1
   CLOSE #2
100  END
```

A.3   COMPUTER PROGRAM FOR CARPET FLOW ANALYSIS: UNIFORM CONCENTRATION PROFILE

```
        OPEN "RESULT.OUT" FOR OUTPUT AS #1
        OPEN "RES1-LOG.OUT" FOR OUTPUT AS #2
REM     UNIFORM CONCENTRATION
        DIM Y(2000), TAU(2000), DUDY(2000), N(2000), G2(2000)
        D = 1 / 1000
        SIGMA = 2650
        mu = .001
        A = 1000 * 9.81 * (2.65 - 1)
        Coo = .62
        Co = .543
        TANPHI = .53
        PHI = ATN(TANPHI)
REM     LAMDA = 3.85
        LAMDA = 3.13
        TAUT = 10
        DELY = .00005
        PRINT #1,
        PRINT #1, "A="; A; DELY; TANPHI; Co; TAUT; D
        i = 0
        Y(0) = 0
        TAU(0) = 0
10      i = i + 1
        Y(i) = Y(i - 1) + DELY
        TAU(i) = TANPHI * A * Coo / (1 / LAMDA + 1) ^ 3 * Y(i)
        G2(i) = TAU(i) * SIGMA * D ^ 2 / LAMDA / mu ^ 2
        IF G2(i) <= 100 THEN
          PRINT #2, "<=100"
          DUDY(i) = TAU(i) / (1 + LAMDA) / (1 + LAMDA / 2) / mu
          N(i) = LAMDA ^ .5 * SIGMA * D ^ 2 * DUDY(i) / mu
          PRINT #2, i; N(i); G2(i); DUDY(i)
```

```
ELSE
  IF G2(i) >= 3000 THEN
  PRINT #2, ">=3000"
  DUDY(i) = (TAU(i) / (.042 * SIGMA * LAMDA ^ 2 * D ^ 2 *
     SIN(PHI))) ^ .5
   N(i) = LAMDA ^ .5 * SIGMA * D ^ 2 * DUDY(i) / mu
    PRINT #2, i; N(i); G2(i); DUDY(i)
  ELSE
   PRINT #2, "100<>3000"
   DUDYL = TAU(i) / (1 + LAMDA) / (1 + LAMDA / 2) / mu
   DUDYI = (TAU(i) / (.042 * SIGMA * LAMDA ^ 2 * D ^ 2 *
     SIN(PHI))) ^ .5
   DUDY(i) = (3000 - G2(i)) / 2900 * DUDYL + (G2(i) - 100)
     / 2900 * DUDYI
   N(i) = LAMDA ^ .5 * SIGMA * D ^ 2 * DUDY(i) / mu
    PRINT #2, i; N(i); G2(i); DUDY(i); DUDYL; DUDYI
  END IF
END IF
IF (TAUT - TAU(i)) > .000001 THEN
  GOTO 10
ELSE
  Y(i) = TAUT * (1 / LAMDA + 1) ^ 3 / TANPHI / A / Coo
  DUDY(i) = (TAUT / (.042 * SIGMA * LAMDA ^ 2 * D ^ 2 *
     SIN(PHI))) ^ .5
END IF
  PRINT #1, Y(0); Co / 2; TAUT
FOR j = 1 TO i
  PRINT #1, Y(j); Co / 2; TAU(i - j); DUDY(i - j); LAMDA
NEXT j
CLOSE #1
CLOSE #2
END
```